ANTI-APOPTOTIC AND APOPTOTIC EFFECTS OF Xrel3 IN HUMAN CERVICAL CANCER CELLS

MARLENE FOUAD AMIN SHEHATA

Anti-apoptotic And Apoptotic Effects of Xrel3 in Human Cervical Cancer Cells

By

© Marlene Fouad Amin Shehata

A thesis submitted to the School of Graduate Studies in partial fulfillment of the requirements for the degree of Master of Science

Division of Basic Medical Sciences

Faculty of Medicine
Memorial University of Newfoundland

July 2003

St.John's Newfoundland

Your file Votre référence
ISBN: 0-612-99114-8
Our file Notre référence
ISBN: 0-612-99114-8

TABLE OF CONTENTS

ABSTRACT ..... **VI**

ACKNOWLEDGEMENT ..... **IX**

LIST OF TABLES ..... **XI**

LIST OF FIGURES ..... **XII**

LIST OF ABBREVIATIONS ..... **XVII**

LIST OF APPENDICES ..... **XX**

CHAPTER 1 INTRODUCTION **1**

1.1 Oncogenesis **2**

1.1.1 Etiology of Cervical Cancer 2

1.1.2 Human Papilloma Virus (HPV) 3

1.2 Apoptosis **8**

1.2.1 Introduction 8

1.2.2 Regulators of apoptosis 10

1.2.2.1 Caspases 11

1.2.2.2 Bcl-2 family of proteins 12

1.2.2.3 p53 14

1.2.2.4 PARP 15

1.3 Rel/NF-κB family **17**

1.3.1 Introduction 17

1.3.2 IκB inhibitor system 28

1.3.3 Role of NF-κB in apoptosis and cell survival. 32

1.3.3.1 NF-κB involvement in apoptosis 32

1.3.3.2 Rel/NF-κB role in cell protection and survival. 33

1.3.4 Xrel3 35

1.4 Cancer Chemotherapy **36**

1.4.1 Introduction 36

1.4.2 Platinums 37

1.4.3 Cisplatin 38

1.4.4 Rel/NF-κB and Chemoresistance 38

1.5 Purpose and hypothesis of this study **39**

CHAPTER 2: MATERIALS AND METHODS **41**

2.1 Materials **41**

2.2 Methods **42**

2.2.1 Cell culture 42

2.2.2 Construction of the pTRE2-Xrel3 plasmid 43

2.2.2.1 Polymerase chain reaction (PCR) 43

2.2.2.2 DNA extraction and purification from agarose gel 44

2.2.2.3 Restriction enzyme cleavage of pTRE2 and pTRE2-Xrel3 plasmids 44

2.2.2.4 Ligation 45

2.2.2.5 Transformation of E. coli with pTRE2-Xrel3 plasmid. 47

2.2.2.6 Plasmid purification using QIAprep Spin Miniprep kit 47

2.2.2.7 Verifying the presence of Xrel3 47

2.2.3 Establishing stable transfection of HeLa cells with Xrel3 48

2.2.4 Selection of the stably transfected clones. 48

2.2.5 Verifying the presence of pTRE2-Xrel3 and pTRE2 49

2.2.5.1 DNA extraction from cultured cells 49

2.2.5.2 Polymerase chain reaction 49

2.2.6 Verification of Xrel3 transcription 49

2.2.6.1 RNA extraction 49

2.2.6.2 Confirming the integrity of the extracted RNAs 50

2.2.6.3 Northern blotting 50

2.2.7 Growth rate and saturation density assay. 52

2.2.8 Drug treatment 52

2.2.9 Cell viability assay 53

2.2.10 Western blotting 53

2.2.11 Statistical Analysis 55

CHAPTER 3 RESULTS 56

3.1 Xrel3 expression in HeLa cells transfected with pTRE2-Xrel3 plasmid 56

3.2 Verification of the size of Xrel3 gene in the transfected HeLa cells 62

3.3 Induction of Xrel3 expression in transfected HeLa cells by doxycycline. 64

3.4 Northern Analyses 67

3.5 Growth Assay 75

3.6 Cell viability assay 80

3.7 Effect of doxycycline induction on protein expression 83

CHAPTER 4: DISCUSSION AND FUTURE DIRECTIONS..132

4.1 Tet-On system and Xrel3 expression.....135

4.2 Effect of Xrel3 expression on growth 136

4.3 Effect of Xrel3 expression on cisplatin-treated HeLa cells. 139

4.4 Modulation of protein expression by Xrel3 overexpression. 141

4.4.1 Xrel3 effect on protein expression at 1 μM cisplatin-treated HeLa cells.142

4.4.2 Xrel3 effect on protein expression at 5 μM cisplatin-treated HeLa cells.145

4.5 Future Directions 148

CHAPTER 5 REFERENCES LIST 151

APPENDIX 1 176

ABSTRACT

Cervical cancer is considered a common yet preventable cause of death in women. It has been estimated that about 420 women out of the 1400 women diagnosed with cervical cancer will die during 5 years from diagnosis (National Cancer Institute of Canada, 2003). This study addresses the role of a member of the Rel/NF-κB family of genes, *Xrel3*, in the growth of the malignant HeLa cervical cells and its effect on chemotherapeutic treatment.

The hypothesis of this study is that Rel/NF-κB promotes chemotherapeutic resistance in cancer cells. In order to study this problem, the amphibian *Xrel3*, a Rel/NF-κB homologue, was used because it was previously shown to be constitutively active when transfected into HeLa cells, which normally do not express Rel/NF-κB. This allowed the opportunity to test whether Xrel3 expression imbues chemoresistant properties to these cells.

The expression of Xrel3 slowed the growth of HeLa cervical cells associated with an increase in expression of the cell cycle inhibitor p21. The expression level of the apoptosis pathway protein caspase-8, its activated product and cleaved poly (ADP-ribose) polymerase, PARP, were also

elevated 6-fold relative to the non-induced state, perhaps associated with the initiation of apoptosis consequent to cell growth arrest.

To determine the effect of chemotherapeutic agents on HeLa cells expressing Xrel3, cells were treated with the DNA-crosslinking and chelating agent, cisplatin. At 1 μM cisplatin, the expression of *Xrel3* initiated an anti-apoptotic effect after 24 hours of treatment, based on the expression of significantly lower levels of the apoptotic proteins, Bax ($P<0.05$), caspase-8 ($P<0.05$) and MDM-2 ($P<0.01$). Furthermore, the level of the tumor suppressor protein p53 was suppressed by 3-fold, along with a reduction of caspase-3 and p21. The expression of the anti-apoptotic BAG-1 isoforms ($P<0.01$) was also increased. The expression of *Xrel3* sensitizes HeLa cells to 1 μM cisplatin after a lag period of three days, however, as assessed by a decrease in numbers of viable cells.

After 24 hours of 5 μM cisplatin treatment, there was a significant increase in the levels of the pro-apoptotic proteins relative to controls, including Bax ($P<0.05$), MDM-2 ($P<0.05$), the cell cycle inhibitor p21 ($P<0.01$), cleaved PARP, caspase-8, and caspase-3. However, p53 was significantly decreased ($P<0.05$) while BCL-2 ($P<0.01$) and BCL- X_L ($P<0.01$) levels were elevated significantly. The level of the anti-apoptotic

protein BAG-1 remained constant ($P<0.01$) in cisplatin-treated Xrel3-expressing cells. Despite the increased expression of BAG-1, the balance between pro- and anti-apoptotic factors shifted towards increased expression of pro-apoptotic proteins. The Human Papillomavirus (HPV) oncoprotein E6 expression was not affected by the transfected *Xrel3* gene.

These results suggested that *Xrel3*, a homolog of c-Rel, causes an anti-apoptotic effect (chemoresistance) when cells are initially exposed to low cisplatin concentrations (1 μM). This result supports the hypothesis of this study. However, with prolonged contact to 1 μM cisplatin or upon 24 hours exposure to 5 μM cisplatin, Xrel3 had a synergistic apoptotic effect when coupled with cisplatin, thus promoting chemosensitivity and cell death. These results support the previously proposed idea that Rel/NF-κB proteins modulate their activity depending on cellular stress.

ACKNOWLEDGEMENT

My sincere thanks and appreciation to my supervisors Drs. Alan Pater and Ken Kao for their support, patience, excellent advice and continuous guidance. I will always recall the times I spent in the lab and your continuous encouragement will never be wiped off by years.

Special thanks to my committee members Drs. Cathy Popadiuk and Robert Gendron for their support. They were always there whenever I needed them.

Also I would like to extend my thanks to Jieying Xiong, Garry Chernenko, Adam Green, Ingrid Pardoe, Malcolm Wells and Bilan Mo. I will never forget the beautiful memories they left me. I will always recall those nice days as long as I live.

My love and gratitude to my parents Drs. Fouad Shehata and Sozit Shoukralla. Their love and support was the steering wheel behind my progress. They never complained about my talks on Molecular Biology of Cancer all through my program. On the contrary, they overwhelmed me by their love, prayers and advice. Also I extend my love to my sister Engineer Marian. She helped me a lot in my thesis. Her computer skills, knowledge,

experience, love and patience will never be erased by years. The frame, design and format of my thesis carry her fingerprints and show her overwhelming love and kindness. Also, my brother Dr.Fady helped me a lot both by advice, prayers and visits. His intelligence and computer talents were my reference and guidance all through my program and thesis writing. Also, my sincere love to my aunt Dr.Faten Shoukralla and my grandma, Julia El-Sawaf who were always there supporting me by prayers, love and advice. Special thanks to my uncle Eng.Samir Shoukralla and his wife Donna and my uncle Eng.Gamal Shehata, Vice President of Telecom Egypt, who helped me with reference letters. Also my uncle Eng. Magdy Shoukralla has always supported me by advice and guidance as well as my uncle Eng. Michael Shoukralla and his wife Carmen who overwhelmed me by their love and support.

I am truly thankful to my rock of salvation, Jesus Christ, who never fails a battle. It is by His power and strength that this project came to materialistic existence.

"Trust in the LORD with all thine heart; and lean not unto thine own understanding. In all thy ways acknowledge him, and he shall direct thy paths." Proverbs 3:5-6

LIST OF TABLES

Table 1: Naturally occurring cancers associated with papillomaviruses.

Table 2: Localization of κB sites in the body determines the functions of Rel/NF-κB.

Table 3: The factors associated with activation of NF-κB transcription family.

Table 4: Steps involved in NF-κB activation.

Table 5: Summary: Effect of Xrel3 expression on HeLa cellular protein extracts.

LIST OF FIGURES

Figure 1.1: A schematic representation of RB/p53 interactions to regulate cell cycle and apoptosis.

Figure 1.2: Summary of the mechanism of action of the tumor suppressor protein, p53.

Figure 1.3: NF-κB and IκB proteins.

Figure 1.4: The steps involved in the activation of NF-κB family of transcription factors.

Figure 1.5: Illustration of the NF-κB pathway.

Figure 2.1: The map of the pTRE2 vector showing the restriction sites (*BamHI and XbaI*) where Xrel3 was integrated.

Figure 3.1: A) The presence of Xrel3 in the pTRE2-Xrel3 transfected HeLa cells. B) Absence of Xrel3 in the pTRE2 transfected HeLa cells.

Figure 3.2: Verification of the size of Xrel3 gene inserted in the pTRE2-Xrel3 plasmid following transfection in HeLa cells.

Figure 3.3: Verification of the integrity of extracted RNAs for Northern blotting.

Figure 3.4: Northern blot analysis for total cellular RNA extracted from doxycycline-treated pTRE2-Xrel3 colonies designated by the numbers 1 to 15 and control pTRE2 colonies given the numbers 1 and 2.

Figure 3.5: Northern blot analysis for total cellular RNA extracted from the non-induced pTRE2-Xrel3 transfected colonies designated by the numbers 1 to 14.

Figure 3.6: Xrel3 transcription in the selected clones -/+ doxycycline.

Figure 3.7: Growth Assay for the highest, intermediate and lowest Xrel3-expressing clones +/- doxycycline.

Figure 3.8: Growth assay for the highest, intermediate and lowest Xrel3-expressing clones +/- doxycycline after treatment with 1 μM cisplatin.

Figure 3.9: Expression of p53 in pTRE2-Xrel3 and control pTRE2 transfected HeLa cells.

Figure 3.10: Expression of p53 in the pTRE2- Xrel3 (Int.) after 24 hours of drug treatment.

Figure 3.11: Expression of p53 in pTRE2-Xrel3 (Int.) after 48 hours of drug treatment.

Figure 3.12: Expression of Bax in pTRE2-Xrel3 (Int.) and pTRE2 transfected HeLa cells after 24 hours of drug treatment.

Figure 3.13: Expression of caspase-3 catalytic subunit at 17 kDa in pTRE2-Xrel3 (Int.) and pTRE2 transfected HeLa cells +/- doxycycline after 24 hours treatment with 1 and 5 μM cisplatin.

Figure 3.14: Expression of caspase-8 at 55 kDa in pTRE2-Xrel3 (Int.) and pTRE2 transfected HeLa cells +/- doxycycline and +/- with 1 μM cisplatin.

Figure 3.15: Expression of caspase-8 at 55 kDa in pTRE2-Xrel3 (Int.) and pTRE2 control cells +/- doxycycline after 24 hours treatment with 1 and 5 μM cisplatin.

Figure 3.16: Expression of MDM-2 in pTRE2-Xrel3 (Int.) compared to the pTRE2 control +/- doxycycline and after 24 hours treatment with 1 and 5 μM cisplatin.

Figure 3.17: Expression of Bcl-2 in pTRE2-Xrel3 (Int.) compared to the pTRE2 control +/- doxycycline and after 24 hours treatment with 1 and 5 μM cisplatin.

Figure 3.18: Expression of Bcl-X_L in pTRE2-Xrel3 (Int.) compared to the pTRE2 control +/- doxycycline and after 24 hours treatment with 1 and 5 μM cisplatin.

Figure 3.19: Expression of PARP in pTRE2-Xrel3 (Int.) compared to the pTRE2 control +/- doxycycline.

Figure 3.20: Expression of PARP 85 kDa catalytic subunit in pTRE2-Xrel3 (Int.) compared to the pTRE2 control +/- doxycycline and after 24 hours treatment with 1 and 5 μM cisplatin.

Figure 3.21: Expression of p21 in pTRE2-Xrel3 (Int.) compared to the pTRE2 control +/- doxycycline and after 24 hours treatment with 1 and 5 μM cisplatin.

Figure 3.22: Expression of cyclin D1 in pTRE2-Xrel3 (Int.) compared to the pTRE2 control +/- doxycycline and after 24 hours treatment with 1 and 5 μM cisplatin.

Figure 3.23: Expression of PCNA in pTRE2-Xrel3 (Int.) compared to the pTRE2 control +/- doxycycline and after 24 hours treatment with 1 and 5 μM cisplatin.

Figure 3.24: Expression of BAG-1 p46 isoform in pTRE2-Xrel3 (Int.) compared to the pTRE2 control +/- doxycycline and after 24 hours treatment with 1 and 5 μM cisplatin.

Figure 3.25: Expression of BAG-1 p29 isoform in pTRE2-Xrel3 (Int.) compared to the pTRE2 control +/- doxycycline and after 24 hours treatment with 1 and 5 μM cisplatin.

Figure 3.26: Expression of HPV 16/18 E6 in pTRE2-Xrel3 (Int.) compared to the pTRE2 control +/- doxycycline and after 24 hours treatment with 1 and 5 μM cisplatin.

Figure 4.1: The mechanism of action of the Tet-On system

LIST OF ABBREVIATIONS

Bcl	B-cell lymphoma
BH	Bcl-2 homology
bp	base pair
cdk	cyclin-dependent kinase
cDNA	complementary DNA
CML	chronic myeloid leukemia
CMV	Cytomegalovirus
DMEM	Dulbecco's modified Eagle's medium
ECL	enhanced chemiluminescence
EDTA	ethylenediamine tetraacetic acid
FasL	Fas ligand
FCS	fetal calf serum
HBAG-1	human BAG-1
HBV	hepatitis B virus
HPV	human papilloma virus
HSV	herpes simplex virus
HTLV	human T-cell leukemia virus

kb	kilobase
kDa	kilodalton
mAb	monoclonal antibody
mRNA	messenger RNA
NLS	Nuclear localization signal
PAGE	Polyacrylamide gel electrophoresis
PARP	poly(ADP) ribose polymerase
PBS	phosphate-buffered saline
PCR	polymerase chain reaction
PCD	programmed cell death
PKC	protein kinase C
PMSF	phenylmethylsulfonyl fluoride
Rb	retinoblastoma
RNA	ribonucleic acid
SD	Standard deviation
SDS	sodium dodecyl sulphate
TEMED	N, N, N', N' –tetra-methylethylenediamine
TNF-α	tumor necrosis factor-alpha

TPA	12-O-tetradecanoyl-phorbol-13-acetate
UV	Ultraviolet

LIST OF APPENDICES

Appendix 1: Computation of the Student's t-test.

Anti-apoptotic And Apoptotic Effects of Xrel3 in Human Cervical Cancer Cells

CHAPTER 1 INTRODUCTION

1.1 Oncogenesis

1.1.1 Etiology of Cervical Cancer

The process of oncogenesis or carcinogenesis fundamentally emerges from defects in the balance between the activity of proto-oncogenes, which promote cell proliferation, and tumor suppressor genes, which regulate the cell cycle. It is known that DNA damage and repair occurs normally in every living cell. When the rate of DNA damage exceeds that of repair, accumulation of DNA damage and defects might trigger the initiation of cancer (Furomoto and Irahara, 2002, Munoz *et al.*, 2003, Garland, 2002).

Uterine cervical cancer is a serious gynecologic malignancy in women. There are two main types of cervical cancer, squamous cell cancer and adenocarcinoma, based on the type of cells that become cancerous. Cervical cancer is initiated when the combined action of a group of carcinogens cause the normal, physiological events associated with cervical metaplastic transformation to go awry and cause the formation of pre-malignant dysplasia (Josefson, 1999). Poor prognosis is usually associated

with positive pelvic lymph nodes, indicating that the tumor cells have become metastatic (Kim *et al.,* 2003).

Recent studies have demonstrated that estrogen, which is the female sex hormone, might have a contributory role in increasing vaginal epithelium proliferation and thus promoting the malignant transformation of the squamous and columnar cells at the junction of the cervical and vaginal epithelium (Park *et al.,* 2003). Infection by the Human Papilloma Virus, HPV, is a necessary requirement for cervical cancer, but not all women infected by this virus develop cervical cancer (Castellsague *et al.,* 2002). Some HPV infections, for instance are associated with benign proliferation or wart formation.

1.1.2 Human Papilloma Virus (HPV)

HPVs are small DNA viruses that are known to be the most common etiological agents in cervical cancer (Ghim *et al.,* 2002). More than 100 types of HPVs have been discovered, isolated and studied (See Table 1) (Sisk and Robertson, 2002). HPVs are implicated in the mucosal and epithelial infections that may range from a benign lesion to a malignant carcinoma (Garland, 2002). HPV has also been reported to be associated

with anal and genital cancers (Heilmann and Kreienberg, 2002). Preliminary findings suggested their involvement in some head and neck cancers as well (Sisk and Robertson, 2002).

The high risk HPV 16 and HPV 18 are associated with malignant transformation and carcinogenesis in 85% of the diagnosed cervical cancer cases (Garland, 2002). Recent studies have shown that 13 different types of HPV are associated with carcinogenesis (Munoz *et al.,* 2003). The most widely known factors associated with HPV are the E6 and E7 oncoproteins, which interact with p53 and Rb tumor suppressors respectively (Furumoto and Irahara, 2002). The interaction of E6 and E7 with these cellular proteins results in their suppression (Ghim *et al.,* 2002), thus disrupting the normal physiological process of programmed cell death in response to DNA damage (See Figure 1.1) (Finzer *et al.,* 2002). In the presence of carcinogens, therefore, the accumulation of DNA damage without apoptosis is presumed to lead to cancer.

It should be made clear that viral infection by itself does not cause cancer. It is the interaction of the viral genome with host genes that disrupts the normal cell cycle and transforms the cell into a pre-malignant state. For instance, some viruses might interact with specific genes (like tumor

suppressor genes mentioned above) in the host cells, switching some systems on or off, thus leaving the cell free to divide in an uncontrolled way and raising the risk of cancer (Zur Hausen *et al.,* 2003).

Other cellular proteins may be affected by HPV infection as well. For instance, cervical cancer cell lines showed overexpression of the anti-apoptotic protein BAG-1, which might contribute to its malignant proliferation (Yang *et al.,* 1998). Therefore, understanding the molecular mechanisms leading to this disease will be of importance for generating means for its early detection and possible prevention and treatment.

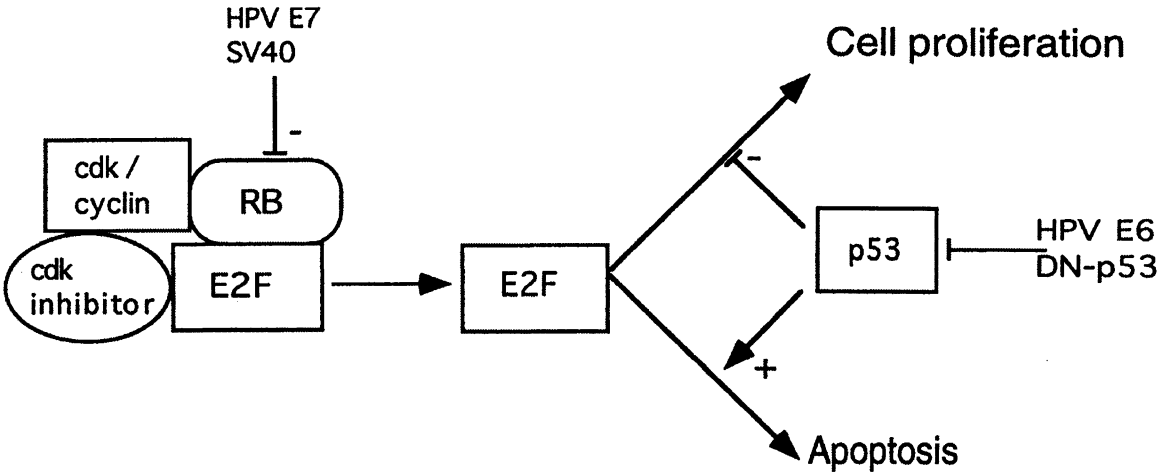

Figure 1.1: A schematic representation of RB/p53 interactions to regulate cell cycle and apoptosis (Adapted from Benett *et al.*, 1998). Cell cycle transition from G_1-S phase is mediated by RB interactions with the E2F transcription factor family, which is considered an important regulator of the cell cycle. Growth factors lead to the phosphorylation of RB in late G_1 phase by cdk/cyclin. This is followed by the release of E2F, allowing transcriptional activation of E2F target genes, which promotes S-phase entry and cell proliferation. HPV E7 and Simian Virus 40 (SV40) promote the release of E2F from RB, whereas HPV E6 and the dominant negative, DN-p53 inhibit p53 activity leading to cell proliferation.

Species	Cancer	Predominant viral types
Humans	Skin carcinomas	HPV-5, -8
	Lower genital tract cancers	HPV-16, -18, -31, -33
	Malignant progression of respiratory papillomas	HPV-6, -11
Cattle	Alimentary-tract carcinoma	HPV-4
	Eye and skin carcinoma	Not characterized
Sheep	Skin carcinoma	Not characterized
Cottontail rabbit	Skin carcinoma	Cotton rabbit papillomavirus (CRPV)

Table 1: Naturally occurring cancers associated with papillomaviruses (Sisk and Robertson, 2002, Zur Hausen *et al.,* 2003).

1.2 Apoptosis

1.2.1 Introduction

Apoptosis, or programmed cell death, is orchestrated by a highly organized group of signaling pathway proteins (for review see Miller and Marx, 1998; Fiers *et al.,* 1999). Apoptosis can be triggered by a variety of events the cell may face. For example, exposure to X-rays, ultraviolet light and chemotherapeutic drugs are factors that can initiate the process of apoptosis (for review, see Miller and Marx, 1998).

One mechanism to protect an organism from the consequences of accumulated DNA damage involves a class of protein-splitting enzymes called caspases, which are activated upon detection of DNA damage and eventually cause cell death (for review, see Thornberry and. Lazebnik, 1998). The control of programmed or physiological cell death acts as a protective mechanism for the organism because accumulation of DNA damage without concomitant repair could lead to the development of cancer, while unregulated apoptosis can cause autoimmune diseases.

The process of apoptosis is essential in stopping the uncontrolled proliferation of cells (for review, see Nicholson, 2000). Any defects in this dynamic process may eventually lead to the development of benign

proliferative lesions or even malignant tumors (for review, see Nicholson, 2000). Apoptosis can be initiated via specific receptors that are members of the tumor necrosis factor (TNF) receptor superfamily (for review, see Ashkenazi and Dixit, 1998). Such "Death receptors" are activated via binding of specific ligands (for review, see Ashkenazi and Dixit, 1998) and once they are activated, they can initiate apoptosis. However, the role of these receptors is not restricted to the initiation of apoptosis, but also includes other functions that differ from apoptosis and sometimes counteract apoptosis such as the recruitment and subsequent ligand binding of growth factors such as the Nerve Growth Factor (NGF) (for review, see Ashkenazi and Dixit, 1998).

Another apoptotic pathway involves the mitochondria. Under stress, these essential organelles can release cytochrome c into the cytoplasm of the cell (for review, see Green and Reed, 1998). This cytochrome c release is a possible activator for caspases by the recruitment of procaspase-9, which undergoes conformational changes that leads to the activation of downstream, effector caspases (for review, see Green and Reed, 1998).

Apoptosis acts as a double-edged sword. Despite its importance in restricting cell proliferation and maintaining constant cell number, excessive

apoptosis is associated with stroke, Alzheimer's disease and other neurodegenerative disorders (for review, see Yuan and Yankner, 2000). Damaged neurons in these disorders commit suicide inappropriately. Alzheimer's disease, for instance, was found to be associated with a genetic component that involves mutations in the chromosomes (1, 14, 21) as well as the tau gene on chromosome 17 and results in unscheduled or unregulated death of brain cells (Rich *et al.,* 2000).

Understanding the details and the signaling pathways of this phenomenon might be helpful in manipulating and intervening in the process of apoptosis. Apoptosis is required to restrict cell proliferation and to maintain a constant cell number. Attempts to suppress apoptosis, however, may be useful to treat neurodegenerative disorders, while attempts to activate apoptosis may be useful in disorders involving overproliferation.

1.2.2 Regulators of apoptosis

Many genes have been implicated in enhancing or inhibiting the process of apoptosis. They act by different mechanisms that ultimately contribute to either tumor suppression or progression, respectively. Four of the most important factors that regulate apoptosis are p53, the caspases, the

Bcl-2 family of proteins and PARP (Reed, 1997; Packham *et al.,* 1997; for review, see Green, 2000).

1.2.2.1 Caspases

Caspases are the executioners of cell death. They receive the signals that enable them to initiate apoptosis. Cells undergoing apoptosis exhibit fragmentation of DNA, condensation of the chromatin, budding of the cell membrane and the formation of apoptotic bodies by dissociation of the cell and its constituents into membrane-enclosed vesicles (for review, see Thornberry and Lazebnik, 1998; Savill and Fadok, 2000). All caspases share a similar structure that consists of three domains: an NH_2-terminal peptide (prodomain), a large subunit (approximately 20 kD) and a small subunit (approximately 10 kD) (for review, see Hengartner, 2000). Caspases are expressed as procaspases, which undergo cleavage to the 2 subunits mentioned above (for review, see Meier *et al.,* 2000). Cleavage of caspases is a sign of active apoptosis. The large and small subunits then associate to form a heterodimer (Boise *et al.,* 1995; Reed, 1997).

The exact mechanism of action of caspases is still unknown. However, several studies have shown that caspases exert both direct and indirect actions on the cell (for review, see Evan et *al.,* 1998). The direct

action of caspases can be exemplified by their ability to act on cell structural integrity by destroying the nuclear lamina (Evan *et al.,* 1998) and cleaving the proteins responsible for regulating the cytoskeleton (Boyd *et al.,* 1995; Evan *et al.,* 1998). The indirect action of caspases is via their ability to inhibit the proteins that promote cell survival and growth (for review, see Hengartner, 2000). Among these proteins is the Bcl-2 family of proteins, which are cleaved by caspases resulting in inactivation of the Bcl-2 proteins and the release of a fragment that has a direct apoptotic effect (for review, see Evan *et al.,* 1998).

Caspases-8, -9, and -10 are known to initiate the caspase activation cascade. However, caspases-3, -6 and -7 propagate the cascade and are activated by the proteolytic cleavage process mediated by other upstream caspases in the caspase cascade pathway (for review, see Hengartner, 2000).

1.2.2.2 Bcl-2 family of proteins

The Bcl-2 family of proteins has several members with various functions (for review, see Nicholson, 2000). The Bcl-2 gene family comprises pro-apoptotic and anti-apoptotic proteins sharing one or more Bcl-2 homology (BH) domains (Reed, 1997). The gene family is made up of 3 main groups (for review, see Hengartner, 2000). Group I includes the anti-

apoptotic members similar to Bcl-2. Group II includes the pro-apoptotic members like Bax and Bak, while group III comprises a diverse collection of proteins that resemble one another structurally, but not necessarily functionally. Bcl-2, BAG-1 and Bcl-x_L provide a cell survival function (Christensen *et al.,* 1999; Stuart *et al.,* 1998; Yang *et al.,* 1998). However, Bax, which promotes apoptosis (Christensen *et al.,* 1999) translocates to the mitochondrial membrane and releases cytochrome c, which can initiate the apoptotic cascade (for review, see Ferrer and Planas, 2003). It also competes for binding with Bcl-2 and with other members of the Bcl-2 superfamily of proteins (for review, see Ferrer and Planas, 2003). Such heterodimerization between anti-apoptotic and pro-apoptotic members of this family is very common and is considered a regulatory mechanism for the decision to undergo apoptosis (Reed, 1997). Thus, the balance between Bcl-2 and Bax is essential for the determination of the apoptotic potential of the cells, in which high apoptotic activity is often associated with a low Bcl-2/Bax level ratio (Reed, 1997).

BAG-1 has been shown to provide an anti-apoptotic effect. Its overexpression in cervical cancer suppressed apoptosis both independently and by increasing Bcl-2 protective activity, which further increased the

resistance of cervical carcinoma to the effect of DNA-damaging agents (Yang *et al.,* 1998; Naishiro, 1999).

1.2.2.3 p53

The tumor suppressor protein p53 has numerous functions (See Figure 1.2) (Rosenthal *et al.,* 1998). Its principle role, however, is as a transcriptional regulator required for the expression of a number of genes involved in cell cycle regulation and apoptosis. The gene encoding p53 can be mutated in many forms of cancer including cervical, uterine, adenocarcinoma, adrenal and colorectal cancers. In cervical cancer, mutation patterns of p53 may vary from point mutation to deletion to base-pair alteration, however 30% of the cases showed a higher percentage of Guanine-Cytosine complementary base pairs compared to the Adenine-Thymine complementary base pairs suggesting that alteration in the base-pairing sequence is the major mutation pattern recognized in p53 (Rosenthal *et al.,* 1998). A recent clinical study showed that the overexpression of p53 in cisplatin-treated tumors might be associated with resistance of the tumor to further cell death and apoptosis (Nakayama *et al.,* 2003).

MDM2 is a p53-regulated protein that has a role in the translocation of p53 from the nucleus and enhances its proteosomal degradation (Rich,

Allen and Wyllie, 2000). Therefore, increased levels of MDM-2 and subsequent low levels of p53 are associated with increased cell growth and proliferation. The p53 tumor suppressor protein can also be targeted for degradation by the E6 oncogene of the Human Papilloma virus (HPV), thus promoting neoplastic proliferations (refer to Figure 1.1) (Rosenthal *et al.,* 1998).

1.2.2.4 PARP

Poly (ADP-ribose) polymerase, PARP, has recently been found to promote cell death, but the exact mechanism of action of PARP remains largely obscure. Many cellular enzymes were found to contain the PARP catalytic subunit, but they have different cellular localizations (Nicoletti and Stella, 2003). Because PARP activation consumes much cellular energy, detection of abnormally high levels of PARP in cells might indicate excessive energy consumption and cellular exhaustion (for review, see Rich *et al.,* 2000). PARP is also known as an apoptosis-inducing factor and high levels of PARP are detected following DNA damage. Thus, this group of enzymes might also be involved in DNA repair, as well as apoptotic responses of the cells (for review, see Rich *et al.*, 2000, summarized in Figure 1.2).

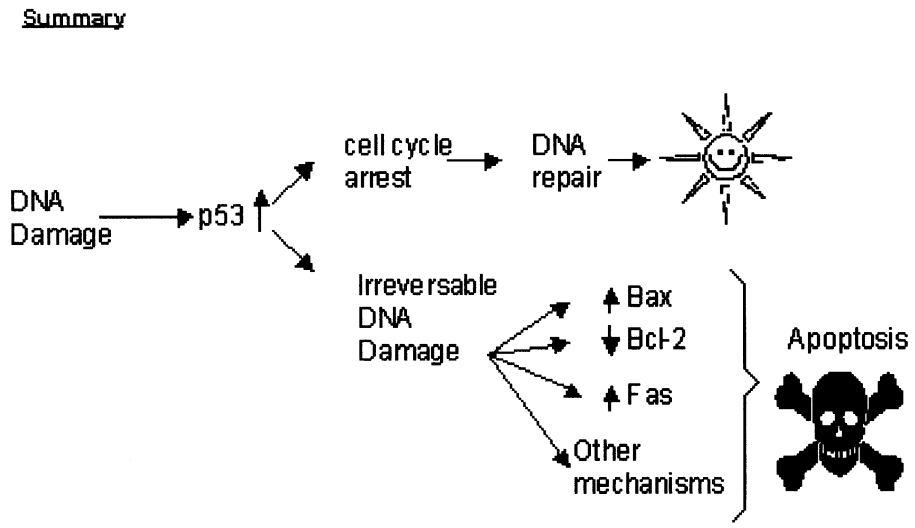

Figure 1.2: Summary of the mechanism of action of the tumor suppressor protein, p53 (Adapted from Famuboni *et al.,* 2002). After DNA damage, the tumor suppressor protein, p53, will be upregulated causing cell cycle arrest and enhancing DNA repair. However, in cases of irreversible DNA damage, p53 has been shown to transcriptionally repress the antiapoptotic gene Bcl-2, while it upregulates the pro-apoptotic proteins Bax and Fas. This in turn, promotes apoptosis. During apoptosis loss of the integrity of the mitochondrial membrane is followed by release of cytochrome c into the cytosol, this in turn leads to activation of caspase cleavage. Bax has been shown to contain p53-binding sites in its promoter site and is upregulated in response to DNA damage and increased p53.

1.3 Rel/NF-κB family

1.3.1 Introduction

The first identified member of the nuclear factor-kappa (κ) B (Rel/NF-κB) family was a protein found to be associated with a decameric oligonucleotide sequence in the enhancer element of the immunoglobulin kappa light chain in B-lymphocytes (Verma *et al.,* 1995; Baeuerle and Baltimore, 1988; Govind, 1999). The Rel/NF-κB family is now known to be made up of a plethora of transcriptional regulators which share a 300 amino acid terminal domain called the Rel homology domain (RHD) (Castranova *et al.,* 1998; Gerondakis *et al.,* 1999). This RHD comprises the DNA binding domain, nuclear localization signal (NLS), dimerization domains and the IκB binding domain (See Figure 1.3) (Liou and Baltimore, 1993; May and Ghosh, 1998). Members of this family include (Verma *et al.,* 1995):

1. NF-κB, including p50, p65, p105 (mice devoid of *p65* generated by targeted "knock-out" gene disruption resulted in defects in fetal development localized to the spleen and liver. However, knock-out

mice devoid of *p105/p50* expression showed no defects during their development).

2. Lyt-10 (p100), including p100 and p52, which are required in spleen development.
3. c-rel (knock-out mice showed defects in the proliferation of B and T cells).
4. relB (knock-out mice showed defects in thymus development).
5. Dorsal, which is involved in the formation of the dorsal-ventral axis of the fruit fly Drosophila (Liou and Baltimore, 1993).

Rel/nuclear factor of kappa B (NF-κB) proteins include those that do not require proteolytic processing and those that do require proteolytic processing. The first group consists of: RelA (known as p65), c-Rel and RelB. The second group includes NF-κB1 (known as p105) and NF-κB2 (known as p100), which further produce p50 and p52 proteins, respectively (See Figure 1.3). Members of these two groups pair with each other with the most commonly detected NF-κB being a heterodimer of p50 and RelA. RelA is responsible for most of NF-κB's transcriptional activity due to the presence of a strong transcriptional activation domain at its C-terminus. p50–c-Rel dimers are less abundant.

Both p50–RelA and p50–c-Rel dimers are regulated by interactions with the inhibitor of κB (IκB) proteins, which cause their cytoplasmic localization. RelB, however, mostly associates with p100 and the p100–RelB dimers are exclusively cytoplasmic. Proteolytic processing of p100 results in the release of p52–RelB dimers, which then translocate to the nucleus. RelB, unlike RelA and c-Rel, can function as an activator or repressor (May and Ghosh, 1998, Verma *et al.,* 1998). Of the above-mentioned proteins, only p50 and p52 are produced from the cytoplasmic precursors p105 and p100, in the presence of ATP as an energy source (May and Ghosh, 1998). However, the other members contain trans-activation domains and can act as activators or inhibitors of transcription based on dimers containing or lacking trans-activation domains (See Figure 1.3) (for review, see Beg and Baldwin 1993).

Figure 1.3: NF-κB and IκB proteins (Adapted from Karin *et al.,* 2002). A schematic representation of various domains in (Rel)/nuclear factor of kappa B (NF-κB) proteins including the Rel Homology Domain, RHD, which comprises the DNA binding domain, nuclear localization signal (NLS), dimerization domains and the IκB binding domain. (Rel)/nuclear factor of κB (NF-κB) proteins include those that do not require proteolytic processing and those that do require proteolytic processing. The first group consists of: RelA (known as p65), c-Rel and RelB and the second group includes NF-κB1 (known as p105) and NF-κB2 (known as p100), which further produce p50 and p52 proteins, respectively. These two groups dimerize, the most commonly detected NF-κB dimer is p50–RelA. RelA is responsible for most of NF-κB transcriptional activity due to the presence of a strong transcriptional activation domain. p50–c-Rel dimers are less abundant. Both p50–RelA and p50–c-Rel dimers are regulated by interactions with the inhibitor of κB (IκB) proteins, which cause their cytoplasmic localization. RelB, however, mostly associates with p100 and the p100–RelB dimers are exclusively cytoplasmic. Proteolytic processing of p100 results in the release of p52–RelB dimers, which translocate to the nucleus. RelB, unlike RelA and c-Rel, can function as an activator or repressor (May and Ghosh, 1998, Verma *et al.,* 1998).

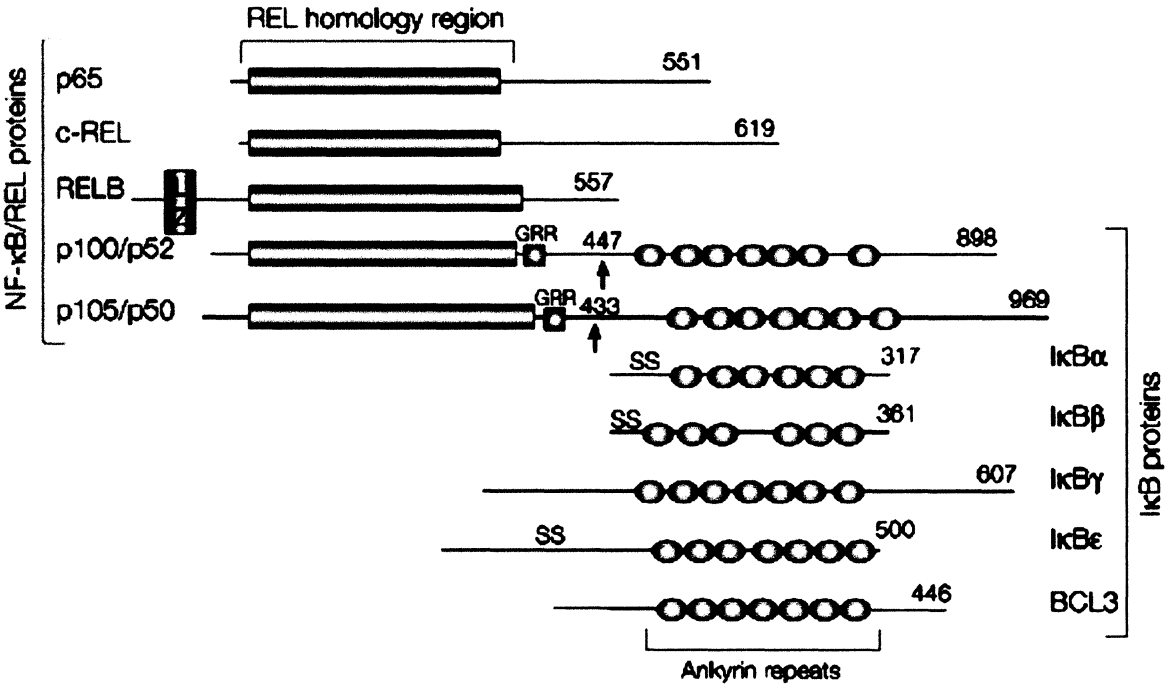
REL homology region
NF-κB/REL proteins
p65
551
c-REL
619
RELB
557
p100/p52
GRR
447
898
p105/p50
GRR
433
969
SS
317
IκBα
SS
361
IκBβ
607
IκBγ
SS
500
IκBε
446
BCL3
IκB proteins
Ankyrin repeats

The functions of the Rel/NF-κB family of proteins are strongly related to the target genes that contain the response elements for the protein (Grilli *et al.,* 1993; Collins *et al.,* 1995; for review, see Verma *et al.,* 1995; Wang *et al.,* 1999). For example, κB response elements are localized in *IL-2, IL-2R, Ig κ* and *MHC Classes (I) and (II) genes*, and here the Rel/NF-κB family of proteins function in modulating the immune system responses by binding to these target sequences and recruiting other immune system and inflammatory reaction mediators (See Figure 1.4 and Table 2). However, the Rel/NF-κB family of proteins is also directly involved in inflammatory reactions and acute phase responses when the κB binding sites are found in the regulatory sequences for the *IL-1, IL-6, TNF-α, TNF-β* and *serum amyloid A protein* genes. Also, the Rel/NF-κB family of proteins is involved in viral infections when the κB sites are found in the HIV-LTR, SV 40, CMV and adenovirus. Other functions of Rel/NF-κB proteins include growth regulation, immune system responses and cell adhesion molecules (see Table 2).

Activation of NF-κB transcription involves the translocation of NF-κB proteins to the nucleus as illustrated in Figure 1.4 (Liou and Baltimore, 1993; May and Ghosh, 1998; Verma *et al.,* 1995; Shain *et al,* 1998). The

factors involved in the transcriptional activation of different members of the Rel/NF-κB family are mentioned in Table 3 (for review, see Verma *et al.*, 1995; Liou and Baltimore, 1993; May and Ghosh, 1998).

Figure 1.4: The steps involved in the activation of NF-κB family of transcription factors. Activators of NF-κB like TNF-alpha, PMA, UV or LPS activate the NF-κB inducible kinase, which in turn phosphorylates at least IKK1 (I kappa B kinase-alpha) and sometimes IKK2 (I kappa B kinase-beta) in the I kappa B-kinase complex. Activators of NF-κB may directly activate the kinase complex as well. This may be followed by phosphorylation of the p105/p65 complex by the kinase complex, which is in turn followed by ubiquitination, proteasomal degradation and the nuclear translocation of NF kappa B. Inside the nucleus; NF kappa B promotes the transcription of immune response genes. The "??????" indicates the possibility of lowered translocation and consequent activation of NF-κB, which occurs in various diseases (Adapted from Ponnappan, 1998).

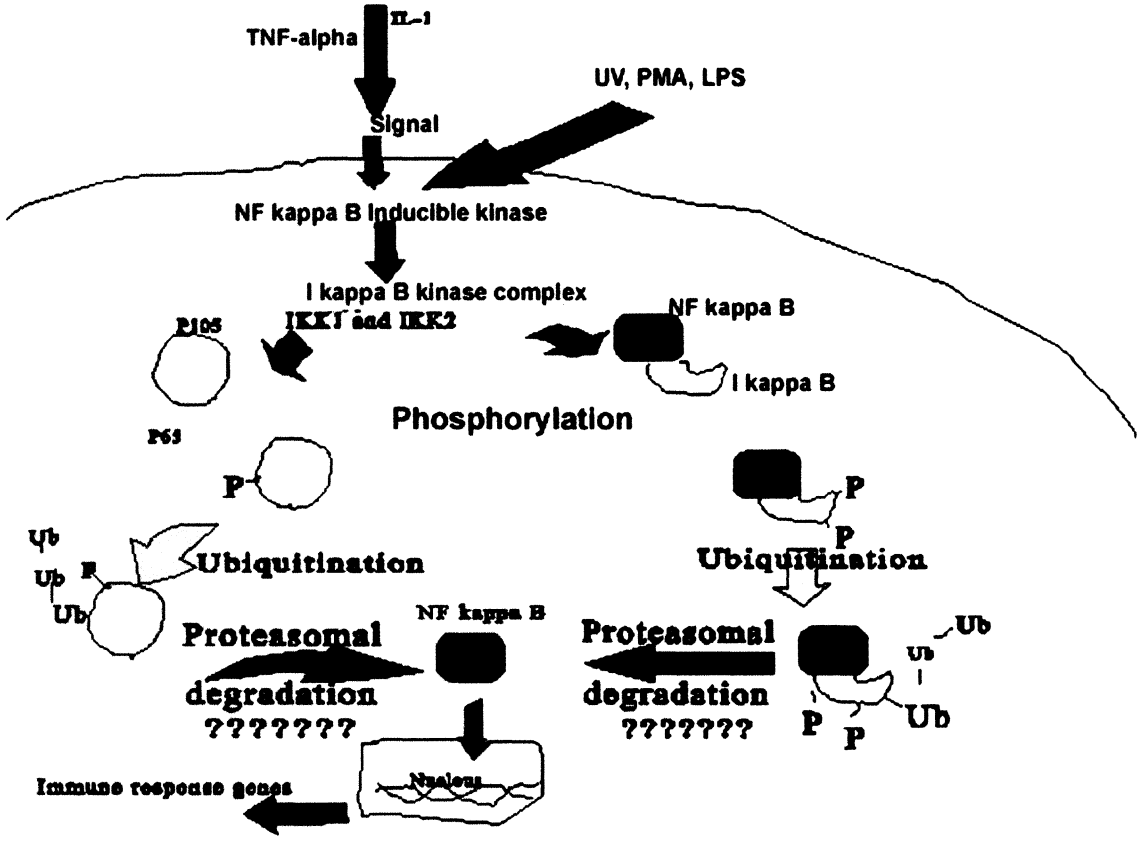
TNF-alpha
IL-1
UV, PMA, LPS
Signal
NF kappa B inducible kinase
I kappa B kinase complex
IKK1 and IKK2
P105
NF kappa B
I kappa B
Phosphorylation
P65
P
Ub
Ubiquitination
Proteasomal
degradation
???????
NF kappa B
Immune response genes
Nucleus

κB sites	Related functions
IL-2, IL-2R, Igκ, MHC Classes I and II	Immune system reaction and responses.
IL-1, IL-6, TNF-α, TNF-β, serum amyloid A protein	Inflammatory reactions and acute phase responses.
HIV-LTR, SV 40, CMV, adenovirus	Viral infections
Rel/NF-κB family (NF-κB1, NF-κB2, c-rel, RelB)	Immune system responses.
p53, c-Myc, Ras, pRB1	Growth regulation.
IκB-α, IκB-γ, p105, p100 and Bcl-3	IκB family members
I-CAM, V-CAM, E-selectin, ELAM1	Cell adhesion molecules

Table 2: Localization of κB binding motifs in the body suggests the functions of Rel/NF-κB (for review, see Verma *et al.,* 1995; Wang *et al,* 1999).

- Cytokines (TNF-α, IL-1, IL-2, IL-6)
- Bacterial lipopolysaccharides
- Phytohemagglutinin (PHA)
- Cross-linking surface CD2, CD3, CD28 and T-cell receptors.
- Proteins secreted by viruses, for example, tax, X, E1A
- Viral infections, for example, HIV-1, Hepatitis B, HSV, HTLV-1
- Antigenic stimulants for the T and B-cells receptors
- Ultraviolet light exposure
- X-irradiation
- Nitric oxide
- Hydrogen peroxide and other oxidizing agents
- Calcium ionophores

Table 3: The factors associated with activation of NF-κB transcription factor (Schottelius *et al.,* 1999; Sun and Ballard, 1999; McFarland *et al.,* 1999; Liou and Baltimore, 1993; Verma *et al.,* 1995; Kawakami *et al.,* 1999; Meyskens *et al.,* 1999; Haddad, 2002).

1.3.2 IκB inhibitor system

The multiple targets of Rel/NF-κB proteins and their multiple modes of regulation indicate that this family possesses diversity in function. Interestingly, their major mode of regulation appears to be well conserved through the IκB inhibitor system. IκB is a protein of 60-70 kDa (Baeuverle and Baltimore, 1988; May and Ghosh, 1998). The IκB inhibitor system comprises seven molecules IκB-α, IκB-β, IκB-γ, Bcl-3, p105, p100 and I κB R (Garcia *et al.,* 1999). The inhibitor of κB (IκB) kinase (IKK) complex is composed of two catalytic subunits, IKKα and IKKβ, and one regulatory subunit, IKKγ.

The IκB inhibitor system regulates NF-κB (p50, p65) by retaining it as a complex in the cytoplasm (Henkel *et al.,* 1993). As a result, the NF-κB family members remain in the cytoplasm in an inactive form. In response to stimuli such as tumour-necrosis factor-α (TNF-α), CD40 ligand (CD40L), interleukin-1 (IL-1) or lipopolysaccharide (LPS), the IKKβ subunit is activated, and phosphorylates the IκB proteins (bound to the NF-κB heterodimers) at two conserved serines. This phosphorylation event triggers the ubiquitin-dependent degradation of IκB by the 26S proteasome, resulting in the nuclear translocation of RelA–p50 (or c-Rel–p50) heterodimers and

transcriptional activation of target genes (See Figure 1.5). In response to other stimuli, such as the TNF family members lymphotoxin B (LTβ) and BAFF, IKKα is activated to induce the phosphorylation of p100 (bound to RelB) at two serine residues at its carboxyl terminus. This phosphorylation event triggers the ubiquitin-dependent degradation of the carboxy-terminal half of p100, releasing its amino-terminal half, the p52 polypeptide, which together with its heterodimer partner, RelB, translocates to the nucleus to activate transcription (Garcia *et al.,* 1999, Baeuverle and Baltimore, 1988; May and Ghosh, 1998, McKenzie *et al.,* 2000) (See Figure 1.5 and Table 4).

Rel/NF-κB family members also cooperate with other transcriptional regulators such as the non-Rel/NF-κB protein Ets-1. Recent data has provided evidence that physical interaction between Ets and NF-kappaB proteins is required for the transcriptional activity of the HIV-1 and HIV-2 enhancers (Bassuk *et al.,* 1997). These interactions represent a potential target for the development of novel immunosuppressive and antiviral therapies.

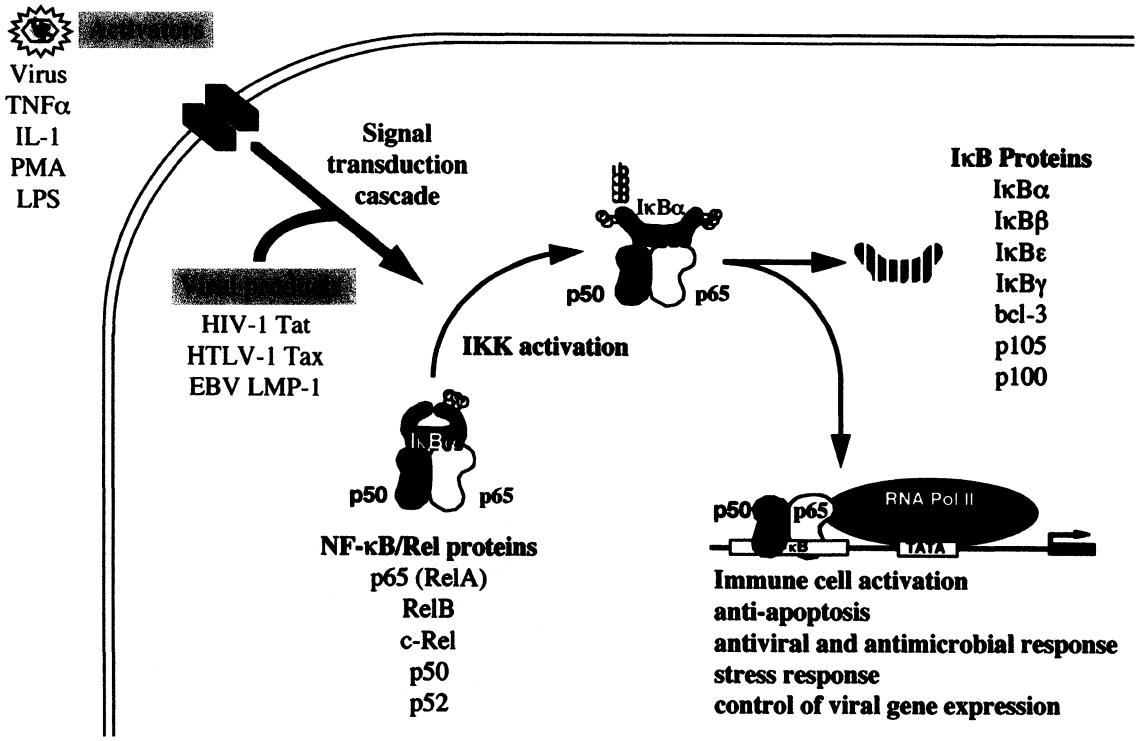

Figure 1.5: Illustration of the Rel/NF-κB pathway. In response to stimuli such as tumour-necrosis factor-α (TNF-α), CD40 ligand (CD40L), interleukin-1 (IL-1) or lipopolysaccharide (LPS), the IKKβ subunit is activated, and phosphorylates the IκB proteins (bound to the NF-κB heterodimers) at two conserved serines. This phosphorylation event triggers the ubiquitin-dependent degradation of IκB by the 26S proteasome, resulting in the nuclear translocation of RelA–p50 (or c-Rel–p50) heterodimers and transcriptional activation of target genes (Adapted from Hiscott *et al.,* 2001).

Steps involved in Rel/NF-κB activation

1. Exposure to a stimulus that activates NF-κB such as UV light.
2. Degradation of IκB or its inactivation by phosphorylation by means of protein kinases (McKenzie et al., 2000).
3. Dissociation of the complex between NF-κB family members and IκB inhibitor system.
4. Translocation of NF-κB proteins to the nucleus.
5. DNA binding of NF-κB proteins.
6. Transcriptional induction by NF-κB proteins.

Table 4: Steps involved in Rel/NF-κB activation (Shain *et al.,* 1998)

1.3.3 Role of NF-κB in apoptosis and cell survival.

The dual role of NF-κB in enhancing or inhibiting apoptosis and cell death has attracted much attention in regard to its role in carcinogenesis (Mercurio and Manning, 1999; Tickle, 1998; Sonenshein, 1997; Muller *et al.,* 2003; Bushdid *et al.,* 1998; Huang *et al.*, 2000; Romano *et al.,* 2000; Bukowski *et al.,* 1998; Bash *et al.,* 1999).

1.3.3.1 NF-κB involvement in apoptosis

The role of Rel/NF-κB proteins in apoptosis has been well studied (Hogerlinden *et al.,* 1999; Manna *et al.,* 2000). NF-κB, for instance, was found to be activated following TNF-α-induced apoptosis in several cell lines (Miyamoto *et al.,* 1994). Treatment of cell lines derived from acute B-cell leukemia and human thymocytes with etoposide was found to activate NF-κB and this activation occurred prior to the initiation of apoptosis (Beg and Baldwin, 1993). Further evidence supporting the involvement of NF-κB in apoptosis is the presence of NF-κB binding sites in the genes encoding *IL-1β converting enzyme protease, c-myc,* and *TNFα,* which are all involved in apoptosis and cell death (Collins *et al.,* 1995; Beg and Baldwin, 1993). Also, several studies showed that p65 is involved in apoptosis. This was based on

an original observation whereby inhibition of apoptosis was achieved by overexpression of a dominant-negative p65 protein (Higgins *et al.,* 1993).

1.3.3.2 Rel/NF-κB role in cell protection and survival.

The role of Rel/NF-κB proteins in cell survival is generally associated with their ability to upregulate the expression of myc (for review, see Foo and Nolan, 1999; Chen *et al.,* 1998). Myc is a protein that mediates the transcriptional activation of cyclin A and cyclin D3, which are cell cycle regulators. A decrease in the myc protein concentration in the cell has been associated with apoptosis. Another pathway that leads to high myc levels is through the stimulation of CD40, a member of TNF receptor family, which results in NF-κB activation (Madrid *et al.,* 1999; Furman *et al.,* 2000) and whose stimulation has been implicated in cell survival and protection (Madrid *et al.,* 1999).

The role of Rel/NF-κB as a factor in both cancerous and normal cell survival is well documented. Recent results, for instance, have shown NF-κB to be activated in the early malignant transformation of mammary cells of the breast (Kim *et al.,* 2000). Furthermore, NF-κB is constitutively active in pancreatic adenocarcinoma in humans (Wang *et al.,* 1999), in T-cell leukemia cells (Mori *et al.,* 1999), in human breast cancer (Cogswell *et al.,*

2000) and in head and neck squamous cell carcinoma cell lines (Ondrey *et al.,* 1999).

In non-cancer cells, NF-κB was reported to be essential for the growth and survival of sympathetic nerve cells independently of the *de novo* protein synthesis (Maggirwar *et al.,* 1998). Further evidence of severe liver degeneration was associated with lack of NF-κB activation (Rudolph *et al.,* 2000). This was based on the death of murine embryonic fibroblasts that lack detectable NF-κB DNA binding activity in response to TNF-α, LPS, IL-1 and do not show IκB kinase activity required for NF-κB activation (Rudolph *et al.,* 2000).

The anti-apoptotic activity of Rel/NF-κB can be regulated by other proteins. For instance, the X chromosome-linked inhibitor of apoptosis (XIAP) induces NF-κB activation by increasing the nuclear translocation of its p65 subunit (Hofer-Warbinek *et al.,* 2000; Stehlik *et al.,* 1998). In addition, CD95, which is known as Fas and possesses an apoptotic effect, was found to stimulate NF-κB degradation by caspases (Ravi *et al.,* 1998), but when an antibody against CD95 was used, caspases were inhibited and the inducibility of NF-κB was restored (Ravi *et al.,* 1998).

1.3.4 Xrel3

Xrel3 encodes an embryonic protein found to be related to the rel family of proteins. The *Xrel3* gene is present in the genome of the amphibian, Xenopus laevis and is expressed in and is essential for the normal development of the head of Xenopus laevis embryos (Lake *et al.,* 2001). *Xrel3* is also normally expressed in the otocysts and notochord of the embryonic larval stages (Lake *et al.,* 2001). Interestingly, Xrel3 overexpression has been implicated in the development of epidermal tumors in embryos (Yang *et al.,* 1998; Lake *et al.,* 2001), but little is known about how these tumors form, or whether they have similar properties to human tumors. Therefore, I was interested in investigating whether the Xrel3 protein had properties that could contribute to human cancer. By applying what is known about the role of Xrel3 in embryos to human cell lines, it may be possible to uncover new knowledge about the mechanism of Rel/NF-κB activity in general. I considered this to be a novel approach to the study of this important family of oncogenes.

In addition to its ability to cause embryonic tumor formation, the rationale for studying the effects of Xrel3 in human cervical cancer cells has basis in practicality. When a DNA vector encoding tagged-Xrel3 was

transiently transfected into HeLa cells, Xrel3 protein constitutively localized in the nuclei, suggesting its ability to be active constantly in mammalian cells (Green, 2003). In addition, HeLa cells do not normally express Rel/NF-κB, so the transfection of Xrel3 into these cells gave me the opportunity to study the activity of an interesting Rel/NF-κB protein in a negative background. Therefore, even though Xrel3 is not a mammalian gene, its homology to the mammalian Rel/NF-κB family indicates that it may serve as a good model for gene regulation by this family enabling us to understand the mechanism of action of the Rel/NF-κB family of transcriptional regulators in cancer cells.

1.4 Cancer Chemotherapy

1.4.1 Introduction

Many chemical agents are used in the treatment of cancer. Some can be used alone in single therapy and others have to be combined or added to other regimens for an effective outcome. The five groups of single chemotherapeutic agents are: alkylating agents, antimetabolites, plant derivatives, antitumor antibiotics and the miscellaneous group which

contains the platinums, procarbazine, mitotane and gallium nitrate (British Medical Association, 2002).

1.4.2 Platinums

The platinum-containing compounds are carboplatin, cisplatin and oxaliplatin. This group of chemotherapeutic drugs is very effective in monotherapy regimens (Gadducci *et al.,* 1997). They are the most active agents in the treatment of ovarian and cervical cancers. However, they are associated with three major drawbacks (Reedijk, 2003):

1. Severe toxicity in the form of nephrotoxicity, ototoxicity, myelosuppression and peripheral neuropathy.
2. Narrow range of tumors upon which they are effective.
3. The development of resistance after a short period of treatment.

New approaches are now designed in an attempt to expand the mechanism of action of platinums. This is done by developing a new generation of platinum-containing compounds that exhibited a broader spectrum of activity on different tumors, lower toxicity potential as well as delayed resistance to treatment (Fuertes *et al.,* 2002; for review, see Jakupec, 2003).

1.4.3 Cisplatin

Cis DiamminedichloroplatinII (cisplatin) is one of the platinum-containing anti-cancer agents. It can be recognized from its chemical name that the cis form is the active form of the drug. The trans form was found to possess no biologic activity (Reedijk, 2003). The mechanism of action of cisplatin is similar to the alkylating agents, but it is not identical. Cisplatin works by promoting DNA cross-linking and chelation (United States Pharmacopeia, 2003). Recent clinical studies have shown that improved cytotoxicity of cisplatin can be attained by increasing the exposure time of the tumor to the drug (Markman, 2003).

1.4.4 Rel/NF-κB and Chemoresistance

Many researches have attempted to investigate the role that NF-κB family might have in chemotherapeutic resistance. Activation of the Rel/NF-κB was found to be associated with chemotherapeutic resistance by suppressing the apoptotic potential of the chemotherapeutic drug. Recent data demonstrate that the protection from apoptosis induced in response to carbonyloxycamptothecin (CPT-11) treatment is effectively inhibited by the transient inhibition of NF-κB in a variety of human colon cancer cell lines (Cusack *et al.*, 2000). This might be due to the cell survival effects

associated with the upregulation of Rel/NF-κB family as previously mentioned. In addition, genetic manipulation aimed at inhibiting Rel/NF-κB, was found to cause sensitization of different tumor cells, like lung cancer cells, to the effect of chemotherapeutic drugs (Jones *et al.,* 2000). This makes the Rel/NF-κB family an attractive set of proteins to study in chemoresistant tumors.

1.5 Purpose and hypothesis of this study

Several attempts are being made to find solutions for the resistance encountered by the usage of chemotherapeutic drugs. An investigation of the upregulation of NF-κB might be a promising field of study in this regard since Rel/NF-κB activation has been associated with chemoresistance. Cisplatin can be used as a monotherapy without any adjuvant chemotherapeutic drugs. Cisplatin is also used in the treatment of gynecologic cancers like ovarian cancers (Gudducci *et al.,* 1997; Reedijk, 2003). Previous studies have shown that the apoptotic effect induced by chemotherapy in cervical cancer involves p53 and the HPV-E6 oncogenes and might be enhanced or attenuated depending on the platinum carrier ligand (Koivusalo *et al.,* 2002).

The purpose of this study was to investigate the effect of *Xrel3* overexpression on the growth of HeLa cells with and without chemotherapeutic treatment. The proposed hypothesis is that Rel/NF-κB is a cause of chemotherapeutic resistance encountered in cancer cells.

My objectives were:

1. To create an inducible *Xrel3* model system to study its role in cancer chemoresistance. The Tet-On system was used to induce the expression of *Xrel3* inserted downstream from the Tet promoter, by the addition of doxycycline in HeLa cells.

2. To determine the effect of induced *Xrel3* expression on the growth of HeLa cervical cancer cells.

3. To determine the effect of induced *Xrel3* expression on the growth of HeLa cells treated with cisplatin.

CHAPTER 2: MATERIALS AND METHODS

2.1 Materials

Tissue culture supplies including 6-wells plates, 100 mm tissue culture plates, 1.5 ml and 2 ml eppendorf tubes were all purchased from Fisher Scientific Co. Dulbecco's modified Eagle medium (DMEM), fetal calf serum; trypsin-ethylenediamine tetraacetic acid (EDTA), genaticin and hygromicin were all purchased from Invitrogen. HeLa cells were purchased from ATCC. Fisher Scientific Co supplied the eppendorf microcentrifuge test tubes for PCR.

RNeasy Mini kit for isolation of total RNA from animal cells, DNeasy kit for DNA extraction from cultured animal cells, Effectene Transfection kit, QIAprep spin Miniprep kit for plasmid extraction from bacteria and Quiaquick Gel Extraction kit for DNA extraction from agarose gels were purchased from Qiagen.

Taq DNA polymerase, dNTP and 10 x Buffer, which were used in PCR, were purchased from Qiagen. The ECL system and Hybond nitrocellulose membrane (Amersham) were used for western blotting. The 1 kb DNA ladder marker, the low melting point agarose, agarose and

acrylamide were purchased from Invitrogen. The Carnation skim milk powder was used for western blotting as a blocking agent. Cisplatin was purchased from Sigma Chemical Co. and X-ray film was purchased from Kodak.

Mouse anti-BAG-1 monoclonal antibody (mAb) was established in our laboratory (Yang et al, 1998). Mouse mAbs for Bcl-X_L, Bcl-2, p21, p53, caspase-3, Cruz marker and secondary anti-mouse antibodies were purchased from Santa Cruz Biotechnology. Mouse mAbs for BAX, PCNA, MDM-2, HPV 16/18-E6 were purchased from Oncogene Co., while mouse mAbs for PARP and caspase-8 were purchased from PharMingen. Sigma Chemical Co. supplied anti-β actin; however Amersham Co. supplied the Rainbow protein marker.

2.2 Methods

2.2.1 Cell culture

All HeLa cells were maintained at 37°C in the presence of 5% CO_2 in a humidified incubator. When the cells reached 80% confluency, the medium was aspirated, the cells were washed with warmed PBS and the washings were aspirated. The cells then were incubated for 15 minutes with 2 ml trypsin-EDTA to detach the cells from the culture dish followed by the

addition of 8 ml DMEM to avoid further cell lysis and pipetting the mixture several times to ensure even distribution of the cells. The cells were passed to fresh culture dishes at different concentrations e.g 1:5, 1:10 and 1:20 according to the purpose of the experiment. HeLa-Tet On cells were recovered from frozen stock and maintained in DMEM containing 10% FCS and 0.03% genaticin until transfection.

After transfection with pTRE2 and pTRE2-Xrel3, cells were maintained in a selective medium containing DMEM + 10% FCS + 0.03% genaticin + 0.02% hygromicin.

The cell numbers were counted with a hemocytometer. The above steps were done during regular passage of the cells where the cells were usually passed at 1:20, 1:10 or 1:5 into fresh plates. Also before growth assays, the above steps were repeated where 2 x 10^4 cells were seeded in each well of the 6 wells plate and the cell numbers were counted with a hemocytometer daily for 6 days.

2.2.2 Construction of the pTRE2-Xrel3 plasmid

2.2.2.1 Polymerase chain reaction (PCR)

PCR was performed to amplify the Xrel3 gene. The protocol provided by Qiagen was followed. The Gene Amp PCR system 2400 was

programmed to run for 30 cycles as follows: 94°C for 3 minutes, 94°C for 1 minute, 61°C for 1 minute, 72°C for 10 minutes and 4°C for 1 hour.

2.2.2.2 DNA extraction and purification from agarose gel

1% agarose gel was prepared in 30 ml 5 x TBE buffer. The electrophoresis apparatus was run for 45 minutes.

The Xrel3 band, which corresponds to 1.6 kb, was clearly identified under U.V light by the Eagle Eye II still video system (Stragagene). This DNA fragment was excised under UV light and then the DNA was extracted by means of the QIAquick gel extraction kit using a vaccum manifold according to the manufacturer's instructions.

2.2.2.3 Restriction enzyme cleavage of pTRE2 and pTRE2-Xrel3 plasmids

The map of the pTRE2 vector (Figure 2.1) shows the restriction sites *BamH I* and *Xba I* that are targeted by the *BamH I* and *Xba I* restriction enzymes.

2.2.2.4 Ligation

The protocol supplied by Invitrogen was followed according to the manufacturer's instructions.

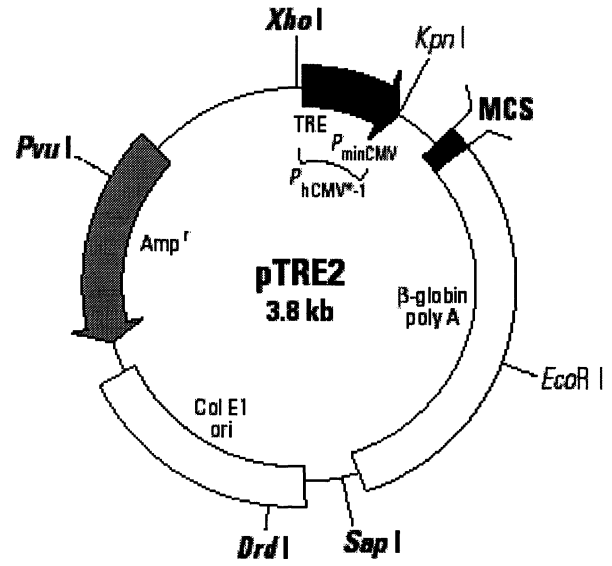

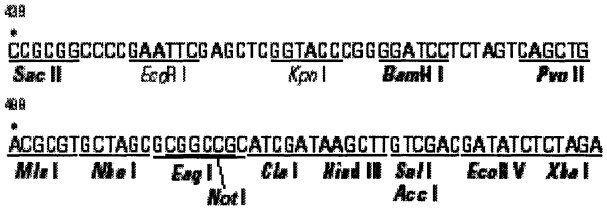

Figure 2.1: The map of the pTRE2 vector showing the restriction sites (*BamHI and XbaI*) where Xrel3 was integrated (Adapted from Clontech, 2003).

2.2.2.5 Transformation of E. coli with pTRE2-Xrel3 plasmid.

The protocol supplied by Clontech lab, Inc was followed with specific modifications. In brief, thawed E.coli competent cells were added to 10 ng of the ligated pTRE2-Xrel3 plasmid solution. This was followed by incubation on ice for 30 minutes, heat shocking in a 42°C water bath for 60 seconds and chilling on ice for 2 minutes. Then, 500 µl LB broth were added followed by 1-hour incubation at 37°C on a shaker. The solution was then spread on ampicillin containing LB agar plates and incubated at 37°C overnight.

2.2.2.6 Plasmid purification using QIAprep Spin Miniprep kit.

The single colonies of bacteria growing on the ampicillin plates were allowed to propagate by incubating each single colony in 50 ml LB broth at 37°C overnight. The protocol provided by Qiagen kit was followed according to the manufacturer's instructions.

2.2.2.7 Verifying the presence of Xrel3

To confirm the presence of Xrel3 in the extracted DNA from the previous step, PCR was used, as previously described. The amplicon was then sequenced commercially.

2.2.3 Establishing stable transfection of HeLa cells with Xrel3

HeLa Tet-On cells, which had been previously established in our lab, were recovered in DMEM + 10% FCS in the presence of 0.03% genaticin. HeLa Tet-On cells were transfected with pTRE2-Xrel3 plasmid and pTRE2 vector, which served as a control. The Effectene Transfection kit protocol was followed according to the manufacturer's instructions. The controls used were the pTRE2 vector and the non-transfected HeLa cells.

After 48 hours, DMEM + 10% FCS + 0.03% geneticin + 0.02% hygromicin was added to each petri dish to serve as a selective medium. The hygromycin resistance gene inserted in the control pTRE2 vector and pTRE2-Xrel3 plasmid offered selective advantage to those cells harboring these plasmids. Conversely, HeLa Tet-On cells not containing pTRE2 or pTRE2-Xrel3 plasmid were killed after 24 hours by the effect of hygromicin selective medium.

2.2.4 Selection of the stably transfected clones.

After transfection, the colonies containing pTRE2 vector and pTRE2-Xrel3 plasmid were selected using the micro-glass cylinder method. After reaching 80% confluency, cells from each separate colony were transferred

to a separate well of 24-wells plates then 6-wells plates, and after incubation to a 100 mm petri dish.

2.2.5 Verifying the presence of pTRE2-Xrel3 and pTRE2 in the selected clones.

2.2.5.1 DNA extraction from cultured cells

The protocol provided by the DNeasy kit purchased from Qiagen was followed.

2.2.5.2 Polymerase chain reaction

To test for the presence of Xrel3, amplification for both clones selected (clones containing pTRE2 vector and those containing pTRE2-Xrel3 plasmid) was performed as previously described. This was followed by electrophoresis on a 1% agarose gel and identifying the Xrel3 band at 1.6 kb in the clones containing the pTRE2-Xrel3 plasmid and its absence in the clones containing the pTRE2 vector.

2.2.6 Verification of Xrel3 transcription

2.2.6.1 RNA extraction

The protocol used the RNeasy kit supplied by Qiagen according to the manufacturer's instructions. Then elution of the RNA was performed by

centrifugation with 50 µl RNase-free water. The concentration of RNA in each sample was determined spectrophotometrically.

2.2.6.2 Confirming the integrity of the extracted RNAs.

RNase-free environment was strictly adhered to throughout the experiments dealing with RNA. The RNA samples (1 µg of each sample) extracted previously were mixed with 2 µl of RNA loading buffer and loaded into the wells of a 1% agarose gel mounted into an electrophoresis apparatus. The gel was prepared as described previously, but using specific RNase-free agarose and sterile water.

2.2.6.3 Northern blotting

To prepare the sample, 20 µg of each RNA sample were heated for 15 minutes at 65°C for denaturing and then placed on ice immediately. The RNA samples were mixed with 5 µl RNA loading buffer.

Gels were prepared using, 850 mls of running buffer 10 x MOPS. Each formaldehyde gel was prepared by boiling 1.3 g agarose gel in 120 mls sterile water accounting for the water that will be evaporated after which 30 mls of 37% formaldehyde were added. The first well used as a marker was separated and stained with ethidium bromide. Transferring the RNA onto a

membrane was performed overnight. This was followed by fixing the RNA onto the membrane by baking the membrane in an oven at 80°C for 2 hours.

To label the probe, Xrel3 DNA was prepared by resolving by electrophoresis the Xrel3 amplified plasmid and then extracting the Xrel3 DNA band using the QIAquick gel extraction kit described previously. 30 ng of the probe were used and labeled according to the manufacturer's instructions.

For prehybridization, 8 ml of pre-warmed 65°C prehybridization solution was added to the membrane in the hybridization bottle with the RNA side facing the solution. The bottle was rotated for 30 minutes in a hybridization oven adjusted to 65°C.

For hybridization, 1.6 x 10^6 cpm/ml of hybridization buffer is required to ensure adequate probe labeling. The amount of the probe required for hybridization was boiled for 10 minutes, chilled on ice immediately for 5 minutes then poured into 45 ml orange-capped tubes in the 65°C water bath. The rotating hybridization bottle after 30 minutes was emptied from the prehybridization solution and filled with pre-warmed 65°C prehybridization solution. The hybridization bottle was rotated in the hybridization oven for 2 hours at 65°C. The blot was washed to high stringency using 492.5 ml sterile

water, 2.5 ml 20 x SSC and 5 ml of 10% SDS for several times at 65°C and exposed to X-ray film at -70°C overnight.

2.2.7 Growth rate and saturation density assay.

Transfected HeLa Tet-On cells with either the pTRE2 vector or the pTRE2-Xrel3 plasmid were grown exponentially. 2 x 10^4 cells were seeded per well of a 6-well plate. The cell numbers were counted daily for 6 days using a hemocytometer. This was done for the pTRE2-Xrel3-transfected cells with and without the presence of doxycyline, which induces Xrel3 expression. Also it was done concomitantly for the pTRE2-transfected HeLa cells with and without doxycycline to serve as a control.

2.2.8 Drug treatment

2 x 10^4 cells were seeded in each well of a 6-wells plate. The following day, 1 μg/ml doxycycline was added to one and not to another plate seeded with pTRE2-Xrel3-transfected HeLa cells and the same was done for pTRE2. Transfected HeLa cells with either pTRE2 or pTRE2-Xrel3 were treated with various concentrations of cisplatin (0.5 μM, 1 μM and 2 μM) from 4 μM cisplatin stock solution in sterile water. Cell numbers were taken after 2 hours of adding the cisplatin. The addition of fresh cisplatin was repeated daily for 6 days. The average of four independent

experiments was plotted. However, the same experiment was repeated 2 more times with the addition of fresh cisplatin every other day.

2.2.9 Cell viability assay

Cell viability was assessed for both pTRE2-Xrel3 transfected cells and pTRE2 control cells with, without doxycycline and with and without cisplatin by trypan blue dye exclusion. Approximately 2 x 10^4 cells/well were seeded in 6-wells plates. After 24 hours, the cells were trypsinized with 500 µl trypsin then 500 µl of 4% trypan blue was added and mixed gently. Then under the light microscope, the viable cells appeared clear and transparent because they were unstained by the dye, however dead cells appeared blue. The number of viable cells was counted daily for 6 days.

2.2.10 Western blotting

Proteins were extracted from 90% confluent cells transfected with both pTRE2-Xrel3 and pTRE2 control cells in the presence and absence of doxycycline, with and without cisplatin. Briefly, the cells were washed with cold PBS to remove the medium, scraped off the petri dish using 300 µl lysis buffer, and transferred to eppendorf tubes and left on ice for 30 minutes. This was followed by microcentrifugation at 4°C for 10 minutes. The supernatant was transferred to a clean eppendorf tube and stored at -70°C.

The concentration was determined using the DC Lowry protein assay kit (Bio-Rad) as advised by the manufacturer. Protein extracts, usually 30 μg, were mixed with equal volumes of 2 x SDS-polyacrylamide gel electrophoresis (PAGE) gel loading buffer (200 mM Tris-HCl (pH 6.8), 4% SDS, 0.2% bromophenol blue, 20% glycerol), boiled for 3 minutes, chilled on ice and resolved in an SDS-PAGE gel. Protein samples were run on a discontinuous 12% polyacrylamide gel, pH 8.8 according to Yang's protocol. Gels were equilibrated in Towbin transfer buffer (25 mM Tris, 20% methanol, 192 mM glycine) for 15 minutes. The proteins were transferred to a Hybond nitrocellulose membrane at 20 V for 45 minutes using a Trans-Blot SD transfer apparatus (Bio-Rad). After transferring, the membranes were blocked in 5% skim milk powder in TBST prepared by mixing 20 mM Tris/HCl (pH 7.6), 137 mM NaCl, 0.1% Tween 20 for 1 hour on a shaker at room temperature. The membranes were then incubated with the primary antibody, at the concentration recommended by the manufacturer, in 5% skim milk powder in TBST overnight at 4°C on a rotator, followed by washing the membrane thrice with TBST for 10 minutes, incubating with the secondary antibody for 1 hour at room temperature, washing thrice with TBST for 10 minutes, detecting the signals

using the enhanced chemilumiscence (ECL) system and exposing the ECL film as advised by the manufacturer. The signals were stripped off the membrane by shaking the membrane with the stripping buffer (100 mM 2-mercaptoethanol, 2% SDS, 62.5 mM Tris/HCl, pH 6.7) at 50°C for 30 minutes, followed by rinsing the membranes thrice with TBST for 10 minutes each time, blocking, and reprobing with β-actin mAb and following the previously explained steps. The density of the bands was quantified using the Eagle Eye II Still Video system (Stratagene).

2.2.11 Statistical Analysis

The statistical analysis was performed using Student's t-test. Differences of $p<0.05$ were considered to be significant (See Appendix 1). Also, the graphs and histograms were generated using the Sigma plot program and Excel of Microsoft Office.

CHAPTER 3 RESULTS

3.1 Xrel3 expression in HeLa cells transfected with pTRE2-Xrel3 plasmid

The *Xrel3* coding region (bases 1 to 2251) was ligated into pTRE2 and stably transfected into HeLa-tet On cells. I selected 15 colonies, which were transfected with the pTRE2-Xrel3 plasmid and 4 colonies transfected with pTRE2 vector alone as a control. DNA from cells of all the 19 colonies was extracted. I then amplified the transgene in the entire DNA extract by PCR to determine if the pTRE2-Xrel3 plasmid was successfully integrated into the genome. The PCR products were first cleaved with *BamHI* and *XbaI* restriction enzymes and then loaded into the wells of a freshly prepared 1% agarose gel and resolved by electrophoresis.

The results showed that the transgene was present in the 15 colonies selected after transfection with pTRE2-Xrel3 plasmid and this was confirmed by the presence of the band at 1.6 kb, which corresponds to the size of the Xrel3 gene, however no Xrel3 gene was detected in the 4 colonies transfected with pTRE2 vector (Figures 3.1 A and B). In DNA from the

colonies transfected with the pTRE2 vector, a band was clearly seen at 3.8 kb, which corresponds to the size of the transfected pTRE2 vector.

Figure 3.1: A) Xrel3 expression in pTRE2-Xrel3 transfected HeLa cells. The *upper panel* shows the presence of Xrel3 band at 1.6 kb in the selected colonies designated by numbers from 1 to 10 as indicated on the top of the figure. The *lower panel* shows the presence of Xrel3 in the remaining colonies designated by numbers 11, 12, 13, 14 and 15 as indicated on the top of the figure.

B) Absence of Xrel3 in the pTRE2 transfected HeLa cells. The *upper panel* shows the different samples loaded as indicated on top of the figure. Starting from the left hand side, the sample wells were loaded with the original sequenced plasmid, colony 10 and 11 transfected with pTRE2-Xrel3 plasmid and colonies 1, 2 and 3 transfected with pTRE2 vector. The *lower panel* shows the rest of the samples loaded as indicated on top of the figure. Starting from the left to the right, the sample wells were loaded with the original sequenced plasmid, colony 1 and 2 transfected with pTRE2-Xrel3 and colonies 2, 3 and 4 transfected with pTRE2 vector.

A)

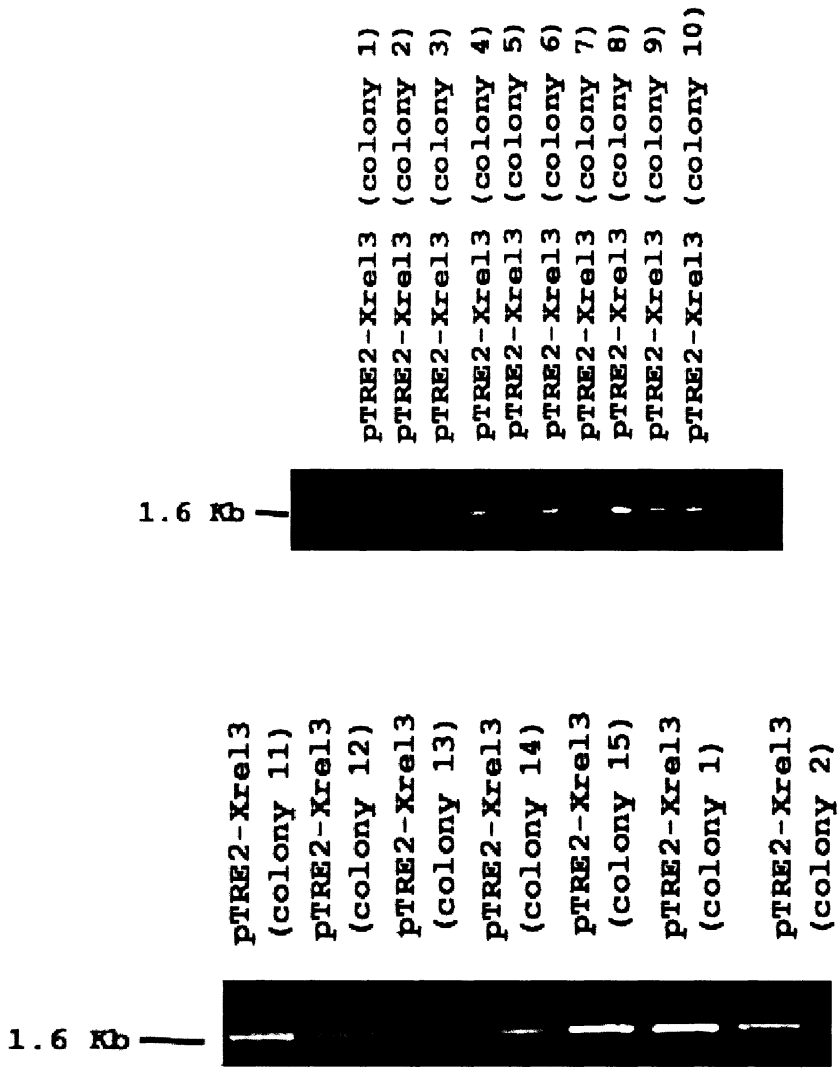
pTRE2-Krel3 (colony 1)
pTRE2-Krel3 (colony 2)
pTRE2-Krel3 (colony 3)
pTRE2-Krel3 (colony 4)
pTRE2-Krel3 (colony 5)
pTRE2-Krel3 (colony 6)
pTRE2-Krel3 (colony 7)
pTRE2-Krel3 (colony 8)
pTRE2-Krel3 (colony 9)
pTRE2-Krel3 (colony 10)
1.6 Kb
pTRE2-Krel3 (colony 11)
pTRE2-Krel3 (colony 12)
pTRE2-Krel3 (colony 13)
pTRE2-Krel3 (colony 14)
pTRE2-Krel3 (colony 15)
pTRE2-Krel3 (colony 1)
pTRE2-Krel3 (colony 2)
1.6 Kb

B)

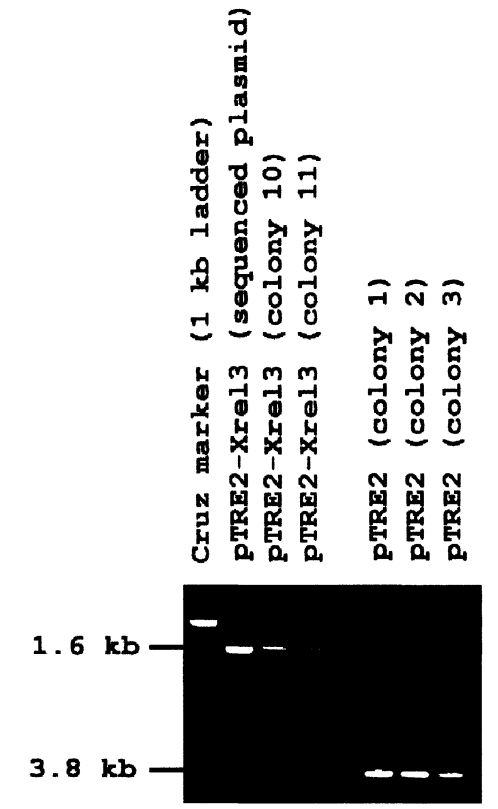
Cruz marker (1 kb ladder)
pTRE2-Xrel3 (sequenced plasmid)
pTRE2-Xrel3 (colony 10)
pTRE2-Xrel3 (colony 11)
pTRE2 (colony 1)
pTRE2 (colony 2)
pTRE2 (colony 3)
1.6 kb
3.8 kb

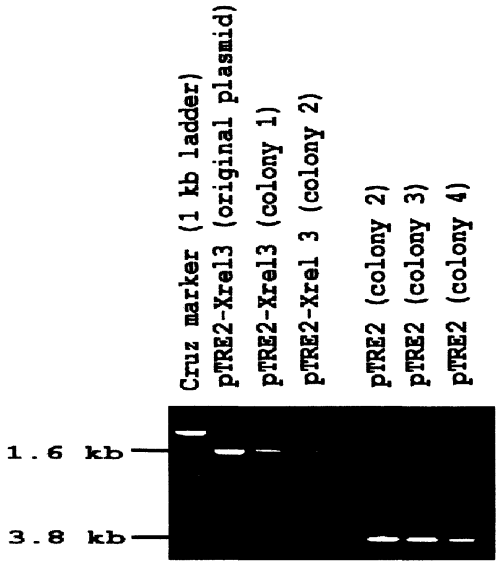
Cruz marker (1 kb ladder)
pTRE2-Xrel3 (original plasmid)
pTRE2-Xrel3 (colony 1)
pTRE2-Xrel 3 (colony 2)
pTRE2 (colony 2)
pTRE2 (colony 3)
pTRE2 (colony 4)
1.6 kb
3.8 kb

3.2 **Verification of the size of Xrel3 gene in the transfected HeLa cells**

To further confirm that the size of the Xrel3 transgene was not altered, I amplified the *Xrel3* gene sequence alone directly from each of the colonies I obtained. The results showed that the size of a band, which appeared upon Xrel3 amplification from the transfected HeLa cells, coincided with Xrel3 amplified from the original plasmid (Figure 3.2). Thus, the size of the inserted *Xrel3* sequence was similar to that of the original plasmid.

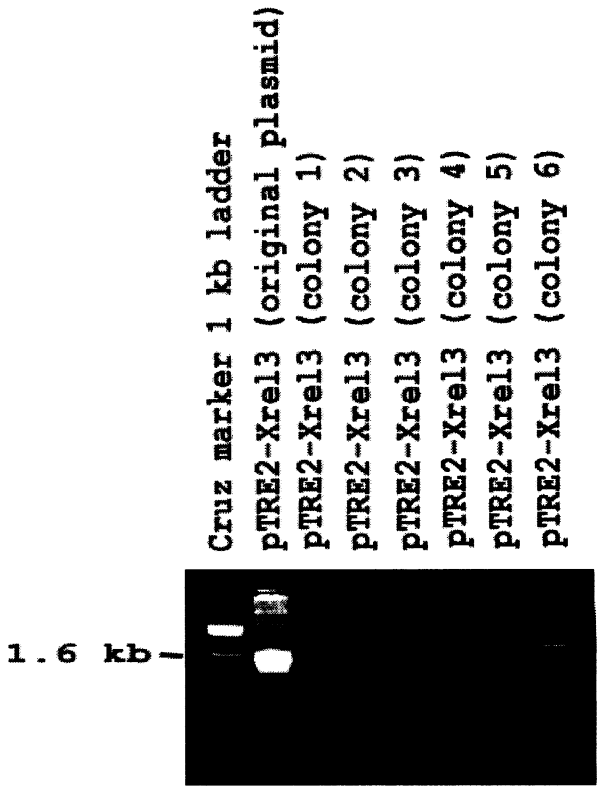

Figure 3.2: Verification of the size of Xrel3 gene inserted in the pTRE2-Xrel3 plasmid following transfection in HeLa cells. Amplification of Xrel3 in the extracted DNA was performed using PCR as described in the Materials and Methods. A clear band of the size of 1.6 kb, coinciding with the size of the Xrel3 gene inserted and amplified, was seen in all the samples. The Xrel3 band, which appeared upon amplification of the gene in the transfected cells, is of the same size as the Xrel3 band, which appeared upon amplification of the gene in the original sequenced plasmid.

3.3 Induction of Xrel3 expression in transfected HeLa cells by doxycycline.

In order to determine whether Xrel3 expression could be induced in the HeLa-Tet On cells transfected with pTRE2-Xrel3, I performed Northern analyses of RNA extracted from both pTRE2-Xrel3 transfected HeLa cells and pTRE2 transfected HeLa cells in the presence or absence of doxycycline. The integrity of the extracted RNAs was verified by the presence of the 28S and 18S bands of comparable intensities (Figure 3.3).

Figure 3.3: Verification of the integrity of extracted RNAs for Northern blotting.

RNA samples show 2 equal bands corresponding to 18S and 28S ribosomal subunits. The numbers represent the number of colonies from 1 to 15 transfected with pTRE2-Xrel3. The letters represent the 4 control colonies transfected with pTRE2 vector.

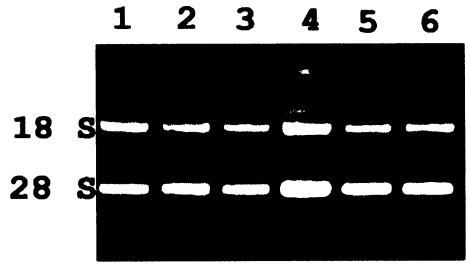
1 2 3 4 5 6
18 S
28 S

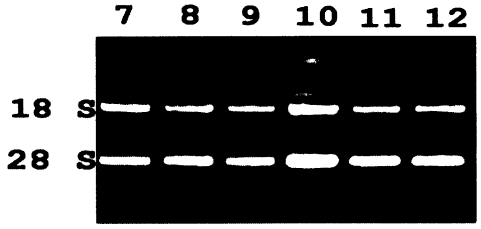
7 8 9 10 11 12
18 S
28 S

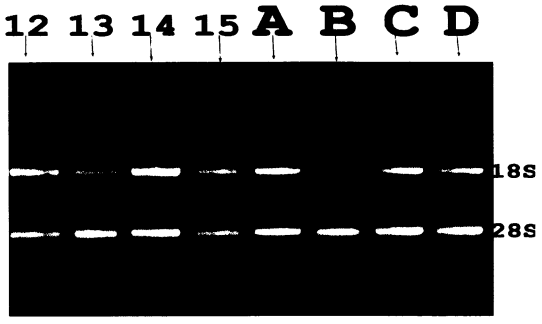
12 13 14 15 A B C D
18S
28S

3.4 Northern Analyses

Based on the results of the Northern blots, I selected the best clones (those that showed a clear signal upon induction and no signal without induction) to work with. The results were as follows:

1. Transcription of *Xrel3* was evident in all of the clones with pTRE2-Xrel3, only after induction by doxycycline (1 μg/ml) (Figure 3.4).

2. The clones with the pTRE2 vector didn't show any transcription of *Xrel3* with and without induction by doxycycline (Figures 3.4 and 3.5). This was determined by the absence of any band at the expected size of *Xrel3 mRNA.*

3. The total cellular RNA extracted from colony number 15, which was transfected with pTRE2-Xrel3 plasmid, failed to show any transcription for *Xrel3* gene after induction by doxycycline (Figure 3.4). This result indicates that colony number 15 does not express *Xrel3.*

4. Colonies numbers 1, 5, 7, 8, 9 and 11 showed leaky transcription of *Xrel3* in the absence of doxycycline, which means that *Xrel3* transgene in these cases might be inserted in a location on the heterochromatin that is of high transcriptional activity in the absence of doxycycline (Figure 3.5).

5. Colonies number 2, 4, 6 and 10 showed non-specific signal (Figure 3.5). This is manifested by the appearance of a band in addition to the one

corresponding to the *Xrel3 mRNA* (colonies 2, 4 and 10) and sometimes the appearance of only one band, but of different size (colony 6).

6. However, colonies number 3, 12, 13, and 14 showed no signal at all without induction and a clear signal after induction by doxycycline. These 4 clones showed different levels of Xrel3 activation (3 >13 >12 >14) and were selected for further study (Figure 3.6).

Figure 3.4: Northern blot analysis of total cellular RNA extracted from doxycycline-treated pTRE2-Xrel3 colonies designated by the numbers 1 to 15 and control pTRE2 colonies given the numbers 1 and 2.

The *upper panel* shows the transcription of Xrel3 upon induction by doxycycline in the pTRE2-Xrel3 transfected colonies designated by the numbers 1 to 7. The first 2 wells were loaded with induced pTRE2 vector, which served as a control.

The *lower panel* shows the transcription of Xrel3 upon induction by doxycycline in the pTRE2-Xrel3 transfected colonies designated by numbers from 8 to 14, but not colony 15 (see text). The first well was loaded with an induced pTRE2 vector to serve as a control. The blots were reprobed with actin to monitor loading of RNA samples.

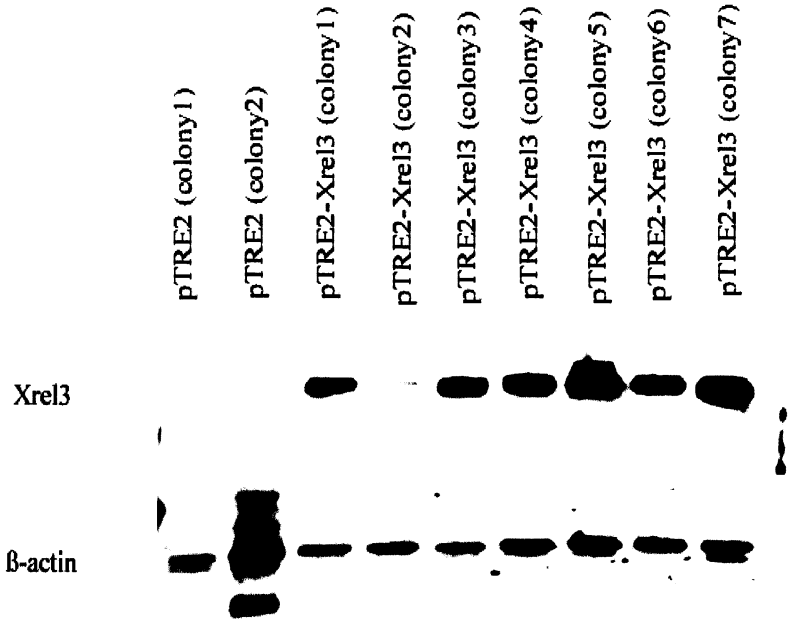
pTRE2 (colony1)
pTRE2 (colony2)
pTRE2-Xrel3 (colony1)
pTRE2-Xrel3 (colony2)
pTRE2-Xrel3 (colony3)
pTRE2-Xrel3 (colony4)
pTRE2-Xrel3 (colony5)
pTRE2-Xrel3 (colony6)
pTRE2-Xrel3 (colony7)
Xrel3
ß-actin

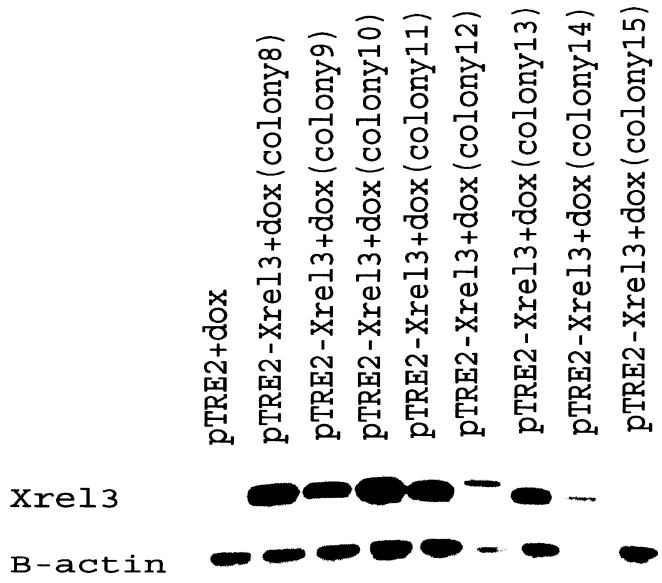
pTRE2+dox
pTRE2-Xrel3+dox(colony8)
pTRE2-Xrel3+dox(colony9)
pTRE2-Xrel3+dox(colony10)
pTRE2-Xrel3+dox(colony11)
pTRE2-Xrel3+dox(colony12)
pTRE2-Xrel3+dox(colony13)
pTRE2-Xrel3+dox(colony14)
pTRE2-Xrel3+dox(colony15)
Xrel3
B-actin

Figure 3.5: Northern blot analysis of total cellular RNA extracted from the non-doxycycline treated pTRE2-Xrel3 transfected colonies designated by the numbers 1 to 14. Both blots were reprobed with GAPDH, a housekeeping gene, which serves as a normalization control. The X-ray films were exposed for 18 hours at -70°C.

The *upper panel* shows Northern blot analysis of the colonies designated by numbers 1 to 6.

A) The effect of +/- doxycycline for colony 1 and 2 was examined.

B) Leaky Xrel3 transcription was observed for colony 1 and 5 in the absence of doxycycline, while an unknown band appeared for colony 2.

C) Colonies 3 and 4 showed no signals without induction, while colony 6 showed a non-specific signal.

D) This was compared to the pTRE2 vector, which showed no signals with or without doxycycline.

The *lower panel* shows the Northern blot analysis of the remaining colonies designated by the numbers 8 to 14.

A) Colonies 7 and 8 showed leakage Xrel3 transcription without doxycycline.

B) Colonies 9, 10 and 11 showed faint signals at the same size of Xrel3.

C) However, colonies 12, 13 and 14 showed no signals at all without doxycycline.

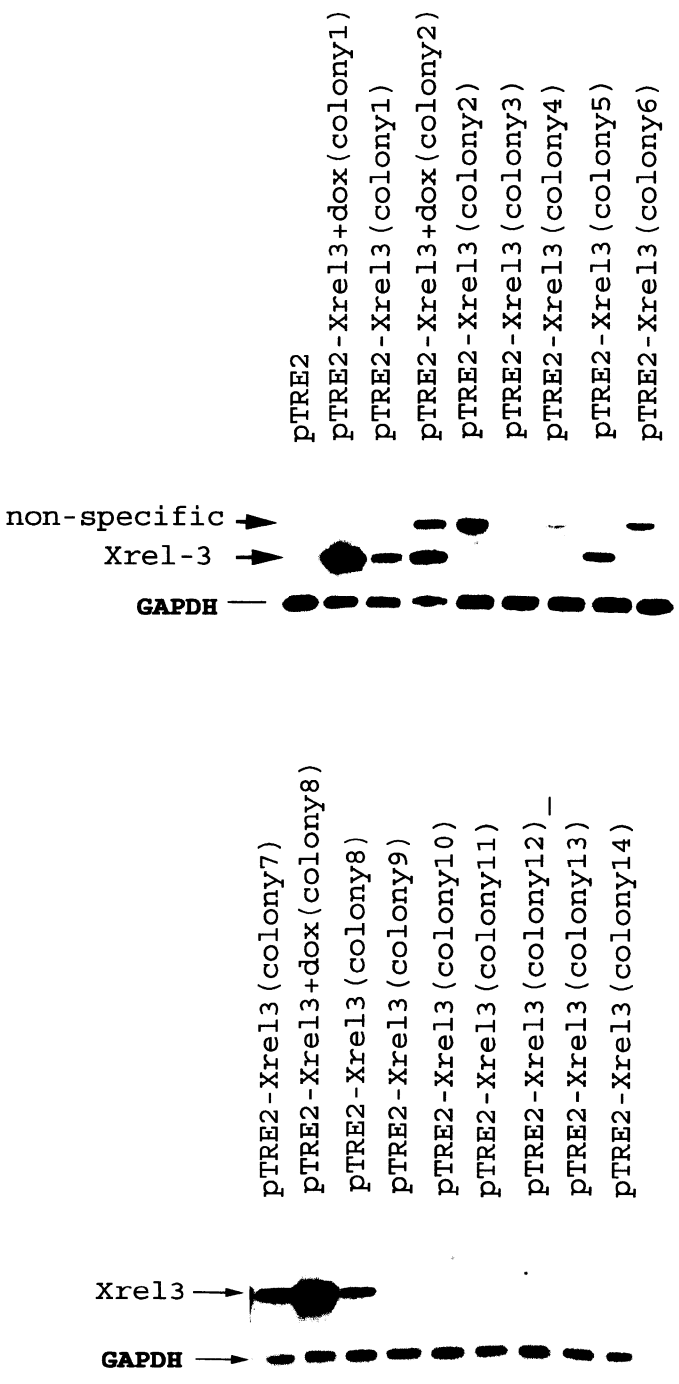
pTRE2
pTRE2-Xrel3+dox(colony1)
pTRE2-Xrel3(colony1)
pTRE2-Xrel3+dox(colony2)
pTRE2-Xrel3(colony2)
pTRE2-Xrel3(colony3)
pTRE2-Xrel3(colony4)
pTRE2-Xrel3(colony5)
pTRE2-Xrel3(colony6)
non-specific
Xrel-3
GAPDH
pTRE2-Xrel3(colony7)
pTRE2-Xrel3+dox(colony8)
pTRE2-Xrel3(colony8)
pTRE2-Xrel3(colony9)
pTRE2-Xrel3(colony10)
pTRE2-Xrel3(colony11)
pTRE2-Xrel3(colony12)
pTRE2-Xrel3(colony13)
pTRE2-Xrel3(colony14)
Xrel3
GAPDH

Figure 3.6: Confirmation of Xrel3 inducible expression in selected clones.

The *upper panel* shows Northern blot analysis of colonies 3,12,13 and 14, which were selected because they showed no signal at all without doxycycline and showed signals of varying intensity with doxycycline. The *lower panel* shows the corresponding densitometry analysis of the results.

Based on the optical density of the individual signals after normalization with GAPDH, clone 3 was designated the highest expressing clone, clone 14 was designated intermediate expressing clone and clone 12 was designated the lowest expressing clone. Xrel3 transcription was quantified by measuring the optical density of the bands after 18 hours exposure. The numbers from 1 to 9 underneath the columns in the lower panel designates the number of columns.

Optical density (% of controls)
0
1
2
pTRE2 + dox
pTRE2-Xrel3 (colony3)
pTRE2-Xrel3 + dox (colony3)
pTRE2-Xrel3 (colony12)
pTRE2-Xrel3 + dox (colony12)
pTRE2-Xrel3 (colony13)
pTRE2-Xrel3 + dox (colony13)
pTRE2-Xrel3 (colony14)
pTRE2-Xrel3 + dox (colony14)
2
4
6
8
10

Xrel3
GAPDH
pTRE2+dox
pTRE2-Xrel3(colony3)
pTRE2-Xrel3+dox(colony3)
pTRE2-Xrel3(colony12)
pTRE2-Xrel3+dox(colony12)
pTRE2-Xrel3(colony13)
pTRE2-Xrel3+dox(colony13)
pTRE2-Xrel3(colony14)
pTRE2-Xrel3+dox(colony14)

3.5 Growth Assay

Approximately 4 x 10^4 cells of each of the highest (clone 3), intermediate (clone 14) and lowest (clone 12) Xrel3 expressing clones were seeded per well in a 6-wells plate. Only one of the 2 plates was treated with doxycycline (1 μg/ml). This was done concomitantly for both the pTRE2-Xrel3 transfected cells and the control cells transfected with just the empty vector. Results showed that the expression of Xrel3 caused a delay in the normal growth of cells. This delay in growth started to appear on the third day of the experiment in all the clones examined (highest, intermediate and lowest-level expressing clone). This effect was absent in the non-induced pTRE2-Xrel3 clones as well as in the control cells. However, clone 14 showed the greatest cellular growth suppression response to Xrel3 induction and was focused on in the future experiments (Figure 3.7). This clone 14 was renamed pTRE2-Xrel3 (Int.).

Figure 3.7: Growth Assay for the highest, intermediate and lowest Xrel3-expressing clones +/- doxycycline. The graph represents the number of cells growing per well versus the number of days. Approximately $4x10^4$ cells were seeded/ well in 6-wells plates. Results show that following induction of Xrel3 expression by doxycycline at day 1, a decline in the growth rate was observed as compared to the non-induced pTRE2-Xrel3 transfected cells. The growth rate was not changed +/- doxycycline in the pTRE2 control HeLa cells, which served as a control. The intermediate level-expressing clone showed the greatest variation in the growth rate +/- induction as determined 5 and 6 days following induction. These results represent the mean ± standard deviation of 6 independent experiments. The bars represent the mean ± standard deviation. Xrel3 expression caused a statistically significant decline in the growth rate. ***Figure A*** shows the difference in growth between the non-induced and induced state of the highest level-expressing clone as compared to the non-induced and induced state of the empty vector.

Figure B shows the difference in growth between the non-induced and induced state of the intermediate level-expressing clone as compared to the non-induced and induced state of the empty vector.

Figure C shows the difference in growth between the non-induced and induced state of the lowest level-expressing clone as compared to the non-induced and induced state of the empty vector.

A)

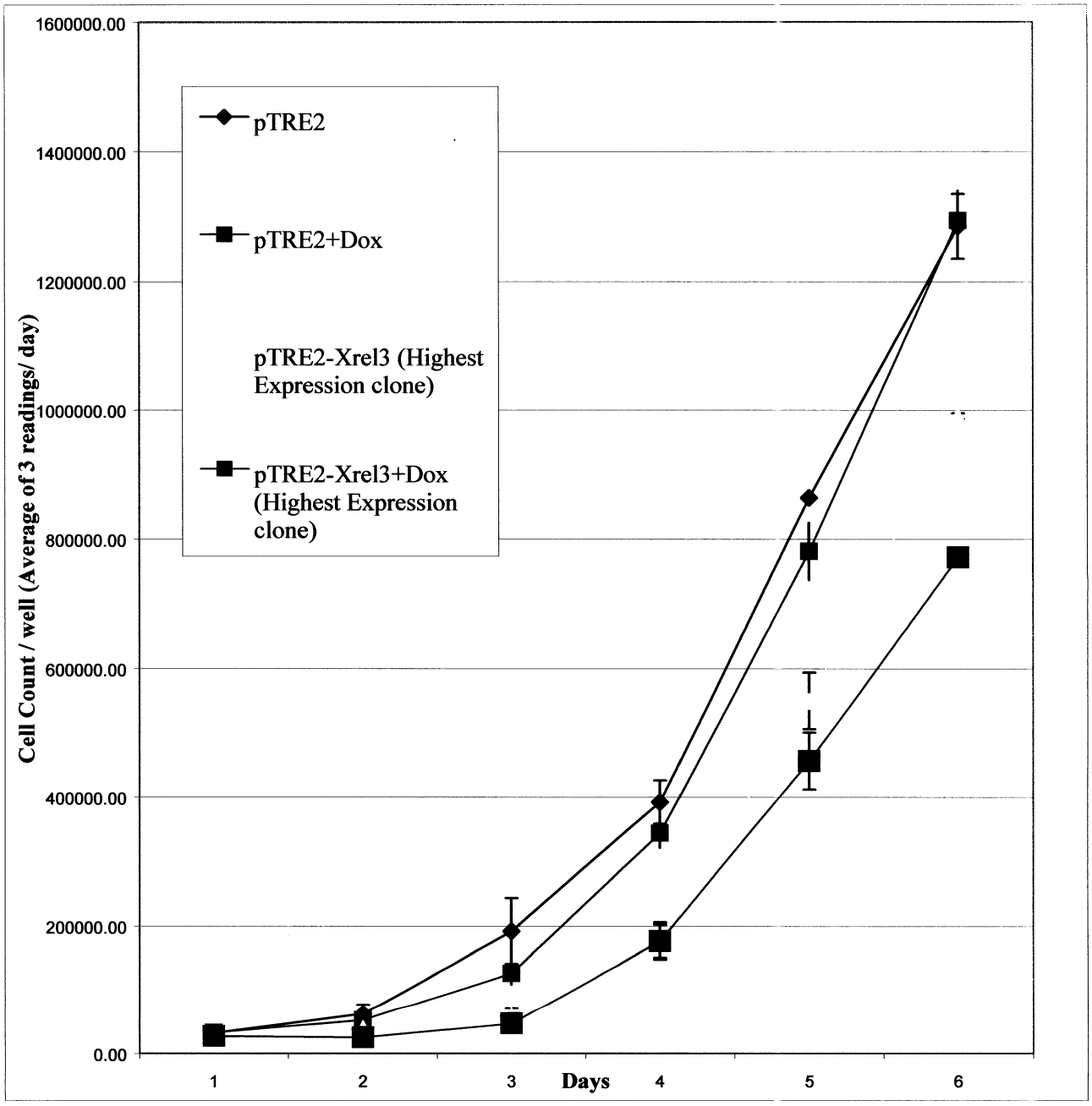
1600000.00
1400000.00
1200000.00
1000000.00
800000.00
600000.00
400000.00
200000.00
0.00
Cell Count / well (Average of 3 readings/ day)
pTRE2
pTRE2+Dox
pTRE2-Xrel3 (Highest Expression clone)
pTRE2-Xrel3+Dox (Highest Expression clone)
1
2
3
Days
4
5
6

B)

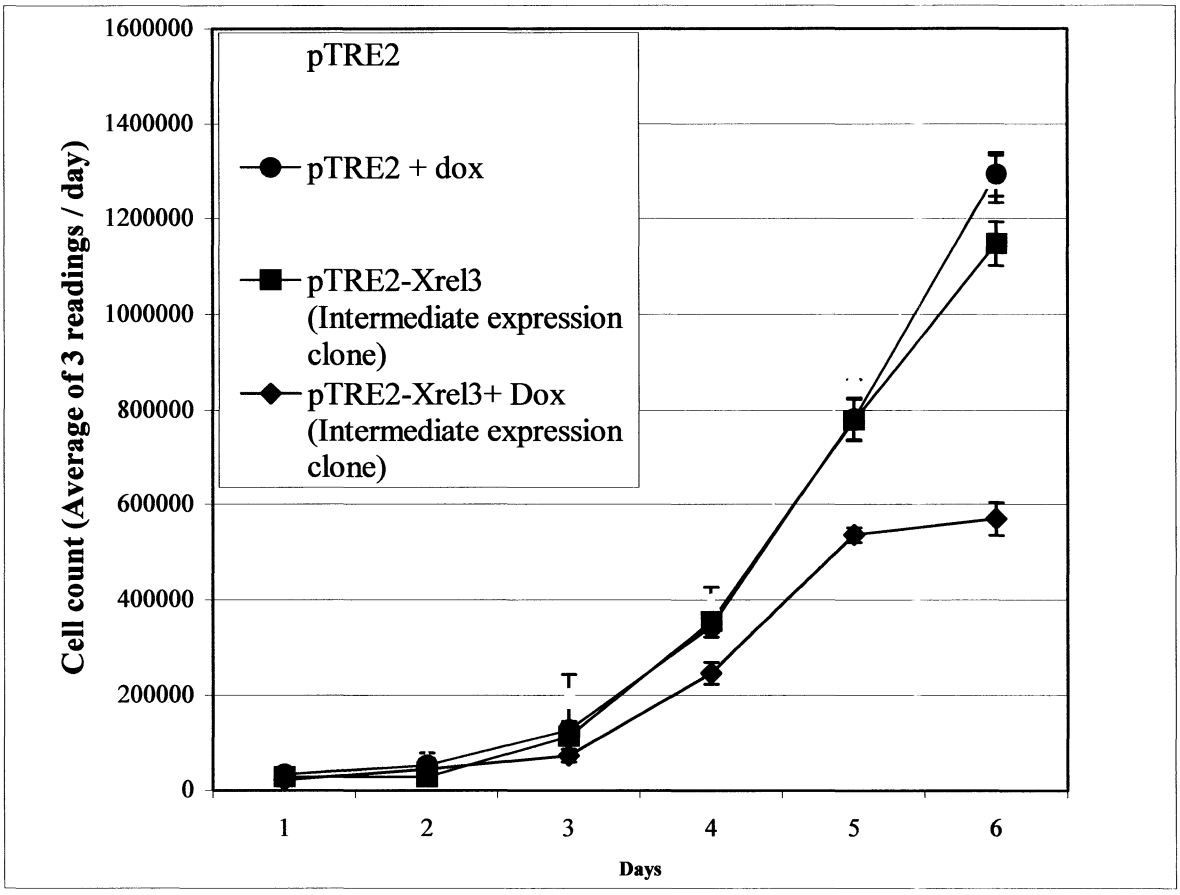
1600000
1400000
1200000
1000000
800000
600000
400000
200000
0
Cell count (Average of 3 readings / day)
pTRE2
pTRE2 + dox
pTRE2-Xrel3 (Intermediate expression clone)
pTRE2-Xrel3+ Dox (Intermediate expression clone)
1
2
3
4
5
6
Days

C)

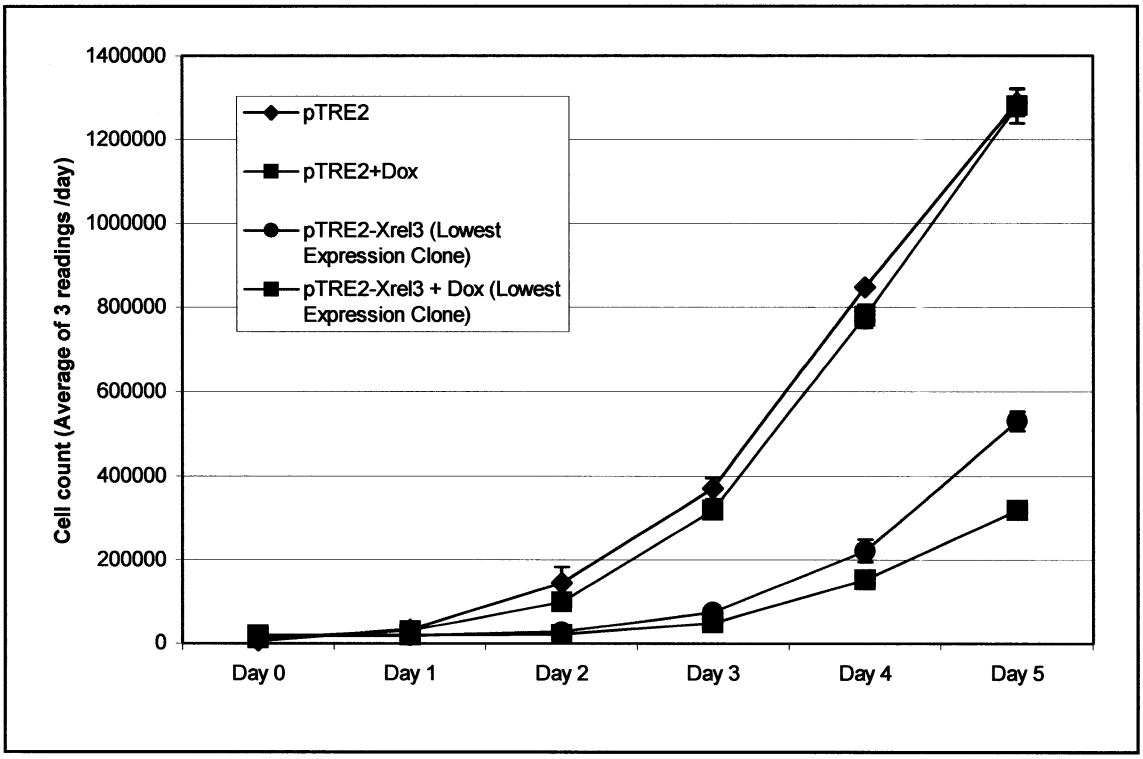
1400000
1200000
1000000
800000
600000
400000
200000
0
Cell count (Average of 3 readings /day)
pTRE2
pTRE2+Dox
pTRE2-Xrel3 (Lowest Expression Clone)
pTRE2-Xrel3 + Dox (Lowest Expression Clone)
Day 0
Day 1
Day 2
Day 3
Day 4
Day 5

3.6 Cell viability assay

Approximately 4 x 10^4 cells of each of pTRE2-Xrel3 (Int.) were seeded per well in a 6-wells plate. This was done for both the pTRE2-Xrel3 (Int.) transfected cells and the control cells transfected with the empty vector. The cells were treated with 1 μM cisplatin for 6 days. On each day of the experiment, the cells were trypsinized and mixed gently with an equal volume of 4 % trypan blue. The cells were counted immediately using a hemocytometer. The viable cells appeared colorless or transparent. However, the dead cells were stained blue. Only the viable cells were counted. The average of 3 readings was taken per day. Results showed that a lower number of viable cells were observed with Xrel3 induction compared to the non-induced and control cells (Figure 3.8). A consistant significant difference was observed between the number of viable cells +/- doxycycline in all of the 6 repeats of the experiment.

Figure 3.8: Growth assay pTRE2-Xrel3 (Int.) +/- doxycycline after treatment with 1 μM cisplatin. The graph represents the difference between the number of cells +/- induction and the decreasing number of viable cells after treatment with 1 μM cisplatin versus the number of days during which the experiment was carried. Less viable cells were observed when induction is coupled with 1 μM cisplatin treatment compared to the pTRE2 control HeLa cells. The number of viable cells, after drug treatment, were counted using trypan blue exclusion assay. An equal volume of the cell suspension and 4% trypan blue were mixed by pipetting and the unstained viable cells only were counted by microscopy. The vertical axis represents X-Y, where X is the number of cells observed +/- doxycycline, and Y is the number of cells observed +/- doxycycline and 1 μM cisplatin. The horizontal axis represents the number of days.

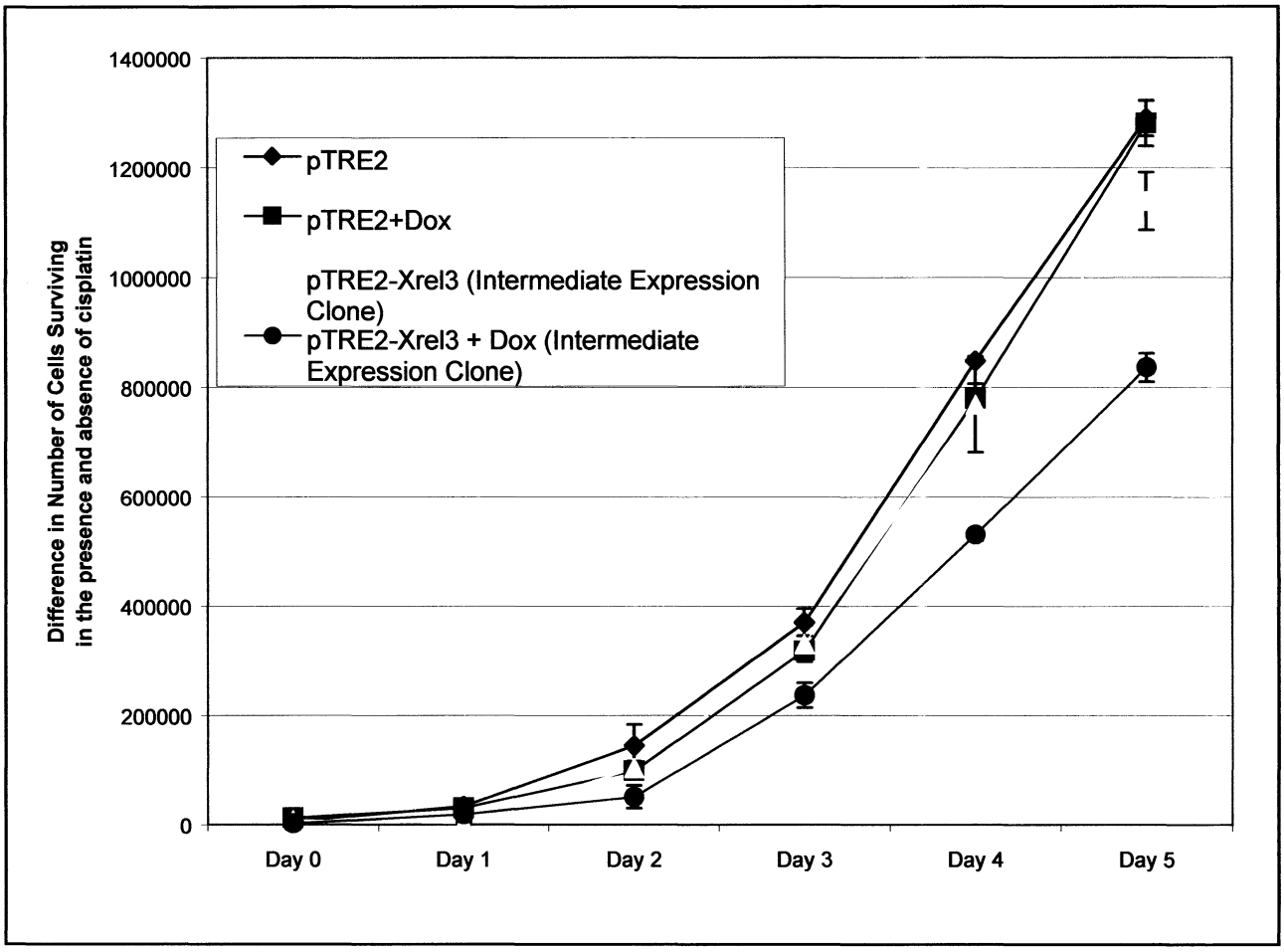
1400000
1200000
1000000
800000
600000
400000
200000
0
Difference in Number of Cells Surviving in the presence and absence of cisplatin
pTRE2
pTRE2+Dox
pTRE2-Xrel3 (Intermediate Expression Clone)
pTRE2-Xrel3 + Dox (Intermediate Expression Clone)
Day 0
Day 1
Day 2
Day 3
Day 4
Day 5

3.7 Effect of doxycycline induction of pTRE2-Xrel3 (INT.) on protein expression

The expression of a variety of pro- and anti-apoptotic factors was determined using Western Blotting analysis. For these experiments, the pTRE2-Xrel3 (Int.) cells were used.

A. Pro-apoptotic factors (Table 5):

1. p53

a) In the absence of cisplatin treatment, the tumor suppressor protein p53 showed an increase of up to 4 fold when compared to the non-induced state (Figure 3.9).

b) At 1 μM cisplatin treatment, the tumor suppressor protein p53 showed a decrease of up to 3 fold (Figures 3.9 and 3.10).

c) At 5 μM cisplatin treatment, the tumor suppressor protein p53 showed a significant decrease of $P<0.05$ relative to the control cells transfected with the empty vector (Figure 3.10).

d) After 48 hours of 1 μM and 5 μM cisplatin treatment, no significant difference was seen in the level of the tumor suppressor protein p53, +/- doxycycline (Figure 3.11). This was the only experiment done after 48 hours of drug treatment in order to examine the effect of prolonged drug treatment on the cells.

Figure 3.9: Expression of p53 in pTRE2-Xrel3 (Int.) and control pTRE2 transfected HeLa cells. The *upper panel* shows a Western blot analysis of the proteins extracted after 24 hours of 1μM cisplatin treatment from pTRE2-Xrel3 (Int.) cells and from pTRE2 control cells +/- doxycycline. The blot was probed with the mouse monoclonal IgG anti-p53 antibody and reprobed with β-actin to serve as a control for equal protein loading. The *lower panel* shows the corresponding densitometry analysis of the results. The values represent the mean ± the standard deviation of 7 independent experiments. Protein expression was quantified by measuring the optical density of the bands at medium exposure of the X-ray film and then dividing the values by the corresponding β-actin values.

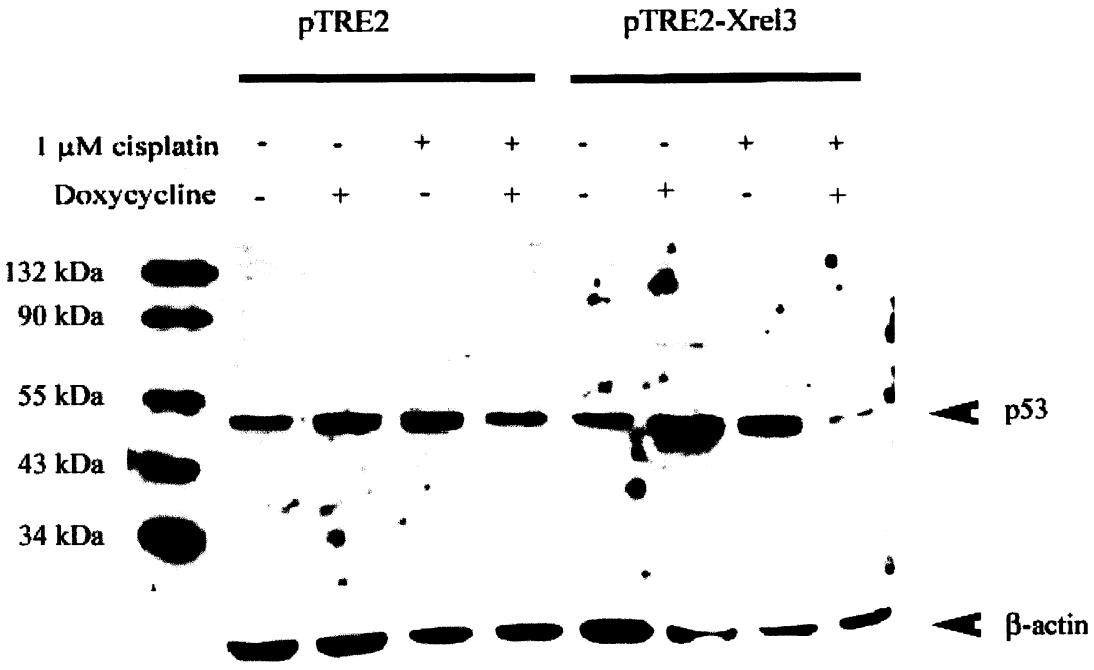

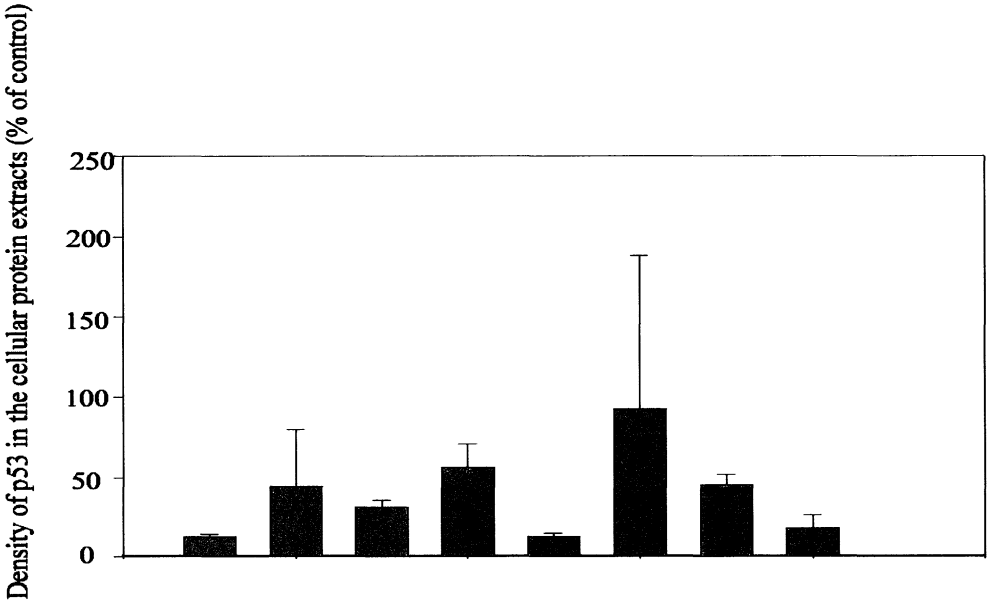

pTRE2 and pTRE2-Xrel3 +/- doxycycline and +/- cisplatin

Figure 3.10: Expression of p53 in pTRE2-Xrel3 (Int.) clone after 24 hours of 1 and 5 μM cisplatin treatment. The *upper panel* shows the Western blot analysis of the proteins extracted after 24 hours of treatment with 1 and 5 μM cisplatin from pTRE2-Xrel3 (Int.) cells +/- doxycycline. The blot was probed with the mouse monoclonal IgG anti-p53 antibody and reprobed with β-actin to serve as a control for equal protein loading. Protein expression was quantified by measuring the optical density of the bands at medium exposure of the X-ray film and then dividing the values by the corresponding β-actin values. The *lower panel* shows the corresponding densitometry analysis of the results. The values represent the mean ± standard deviation of 3 independent experiments. $^{**}P<0.01$ is the statisitical significance of the difference in p53 expression between pTRE2-Xrel3 (Int.) clone treated with 5 μM cisplatin and the corresponding non-induced clone.

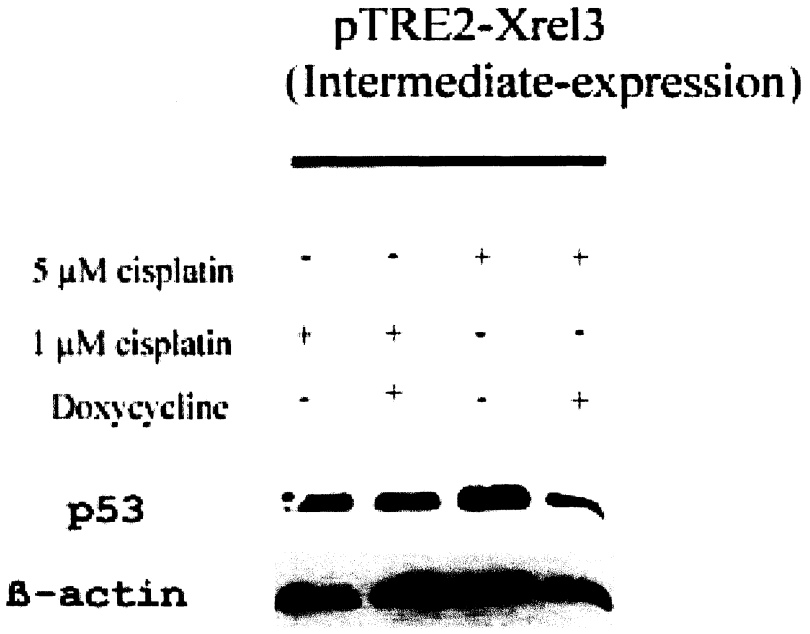
pTRE2-Xrel3
(Intermediate-expression)
5 μM cisplatin - - + +
1 μM cisplatin + + - -
Doxycycline - + - +
p53
ß-actin

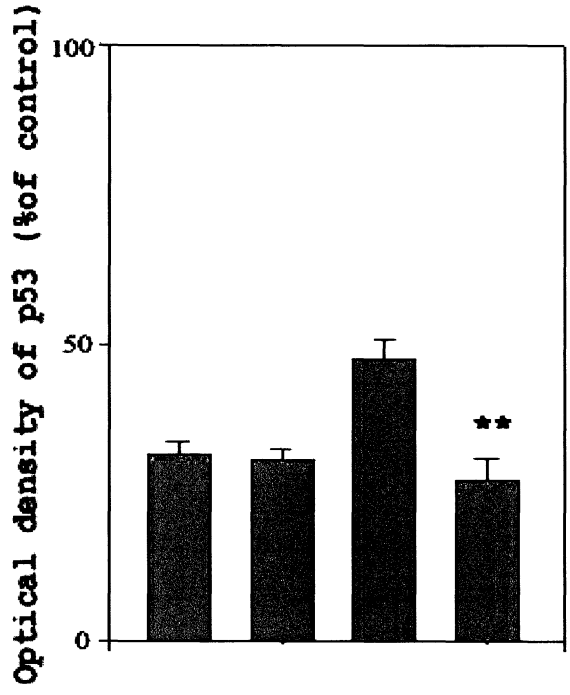
Optical density of p53 (%of control)
100
50
0
**
pTRE2-Xrel3 transfected HeLa cells

Figure 3.11: Expression of p53 in the intermediate Xrel3-expressing clones after 48 hours of drug treatment. The *upper panel* shows the Western blot analysis of the proteins extracted after 48 hours of treatment with 1 and 5 μM cisplatin from pTRE2-Xrel3 (Int.) cells +/- doxycycline. The blot was probed with the mouse monoclonal IgG anti-p53 antibody and reprobed with β-actin to serve as a control for equal protein loading. Protein expression was quantified by measuring the optical density of the bands at medium exposure of the X-ray film and then dividing the values by the corresponding β-actin values. The *lower panel* shows the corresponding densitometry analysis of the results.

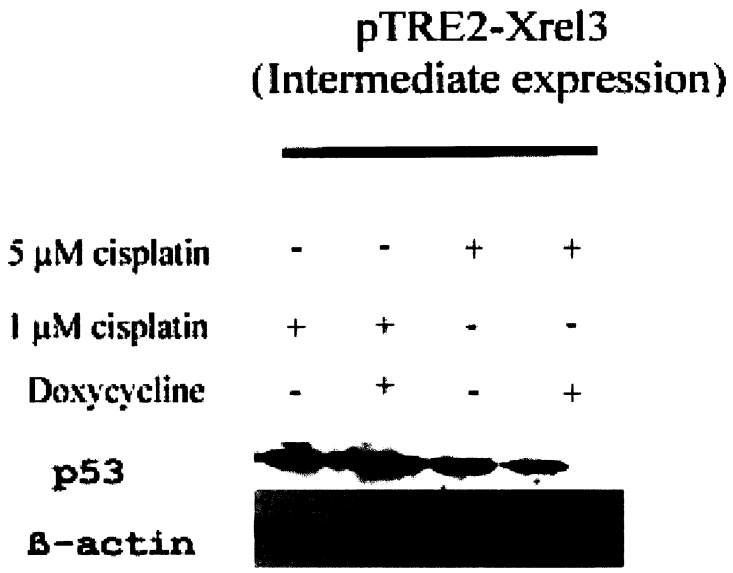

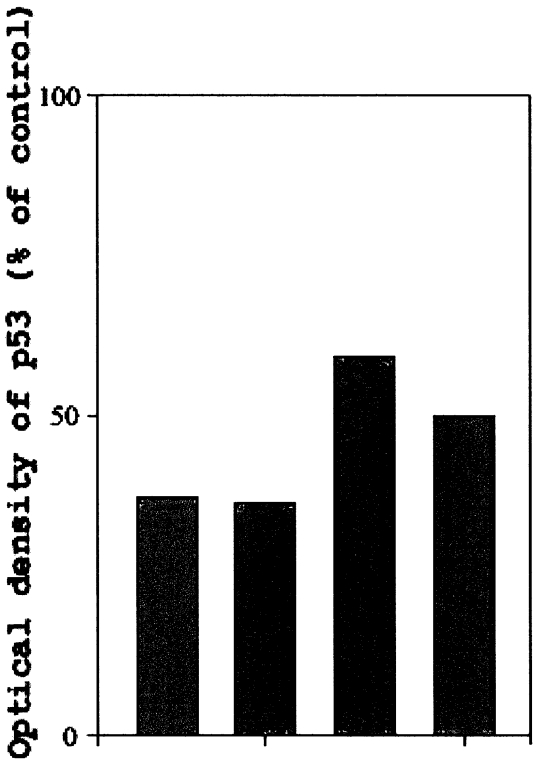

pTRE2-Xrel3 transfected HeLa cells after 48 hours

2. Bax

a) At 1 μM cisplatin treatment, a significant decrease of the apoptotic protein Bax of $P<0.05$ was observed relative to the non-induced state (Figure 3.12).

b) At 5 μM cisplatin treatment, a significant increase of the apoptotic protein Bax of $P<0.05$ relative to the control cells transfected with just the empty vector was observed (Figure 3.12).

3. Caspase-3

a) At 1 μM cisplatin treatment, the 17-kDa catalytic subunit of the apoptotic factor caspase-3 showed a decrease of 0.3 fold relative to the non-induced state (Figure 3.13).

b) At 5 μM cisplatin treatment, the 17- kDa catalytic subunit of the apoptotic factor caspase-3 showed a significant increase of $P<0.05$ relative to the 1 μM cisplatin treatment (Figure 3.13).

Figure 3.12: Expression of Bax in pTRE2-Xrel3 (Int.) and pTRE2 transfected HeLa cells after 24 hours of 1 and 5 μM cisplatin treatment. The *upper panel* shows the Western blot analysis of the proteins extracted after 24 hours of treatment with 1 and 5 μM cisplatin from pTRE2-Xrel3 (Int.) cells +/- doxycycline. Protein expression was quantified by measuring the optical density of the bands at medium exposure of the X-ray film and then dividing the values by the corresponding β-actin values. The *lower panel* shows the corresponding densitometry analysis of the results. The values represent the mean ± standard deviation. *$P<0.05$ is the statistical significance of the difference in Bax expression with Xrel3 induction relative to the non-induced state at 1 μM cisplatin, +$P<0.05$ is the statistical significance of the difference in Bax expression with Xrel3 induction relative to control at 5 μM cisplatin and **$P<0.01$ is the statistical significance of the difference in Bax expression in control cells with doxycycline as compared to without doxycycline at 5 μM cisplatin.

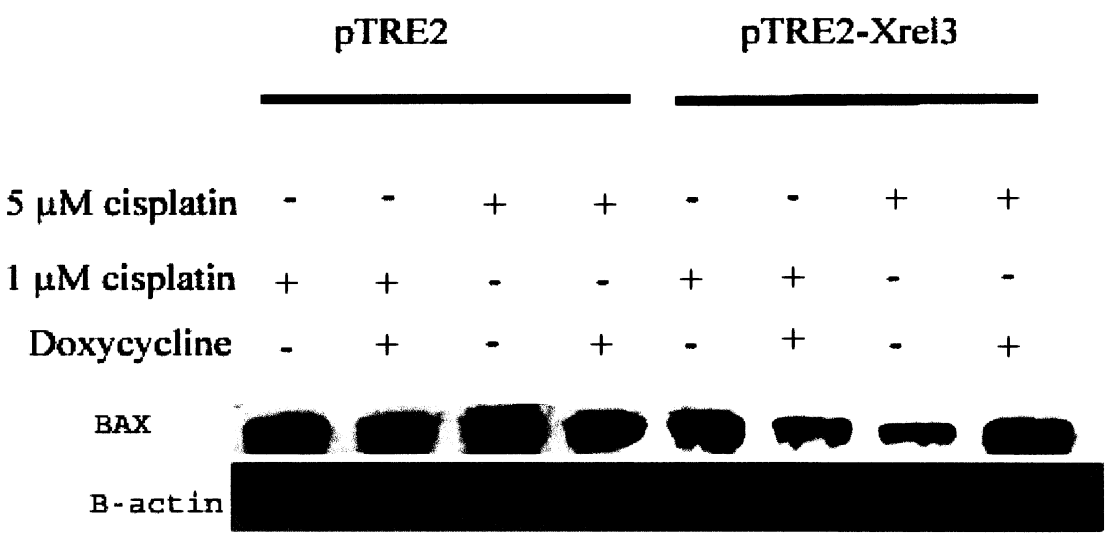

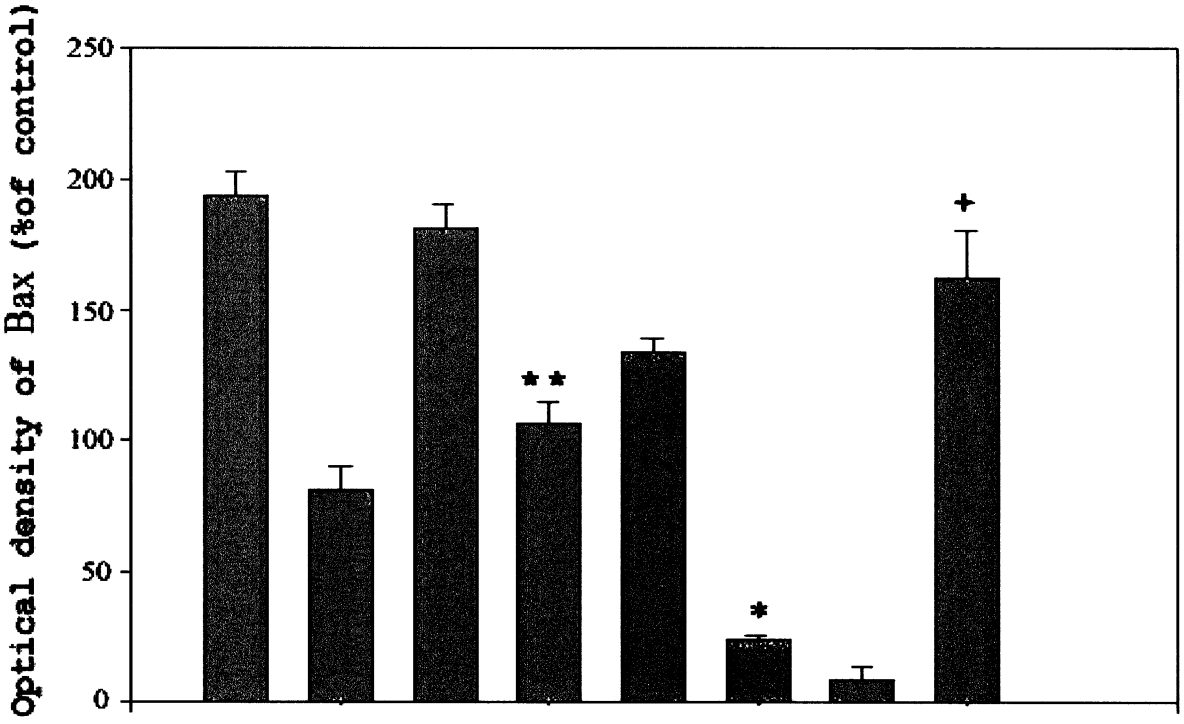

pTRE2 and pTRE2-Xrel3 +/- doxycycline and in the presence of 1 or 5 μM cisplatin

Figure 3.13: Expression of caspase-3 catalytic subunit at 17 kDa in pTRE2-Xrel3 (Int.) and pTRE2 transfected HeLa cells +/- doxycycline after 24 hours treatment with 1 and 5 μM cisplatin. The *upper panel* shows the Western blot analysis of the proteins extracted after 24 hours of treatment with 1 and 5-μM cisplatin from pTRE2-Xrel3 (Int.) cells compared to the control cells +/- doxycycline. Protein expression was quantified by measuring the optical density of the bands at medium exposure of the X-ray film and then dividing the values by the corresponding β-actin values. The *lower panel* shows the corresponding densitometry analysis of the results. The values represent the mean ± standard deviation. **$P<0.01$ is the statistical significance of the difference in caspase-3 expression with Xrel3 induction relative to the non-induced state at 5 μM cisplatin and *$P<0.01$ is the statistical significance of the difference in caspase-3 expression in control cells with doxycycline as compared to without doxycycline at 1 and 5-μM cisplatin.

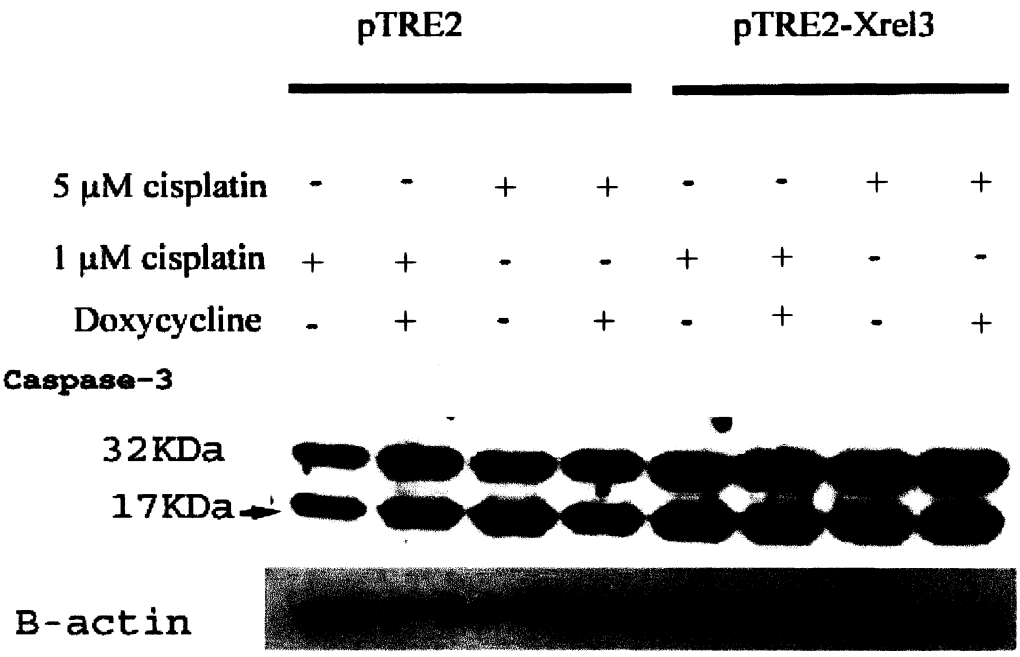

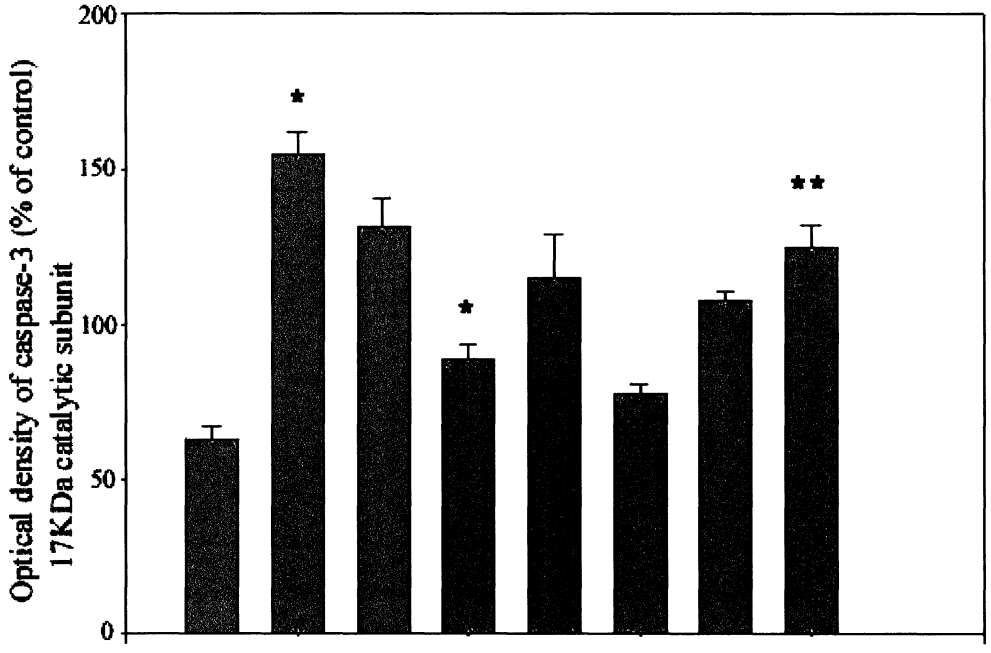

pTRE2 and pTRE2-Xrel3 +/- doxycycline and in the presence of 1 or 5 μM cisplatin

4. Caspase-8

a) In the absence of drug treatment, the 55-kDa catalytic subunit of the apoptotic factor caspase-8 showed an increase of up to 6 fold relative to the non-induced state (Figure 3.14).

b) At 1 μM cisplatin treatment, the 55-kDa catalytic subunit of the apoptotic factor caspase-8 showed a significant decrease of $P<0.05$ relative to control (Figures 3.14 and 3.15).

c) At 5 μM cisplatin treatment, the 55-kDa catalytic subunit of the apoptotic factor caspase-8 showed a significant increase of $P<0.05$ relative to the 1 μM cisplatin treatment (Figure 3.15).

5. MDM-2

a) At 1 μM cisplatin treatment, MDM-2 showed a significant decrease of $P<0.01$ relative to both the non-induced state and to the control (Figure 3.16).

b) At 5 μM cisplatin treatment, MDM-2 showed a significant increase of $P<0.05$ relative to the non-induced state (Figure 3.16).

Figure 3.14: Expression of caspase-8 at 55 kDa cleaved product in pTRE2-Xrel3 (Int.) and pTRE2 transfected HeLa cells +/- doxycycline and +/- with 1 μM cisplatin. The *upper panel* shows the Western blot analysis of the proteins extracted after 24 hours of treatment with 1 μM cisplatin from pTRE-Xrel3 (Int.) cells in comparison with the pTRE2 control clone +/- doxycycline. Protein expression was quantified by measuring the optical density of the bands at medium exposure of the X-ray film and then dividing the values by the corresponding β-actin values. The *lower panel* shows the corresponding densitometry analysis of the results. The values represent the mean ± standard deviation. +$P<0.05$ is the statistical significance of the difference in caspase-8 expression with Xrel3 induction relative to the control cells transfected with the empty vector at 1 μM cisplatin.

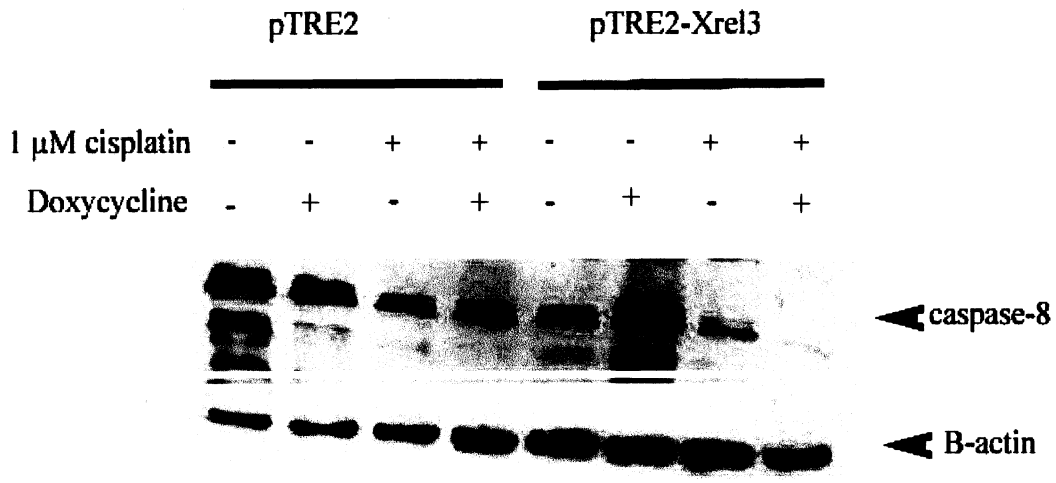
pTRE2
pTRE2-Xrel3
1 μM cisplatin - - + + - - + +
Doxycycline - + - + - + - +
caspase-8
B-actin

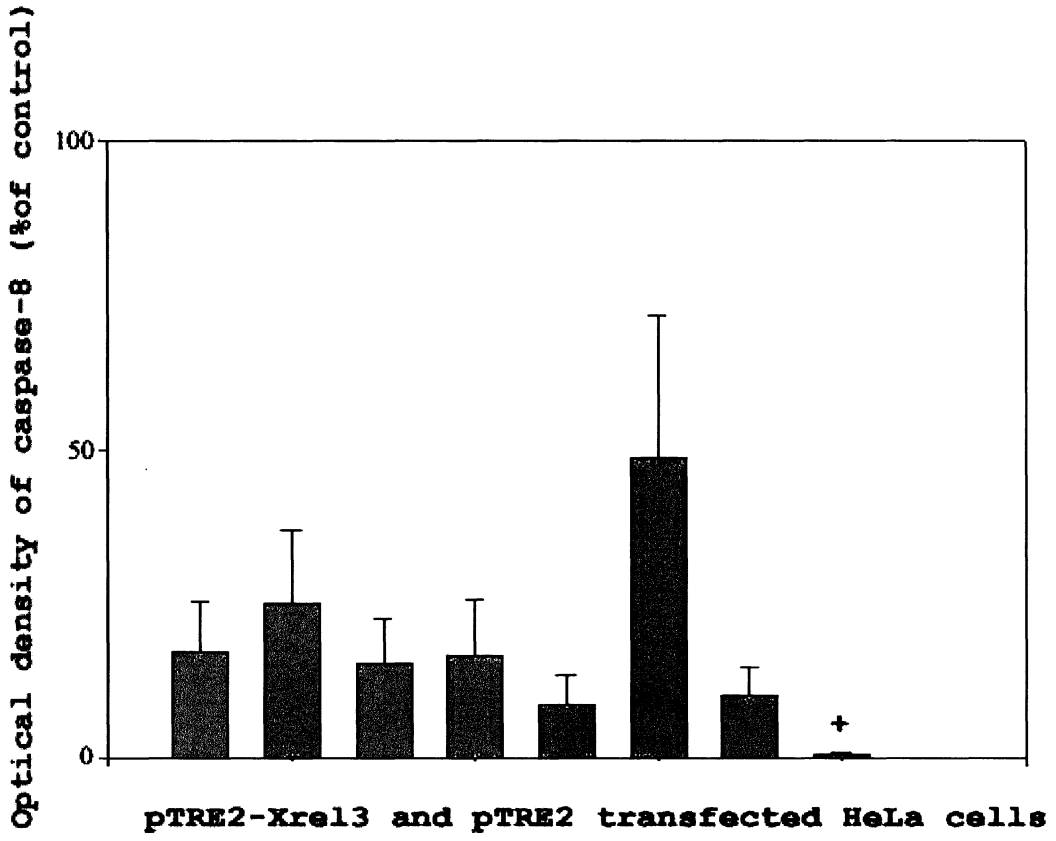
Optical density of caspase-8 (%of control)
100
50
0
+
pTRE2-Xrel3 and pTRE2 transfected HeLa cells

Figure 3.15: Expression of caspase-8 at 55 kDa cleaved product in pTRE2-Xrel3 (Int.) and pTRE2 control clone +/- doxycycline after 24 hours treatment with 1 and 5 μM cisplatin. The *upper panel* shows the Western blot analysis of the proteins extracted after 24 hours of treatment with 1 and 5 μM cisplatin from pTRE2-Xrel3 (Int.) cells compared with the pTRE2 control cells +/- doxycycline. The blot was probed with the mouse monoclonal IgG anti-caspase-8 antibody and reprobed with β-actin to serve as a control for equal protein loading.

Protein expression was quantified by measuring the optical density of the bands at medium exposure of the X-ray film and then dividing the values by the corresponding β-actin values.

The *lower panel* shows the corresponding densitometry analysis of the results. The values represent the mean ± standard deviation of 3 independent experiments. +$P<0.05$ is the statistical significance of the difference in caspase-8 expression with Xrel3 induction relative to the control at 1 μM cisplatin, **$P<0.05$ is the statistical significance of the difference in caspase-8 expression with induction and 5 μM cisplatin relative to the 1 μM cisplatin treatment, *$P<0.05$ is the statistical significance of the difference in caspase-8 expression with doxycycline as compared to without doxycycline.

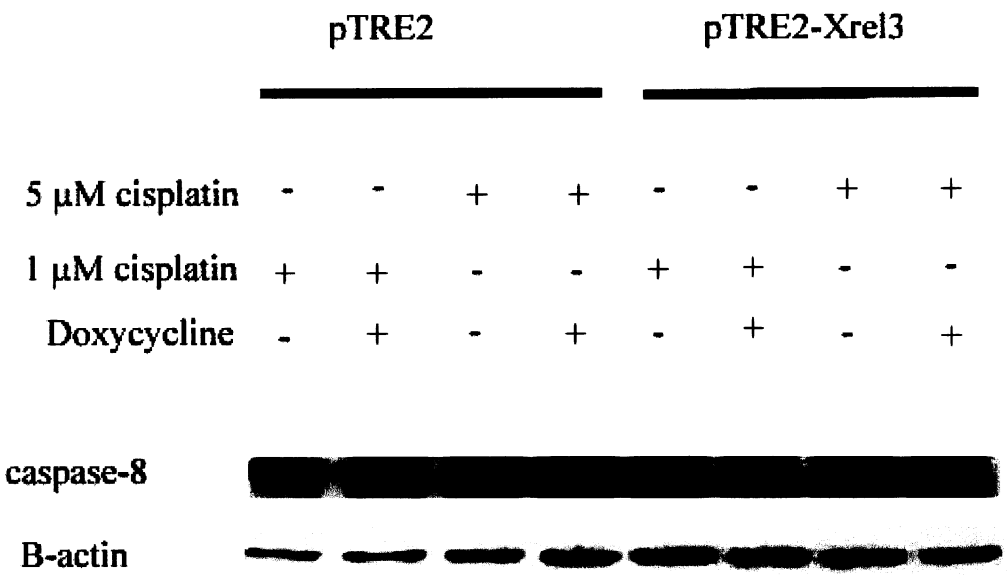
pTRE2
pTRE2-Xrel3
5 μM cisplatin - - + + - - + +
1 μM cisplatin + + - - + + - -
Doxycycline - + - + - + - +
caspase-8
B-actin

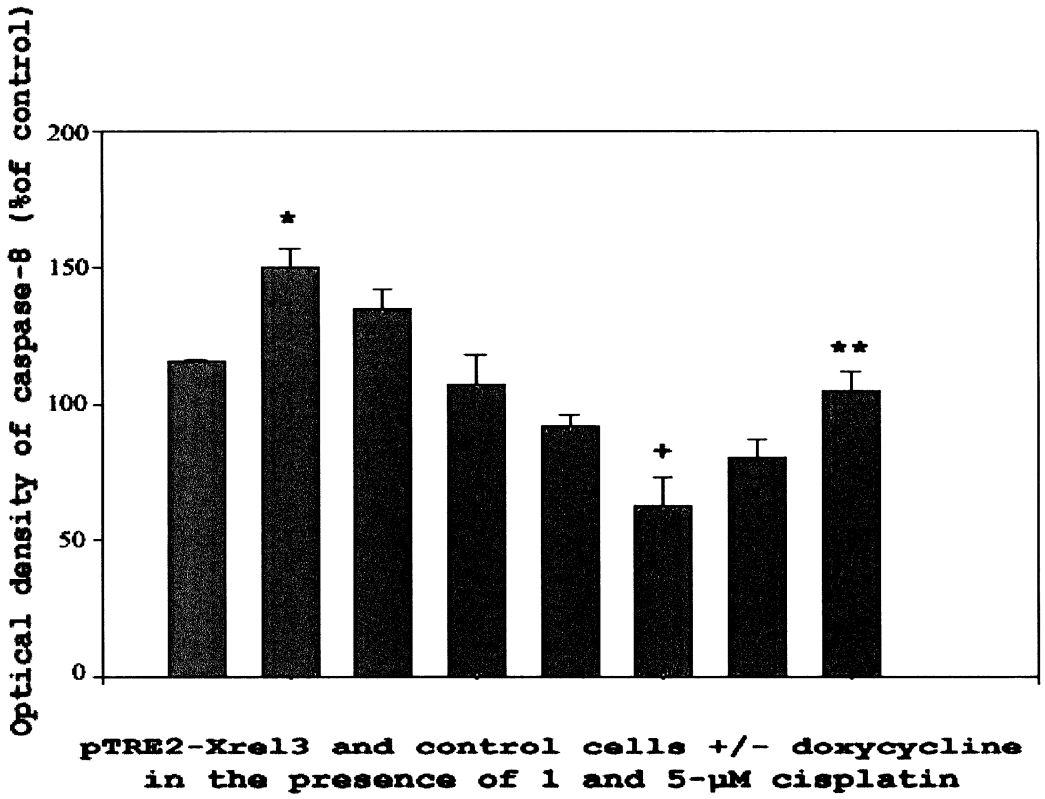
Optical density of caspase-8 (%of control)
200
150
100
50
0
*
**
+
pTRE2-Xrel3 and control cells +/- doxycycline
in the presence of 1 and 5-μM cisplatin

Figure 3.16: Expression of MDM-2 in pTRE2-Xrel3 (Int.) compared to the pTRE2 control +/- doxycycline and after 24 hours treatment with 1 and 5 μM cisplatin. The *upper panel* shows the Western blot analysis of the proteins extracted after 24 hours of treatment with 1 and 5 μM cisplatin from pTRE2-Xrel3 (Int.) in comparison with the pTRE2 control cells +/- doxycycline. The blot was probed with the mouse monoclonal IgG anti-MDM-2 antibody and reprobed with β-actin to serve as a control for equal protein loading.

Protein expression was quantified by measuring the optical density of the bands at medium exposure of the X-ray film and then dividing the values by the corresponding β-actin values.

The *lower panel* shows the corresponding densitometry analysis of the results. The values represent the mean ± standard deviation of 3 independent experiments. **$P<0.01$ is the statistical significance of the difference in MDM-2 expression at 1 μM cisplatin with Xrel3 induction relative to the non-induced and to the control state as well and *$P<0.05$ is the statistical significance of the difference in MDM-2 expression with Xrel3 induction at 5 μM cisplatin relative to the non-induced state.

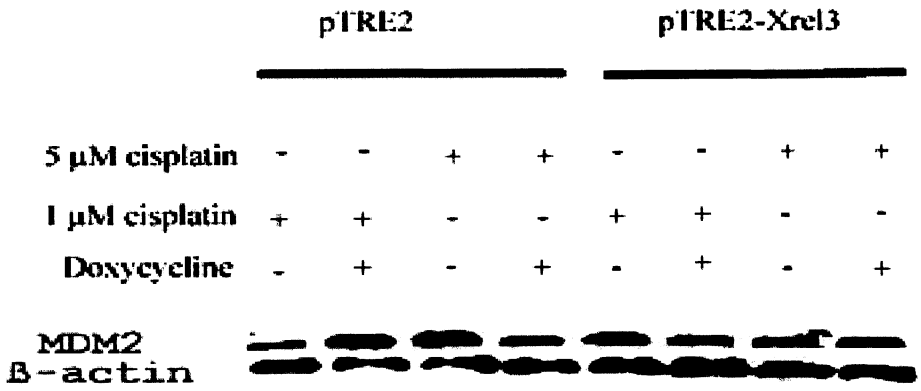
pTRE2
pTRE2-Xrel3
5 μM cisplatin - - + + - - + +
1 μM cisplatin + + - - + + - -
Doxycycline - + - + - + - +
MDM2
B-actin

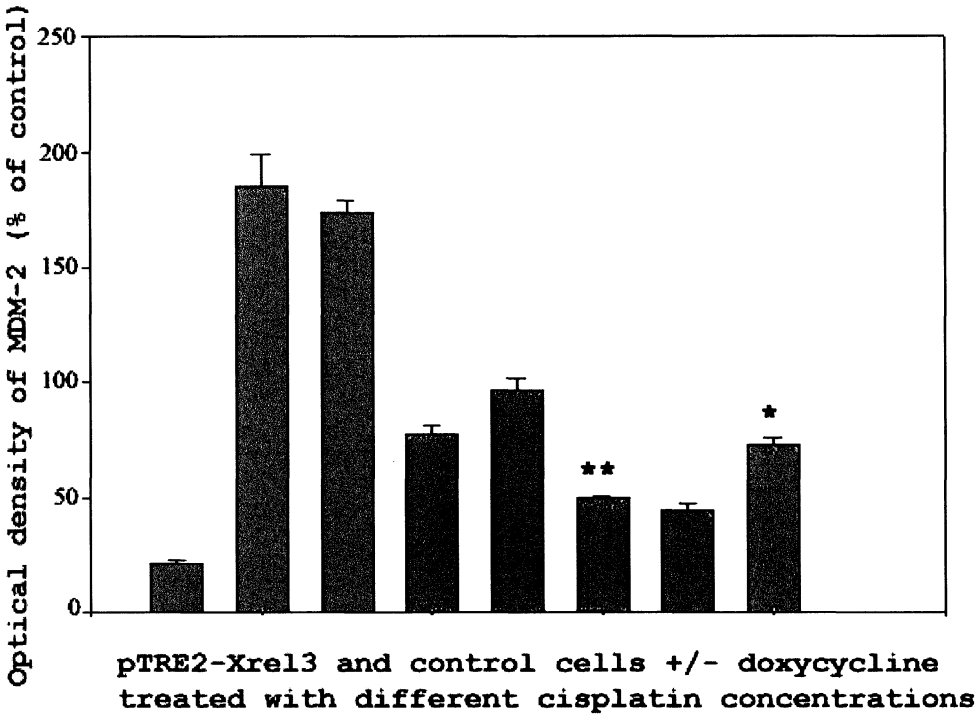
Optical density of MDM-2 (% of control)
250
200
150
100
50
0
**
*
pTRE2-Xrel3 and control cells +/- doxycycline
treated with different cisplatin concentrations

6. Bcl-2

a) At 1 μM cisplatin treatment, a significant decrease in Bcl-2 of $P<0.01$ relative to the control cells transfected with the empty vector and relative to the non-induced state was observed (Figure 3.17).

b) At 5 μM cisplatin treatment, a significant increase in Bcl-2 of $P<0.01$ relative to the control cells transfected with just the empty vector and relative to the non-induced state was observed (Figure 3.17).

7. Bcl-X_L

a) At 1 μM cisplatin treatment, a significant decrease of $P< 0.01$ relative to the control cells transfected with just the empty vector and $P<0.05$ relative to the non-induced state was observed (Figure 3.18).

b) At 5 μM cisplatin treatment, a significant increase of $P<0.01$ relative to the control cells transfected with the empty vector and $P<0.05$ relative to the non-induced state was observed (Figure 3.18).

Figure 3.17: Expression of Bcl-2 in pTRE2-Xrel3 (Int.) compared to the pTRE2 control +/- doxycycline and after 24 hours treatment with 1 and 5 μM cisplatin. The *upper panel* shows a Western blot analysis of the proteins extracted after 24 hours of treatment with 1 and 5 μM cisplatin from pTRE2-Xrel3 (Int.) cells in comparison with the pTRE2 control cells +/- doxycycline. The blot was probed with the mouse monoclonal IgG anti-Bcl-2 antibody and reprobed with β-actin to serve as a control for equal protein loading. Protein expression was quantified by measuring the optical density of the bands at medium exposure of the X-ray film and then dividing the values by the corresponding β-actin values. The *lower panel* shows the corresponding densitometry analysis of the results. The values represent the mean ± standard deviation of 3 independent experiments. ** $P<0.005$ is the statistical significance of the difference in Bcl-2 expression with Xrel3 induction relative to both control and non-induced cells.

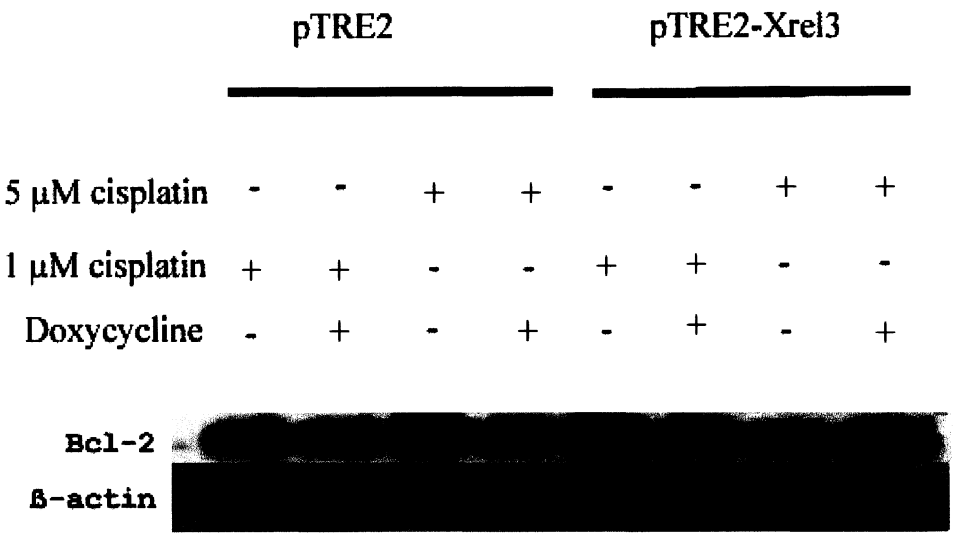
pTRE2
pTRE2-Xrel3
5 μM cisplatin - - + + - - + +
1 μM cisplatin + + - - + + - -
Doxycycline - + - + - + - +
Bcl-2
ß-actin

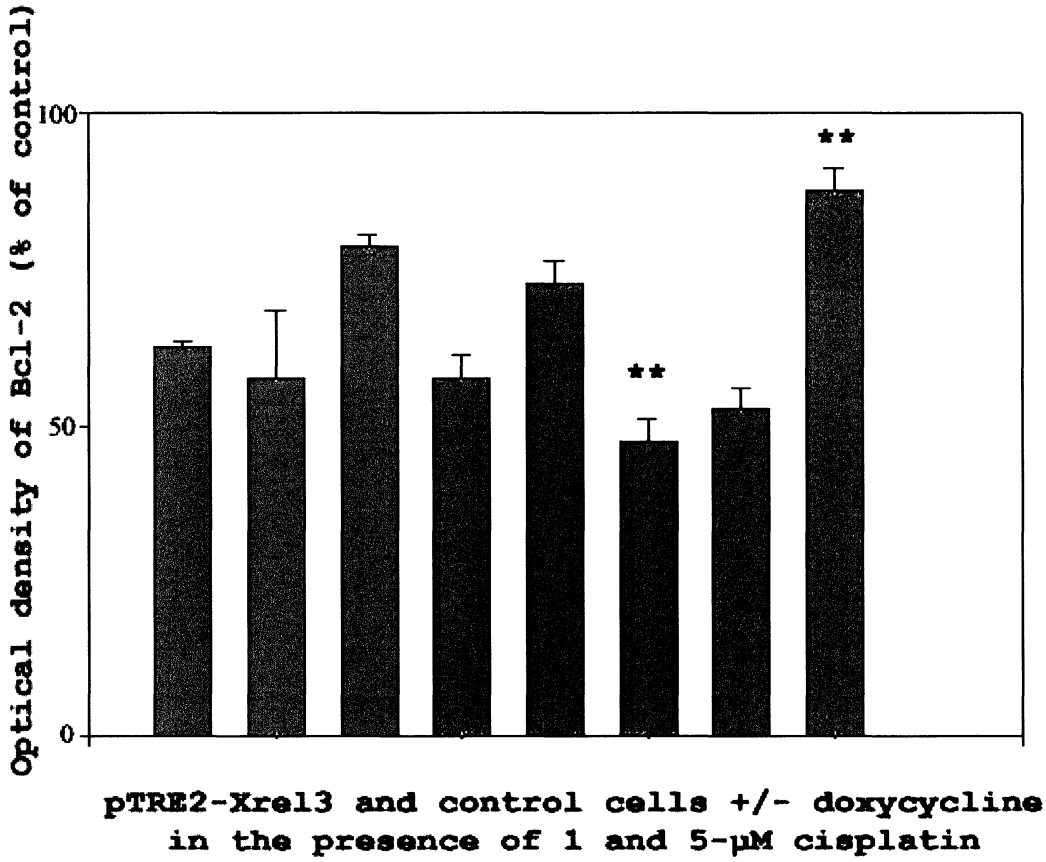
Optical density of Bcl-2 (% of control)
100
50
0
**
**
pTRE2-Xrel3 and control cells +/- doxycycline
in the presence of 1 and 5-μM cisplatin

Figure 3.18: Expression of Bcl-X_L in pTRE2-Xrel3 (Int.) compared to the pTRE2 control +/- doxycycline and after 24 hours treatment with 1 and 5 μM cisplatin. The *upper panel* shows the Western blot analysis of the proteins extracted after 24 hours of treatment with 1 and 5 μM cisplatin from pTRE2-Xrel3 (Int.) cells in comparison with the pTRE2 control cells +/- doxycycline. The blot was probed with the mouse monoclonal IgG anti-Bcl-X_L antibody and reprobed with β-actin to serve as a control for equal protein loading.

Protein expression was quantified by measuring the optical density of the bands at medium exposure of the X-ray film and then dividing the values by the corresponding β-actin values.

The *lower panel* shows the corresponding densitometry analysis of the results. The values represent the mean ± standard deviation. ** $P<0.01$ is the statistical significance of the difference in Bcl-X_L expression with Xrel3 induction relative to the non-induced state at 1 and 5 μM cisplatin.

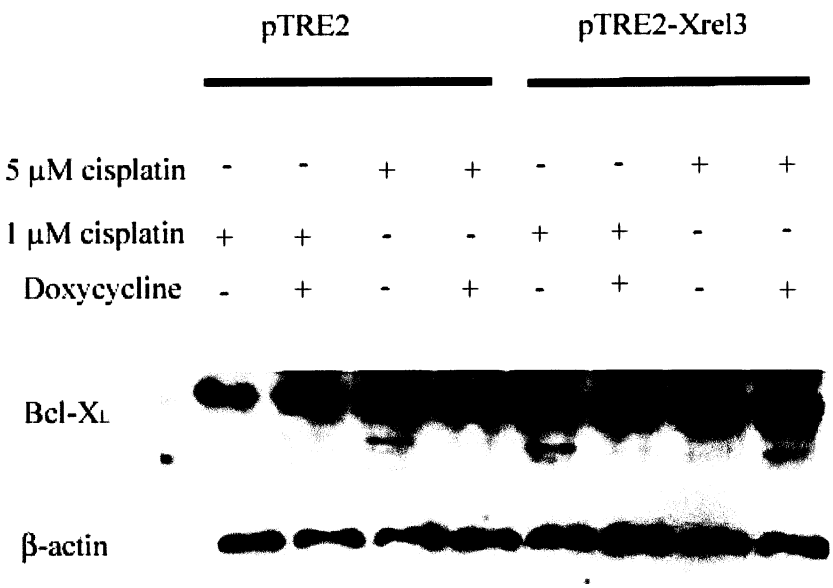
pTRE2
pTRE2-Xrel3
5 μM cisplatin - - + + - - + +
1 μM cisplatin + + - - + + - -
Doxycycline - + - + - + - +
Bcl-XL
β-actin

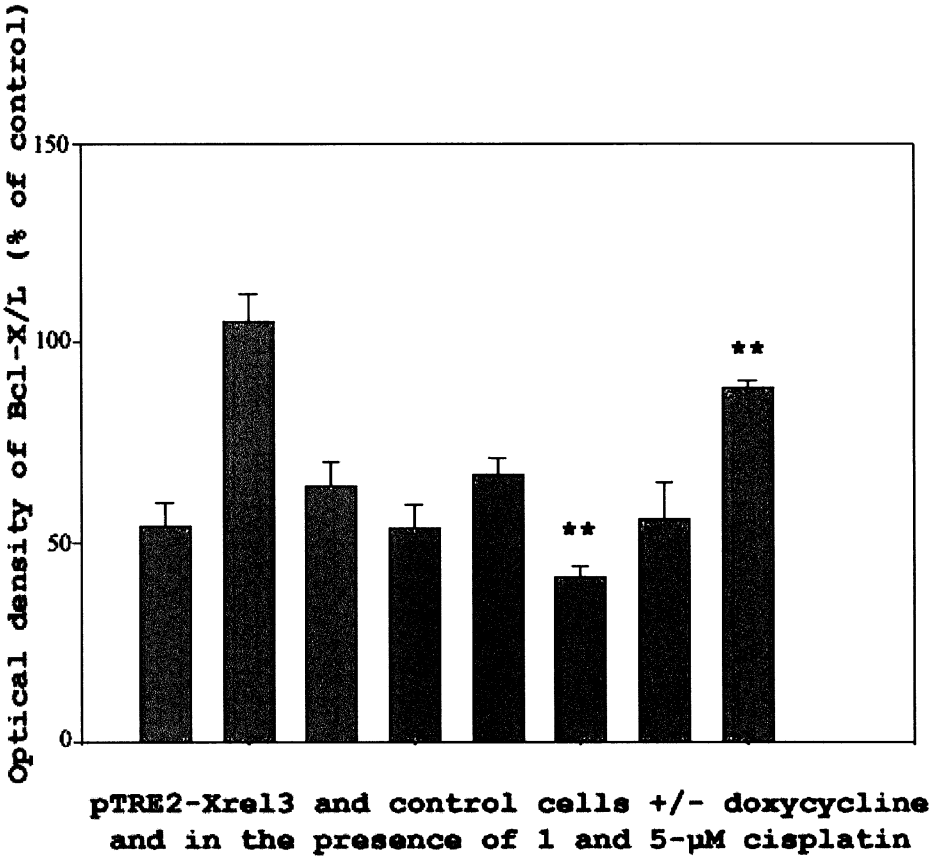
Optical density of Bcl-X/L (% of control)
150
100
50
0
**
**
pTRE2-Xrel3 and control cells +/- doxycycline
and in the presence of 1 and 5-μM cisplatin

8. PARP

a) In the absence of drug treatment, the 85-kDa catalytic subunit of the apoptotic factor PARP showed a significant increase of $P<0.01$ relative to the non-induced state and relative to the control (Figure 3.19).

b) At 1 μM cisplatin treatment, the 85-kDa catalytic subunit of the apoptotic factor PARP showed a 2-fold increase relative to the non-induced state (Figure 3.20).

c) At 5 μM cisplatin treatment, the 85-kDa catalytic subunit of the apoptotic factor PARP showed a 3.1 fold increase relative to the non-induced state (Figure 3.20).

Figure 3.19: Expression of PARP in pTRE2-Xrel3 (Int.) cells compared to the pTRE2 control cells +/- doxycycline. The *upper panel* shows the Western blot analysis of the proteins extracted after 24 hours from pTRE2-Xrel3 (Int.) cells in comparison with the pTRE2 control cells +/- doxycycline. The blot was probed with the mouse monoclonal IgG anti-human PARP antibody and reprobed with β-actin to serve as a control for equal protein loading. Protein expression was quantified by measuring the optical density of the bands at medium exposure of the X-ray film and then dividing the values by the corresponding β-actin values. The *lower panel* shows the corresponding densitometry analysis of the results. The values represent the mean ± standard deviation of 3 independent experiments. ** $P<0.005$ is the statistical significance of the difference in PARP expression of the 85 kDa catalytic subunit indicating apoptosis with Xrel3 induction without treatment relative to both control and non-induced cells.

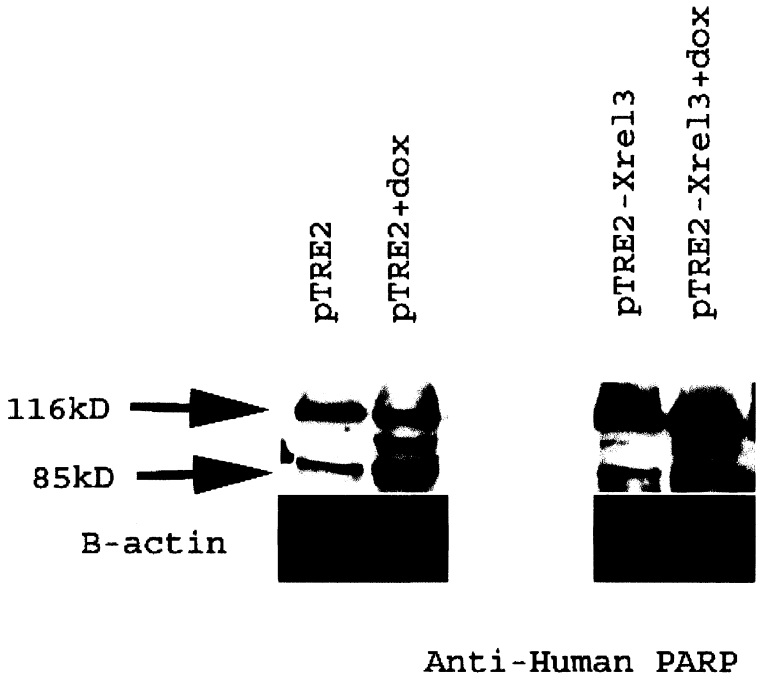
pTRE2
pTRE2+dox
pTRE2-Xrel3
pTRE2-Xrel3+dox
116kD
85kD
B-actin
Anti-Human PARP

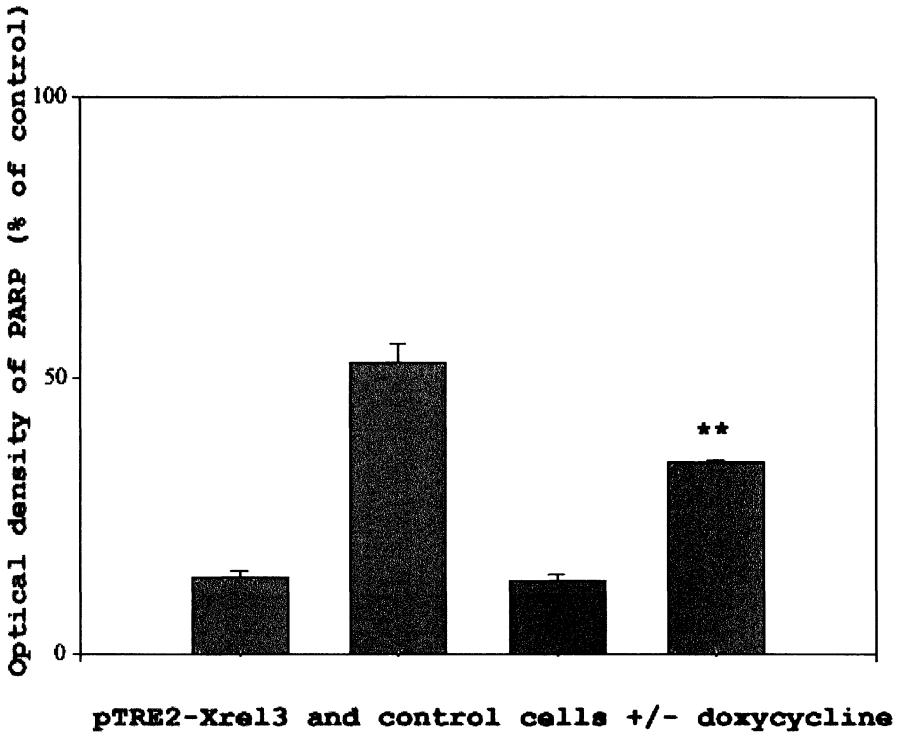
Optical density of PARP (% of control)
100
50
0
**
pTRE2-Xrel3 and control cells +/- doxycycline

Figure 3.20: Expression of PARP 85 kDa catalytic subunit in pTRE2-Xrel3 (Int.) compared to the pTRE2 control +/- doxycycline and after 24 hours treatment with 1 and 5 μM cisplatin. The *upper panel* shows the Western blot analysis of the proteins extracted after 24 hours of treatment with 1 and 5 μM cisplatin from pTRE2-Xrel3 (Int.) cells in comparison with the pTRE2 control cells +/- doxycycline. The blot was probed with the mouse monoclonal IgG anti-human PARP antibody and reprobed with β-actin to serve as a control for equal protein loading.

Protein expression was quantified by measuring the optical density of the bands at medium exposure of the X-ray film and then dividing the values by the corresponding β-actin values.

The *lower panel* shows the corresponding densitometry analysis of the results. The values represent the mean ± standard deviation of 5 independent experiments.

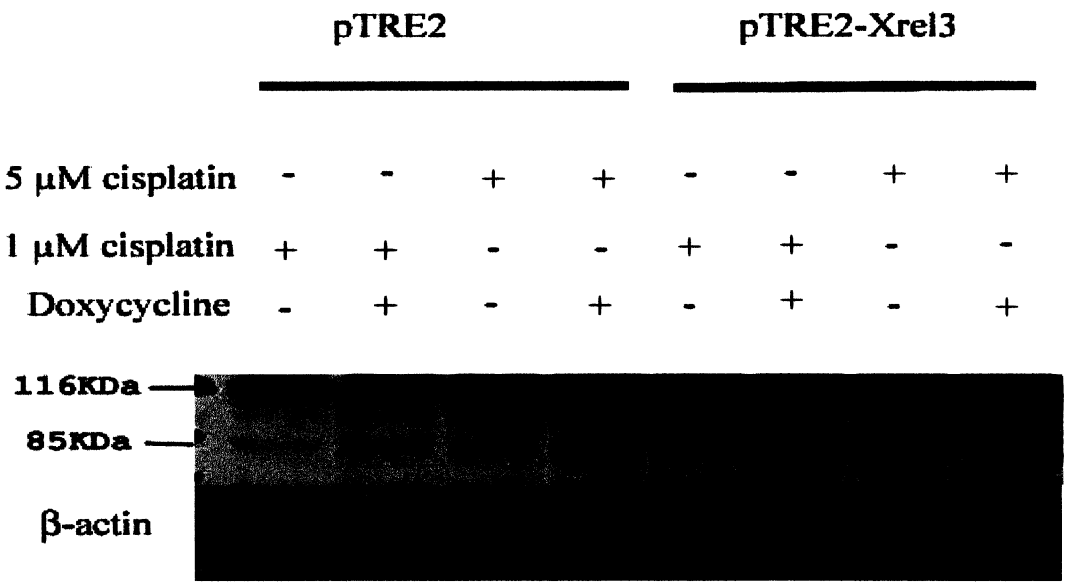

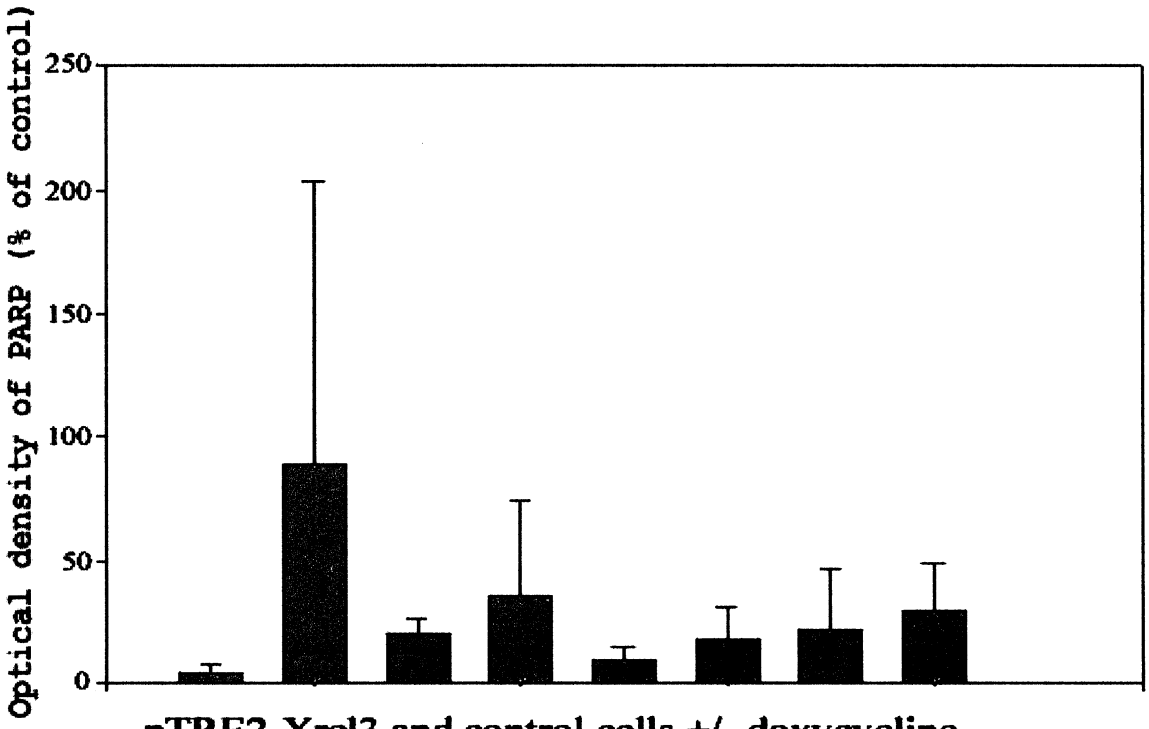

pTRE2-Xrel3 and control cells +/- doxycycline in the presence of 1 or 5 μM cisplatin

B. Cell Cycle Regulators

1. p21

a) In the absence of drug treatment a significant increase in p21 was observed relative to the non-induced and control cells (Figure 3.21 A).

b) At 1 μM cisplatin treatment, a decrease in p21 of up to 0.4 fold was observed relative to the non-induced state (Figure 3.21 B).

c) At 5 μM cisplatin treatment, a significant increase in the cell cycle regulator p21 of $P<0.01$ relative to the control cells transfected with the empty vector was observed (Figure 3.21 B).

2. Cyclin D1

a) At 1 μM cisplatin treatment, an increase in cyclin D1 of 0.4 fold relative to the control was observed (Figure 3.22).

b) At 5 μM cisplatin treatment, an increase in the cyclin D1 of 0.2 fold relative to the non-induced state was observed (Figure 3.22).

3. PCNA

a) At 1 μM cisplatin treatment, the proliferating cell nuclear antigen (PCNA) showed a significant decrease of $P<0.01$ relative to the control cells transfected with the empty vector and $P<0.05$ relative to the non-induced state (Figure 3.23).

b) At 5 μM cisplatin treatment, PCNA showed a significant increase of $P<0.01$ relative to the non-induced state and the control (Figure 3.23).

Figure 3.21: Expression of p21 in pTRE2-Xrel3 (Int.) compared to the pTRE2 control +/- doxycycline and after 24 hours treatment with 1 and 5 μM cisplatin. *Figure (A)* shows the Western blot analysis of the proteins extracted from the pTRE2-Xrel3 (Int.) cells +/- doxycycline and without drug treatment. *Figure (B)* shows the Western blot analysis of pTRE2-Xrel3 (Int.) cells in comparison with the pTRE2 control clone +/- doxycycline and +/- with 1 and 5 μM cisplatin. Protein expression was quantified by measuring the optical density of the bands at medium exposure of the X-ray film and then dividing the values by the corresponding β-actin values. *Figure (C)* shows the corresponding densitometry analysis of the results. The values represent the mean ± standard deviation of 4 independent experiments. **P<0.01 is the statistical significance of the difference in p21 expression with Xrel3 induction at 5 μM cisplatin relative the control.

(A)

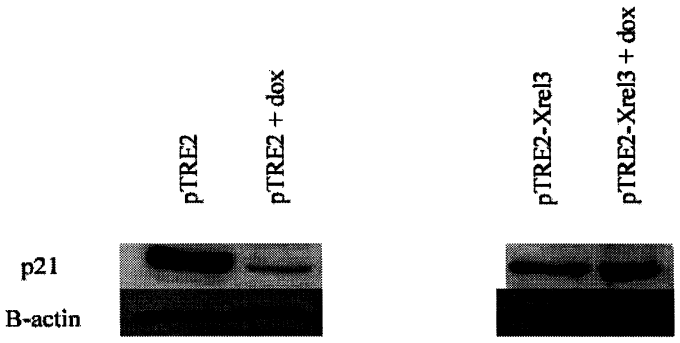
pTRE2
pTRE2 + dox
pTRE2-Xrel3
pTRE2-Xrel3 + dox
p21
B-actin

(B)

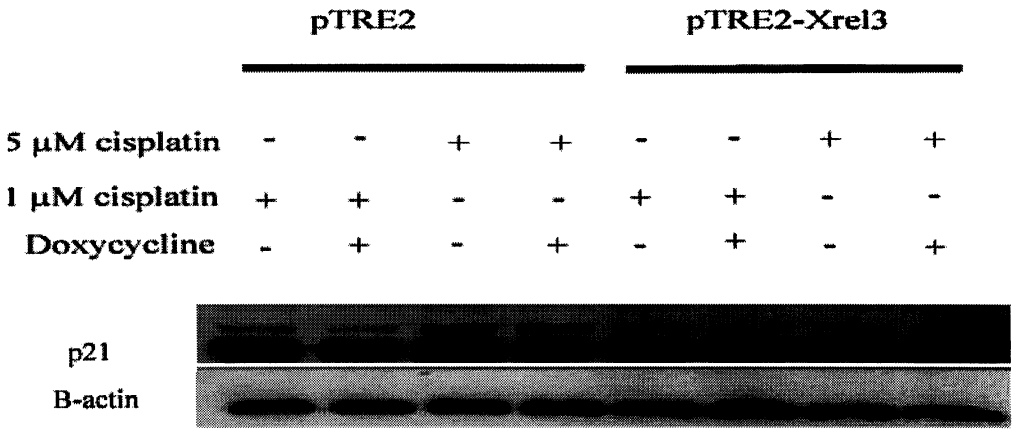
pTRE2
pTRE2-Xrel3
5 μM cisplatin - - + + - - + +
1 μM cisplatin + + - - + + - -
Doxycycline - + - + - + - +
p21
B-actin

(C)

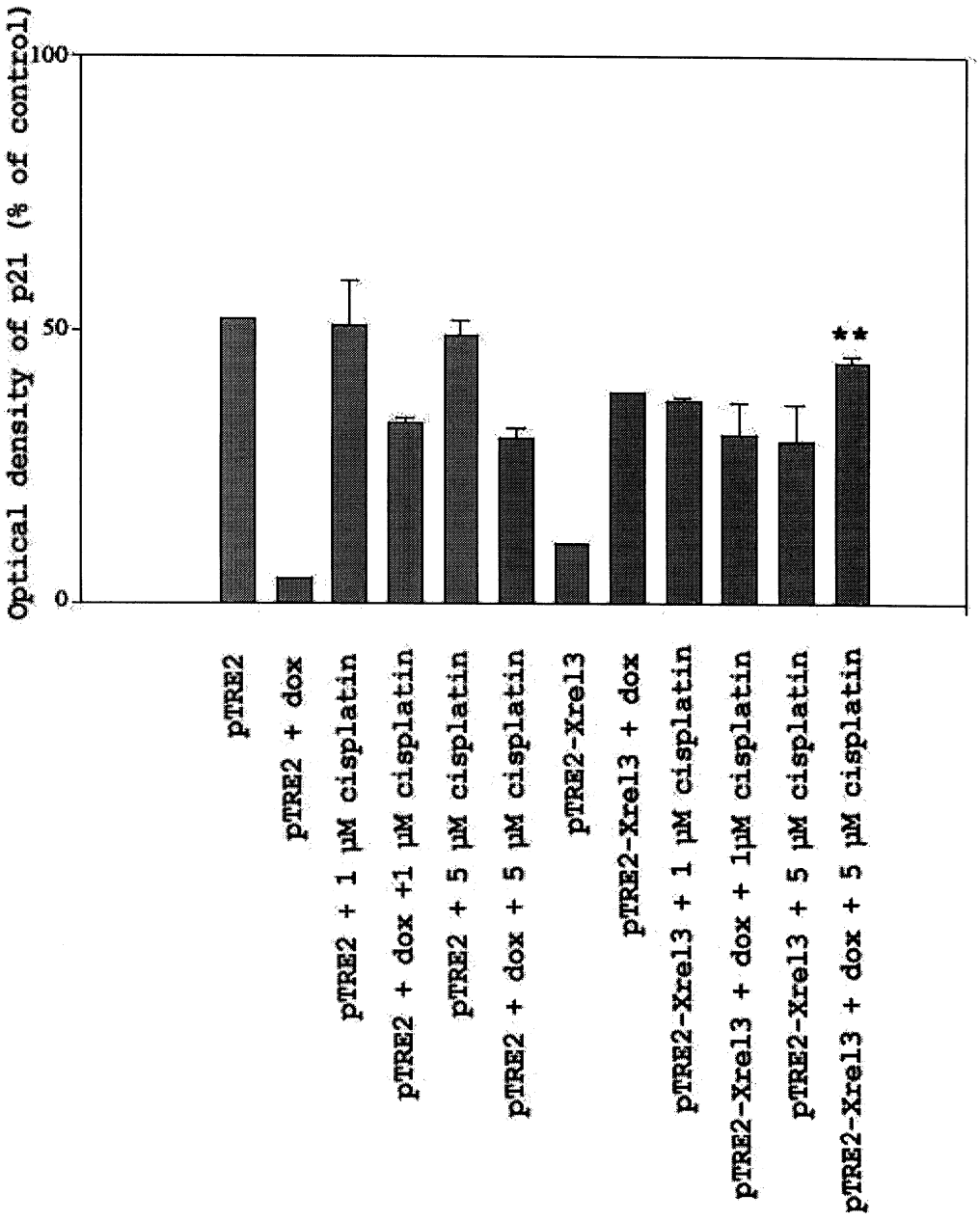
Optical density of p21 (% of control)
100
50
0
**
pTRE2
pTRE2 + dox
pTRE2 + 1 μM cisplatin
pTRE2 + dox +1 μM cisplatin
pTRE2 + 5 μM cisplatin
pTRE2 + dox + 5 μM cisplatin
pTRE2-Xrel3
pTRE2-Xrel3 + dox
pTRE2-Xrel3 + 1 μM cisplatin
pTRE2-Xrel3 + dox + 1μM cisplatin
pTRE2-Xrel3 + 5 μM cisplatin
pTRE2-Xrel3 + dox + 5 μM cisplatin

Figure 3.22: Expression of cyclin D1 in pTRE2-Xrel3 (Int.) compared to the pTRE2 control +/- doxycycline and after 24 hours treatment with 1 and 5 μM cisplatin. The *upper panel* shows the Western blot analysis of the proteins extracted after 24 hours of treatment with 1 and 5 μM cisplatin from pTRE2-Xrel3 (Int.) cells in comparison with the pTRE2 control cells +/- doxycycline. Protein expression was quantified by measuring the optical density of the bands at medium exposure of the X-ray film and then dividing the values by the corresponding β-actin values.

The *lower panel* shows the corresponding densitometry analysis of the results. The values represent the mean ± standard deviation of 3 independent experiments.

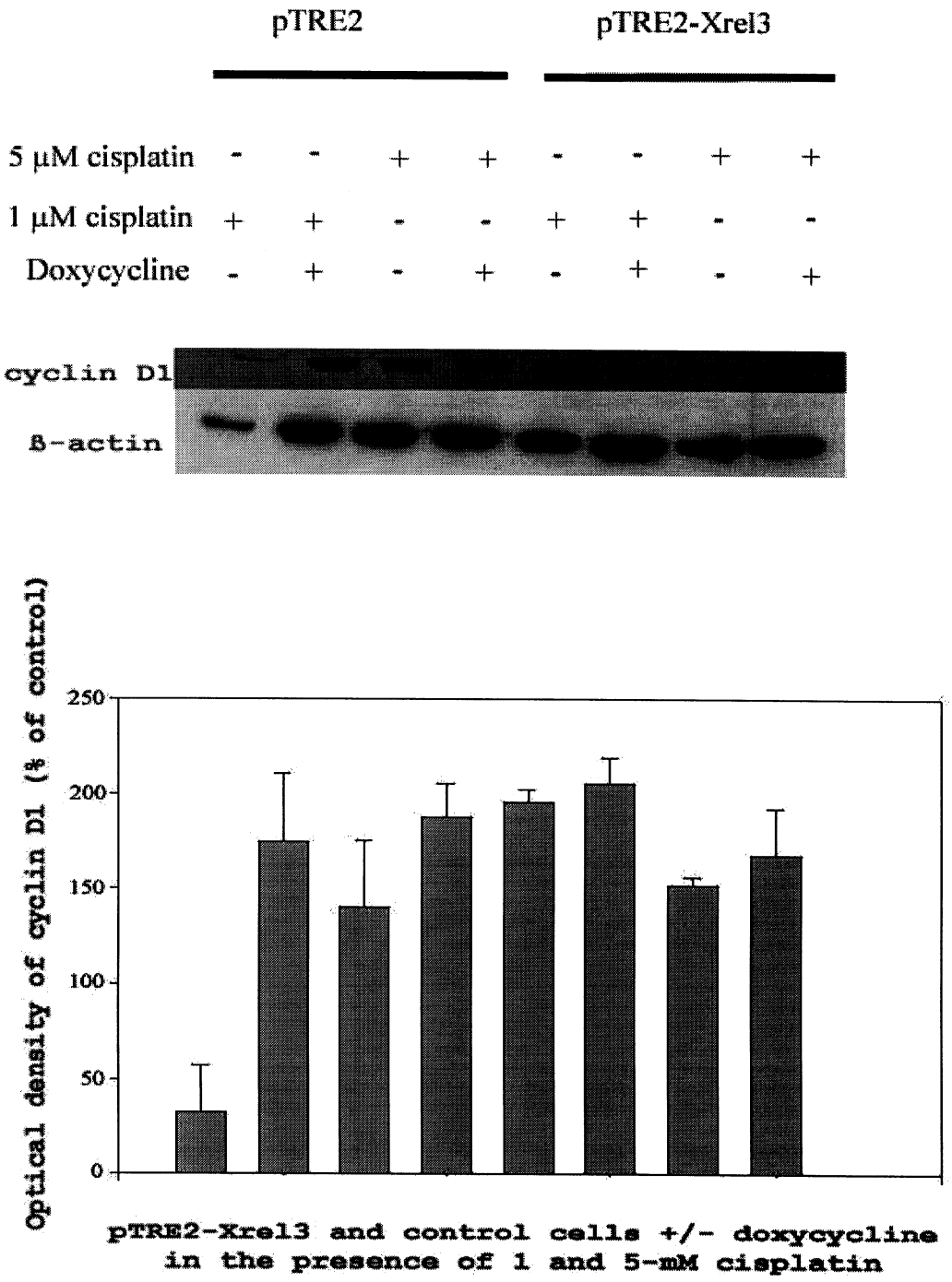
pTRE2
pTRE2-Xrel3
5 μM cisplatin - - + + - - + +
1 μM cisplatin + + - - + + - -
Doxycycline - + - + - + - +
cyclin D1
β-actin
Optical density of cyclin D1 (% of control)
250
200
150
100
50
0
pTRE2-Xrel3 and control cells +/- doxycycline
in the presence of 1 and 5-mM cisplatin

Figure 3.23: Expression of PCNA in pTRE2-Xrel3 (Int.) compared to the pTRE2 control +/- doxycycline and after 24 hours treatment with 1 and 5 μM cisplatin. The *upper panel* shows the Western blot analysis of the proteins extracted from pTRE2-Xrel3 (Int.) cells in comparison with the pTRE2 control cells +/- doxycycline. Protein expression was quantified by measuring the optical density of the bands at medium exposure of the X-ray film and then dividing the values by the corresponding β-actin values. The *lower panel* shows the corresponding densitometry analysis of the results. The values represent the mean ± standard deviation of 3 independent experiments. **P<0.01 is the statistical significance of the difference in PCNA expression with Xrel3 induction at 1 and 5 μM cisplatin relative to both the non-induced and the control.

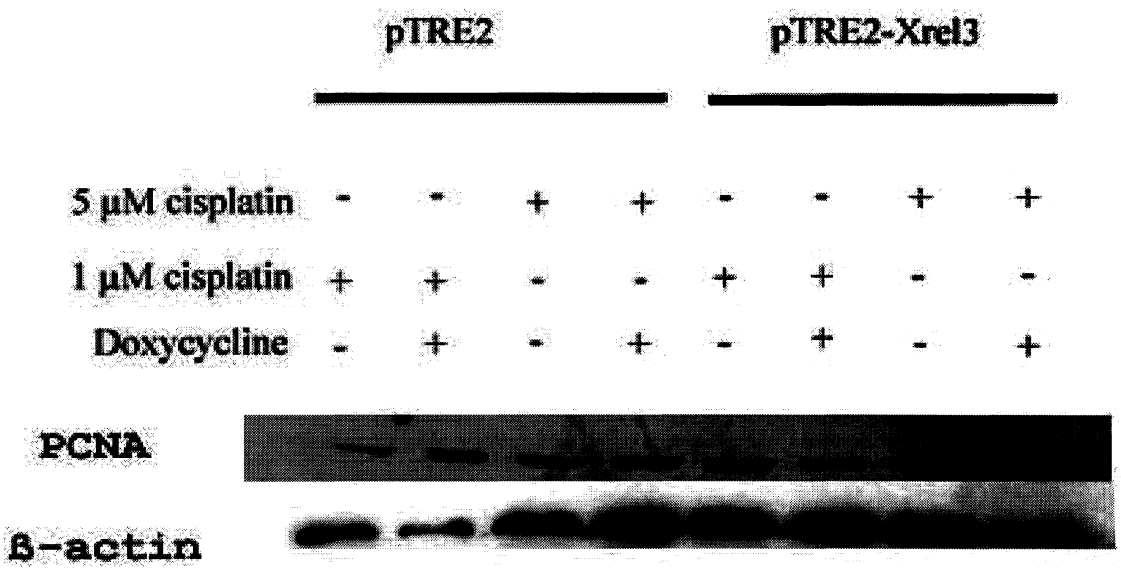
pTRE2
pTRE2-Xrel3
5 μM cisplatin - - + + - - + +
1 μM cisplatin + + - - + + - -
Doxycycline - + - + - + - +
PCNA
ß-actin

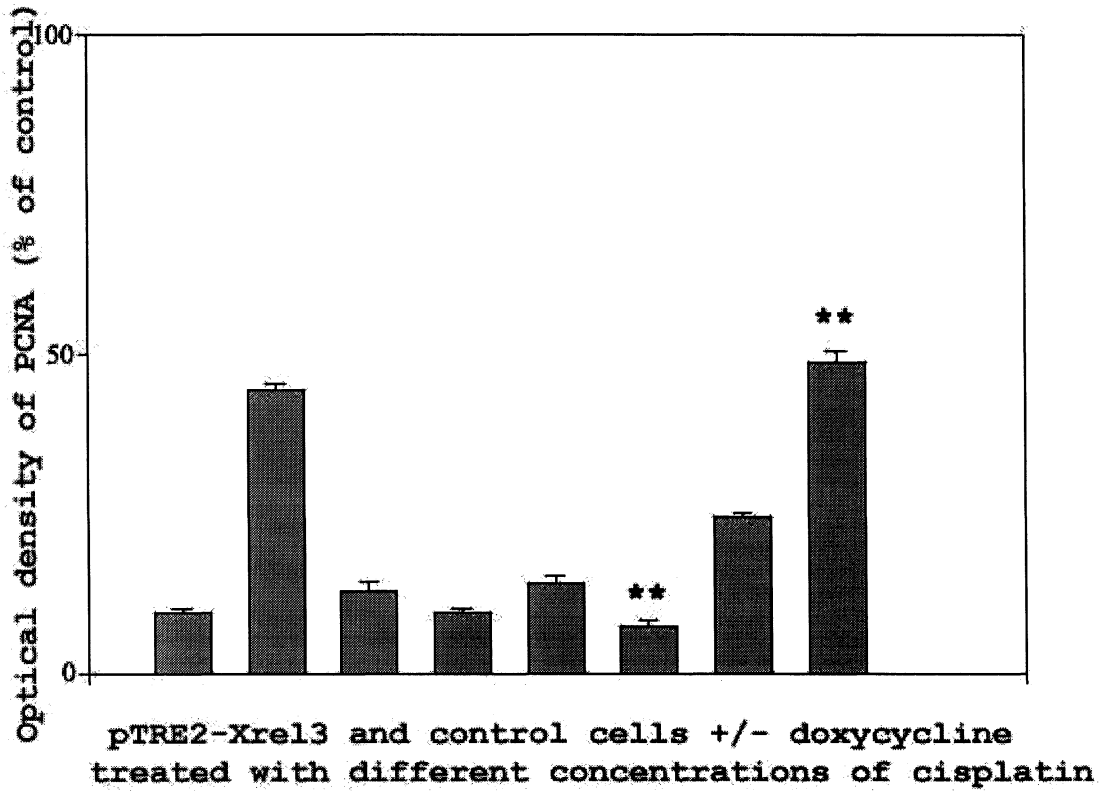
Optical density of PCNA (% of control)
100
50
0
**
**
pTRE2-Xrel3 and control cells +/- doxycycline
treated with different concentrations of cisplatin

C. Anti-apoptotic factors

BAG-1

a) At 1 μM cisplatin treatment, the p29 isoform of BAG-1 showed a significant increase of $P<0.05$ relative to the non-induced state and the control cells (Figure 3.25). Also the p33, p46 and p50 isoforms of BAG-1 showed a significant increase of $P<0.01$ relative to both the non-induced and control cells (Figure 3.24).

b) At 5 μM cisplatin treatment, the p29 isoform of BAG-1 showed a significant decrease of $P<0.01$ relative to the non-induced state (Figure 3.25). Also, the p33, p46 and p50 isoforms of BAG-1 showed an increase of $P<0.01$ relative to the non-induced state (Figure 3.24).

D. HPV 16/18 E6

No significant changes were observed in the 2 subunits at 1 μM cisplatin treatment +/- doxycycline (Figure 3.26).

Figure 3.24: Expression of BAG-1 p46 isoform in pTRE2-Xrel3 (Int.) compared to the pTRE2 control +/- doxycycline and after 24 hours treatment with 1 and 5 μM cisplatin. The *upper panel* shows Western blot analysis of the proteins extracted after 24 hours of treatment with 1 and 5 μM cisplatin from pTRE2-Xrel3 (Int.) cells in comparison with the pTRE2 control cells +/- doxycycline. The *lower panel* shows the corresponding densitometry analysis of the results. The values represent the mean ± standard deviation of 5 independent experiments.

** $P<0.01$ is the statistical significance of the difference in BAG-1 p46 isoform expression with Xrel3 induction relative to the non-induced state,

++$P<0.01$ is the statistical significance of the difference in BAG-1 p46 isoform expression with Xrel3 induction relative to the control.

Similar results were obtained for p33 and p50 isoforms of BAG-1.

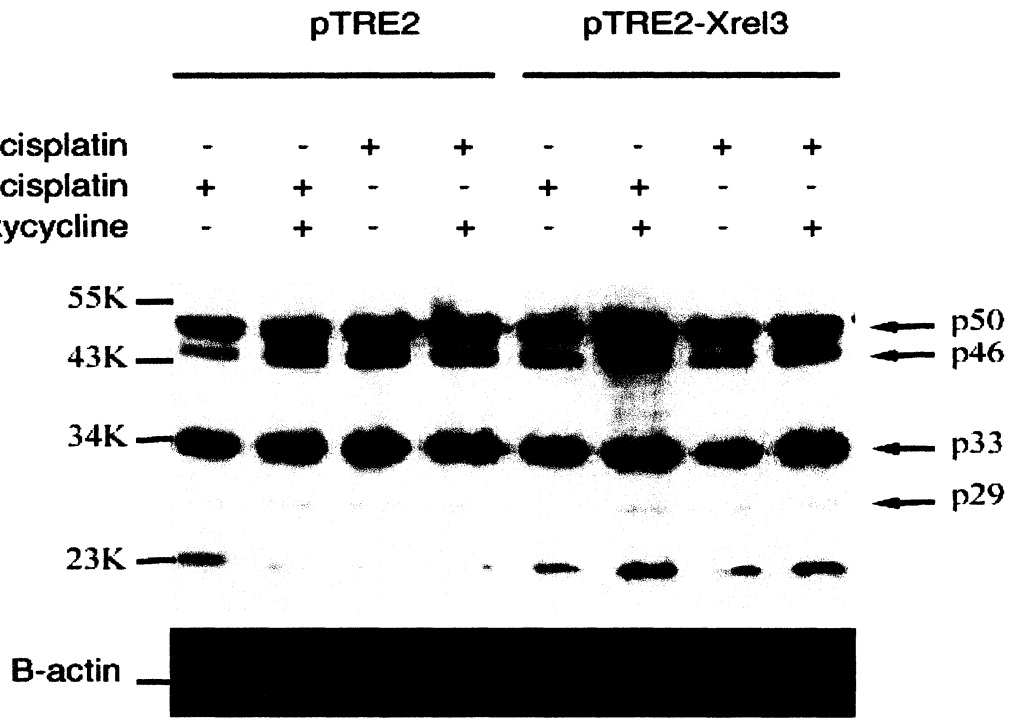
pTRE2
pTRE2-Xrel3
5 μM cisplatin - - + + - - + +
1 μM cisplatin + + - - + + - -
Doxycycline - + - + - + - +
55K
43K
34K
23K
B-actin
p50
p46
p33
p29

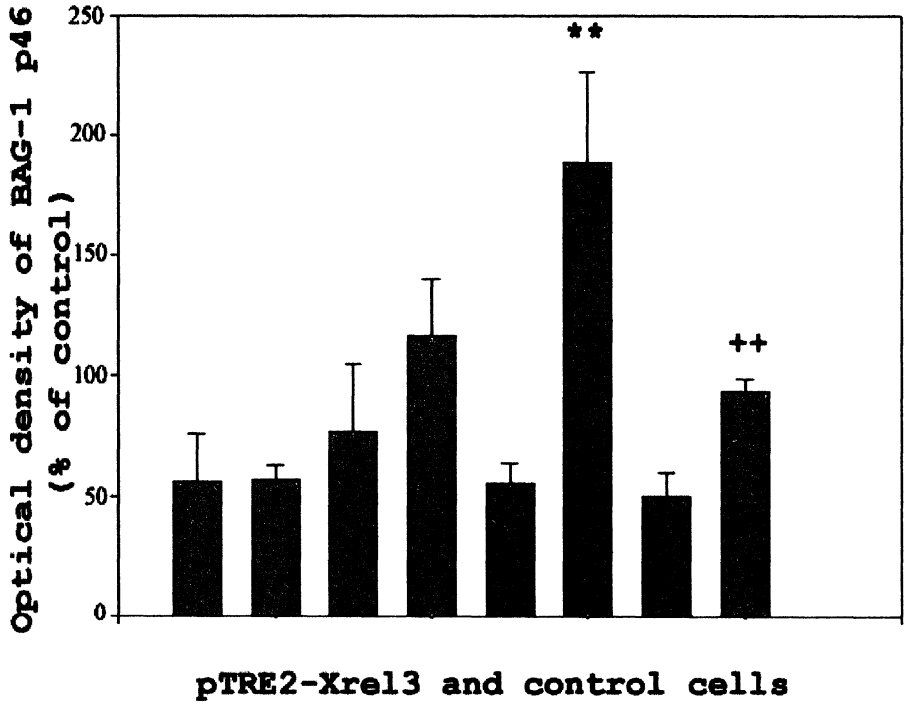
Optical density of BAG-1 p46 (% of control)
250
200
150
100
50
0
**
++
pTRE2-Xrel3 and control cells

Figure 3.25: Expression of BAG-1 p29 isoform in pTRE2-Xrel3 (Int.) cells compared to the pTRE2 control cells +/- doxycycline and after 24 hours treatment with 1 and 5 μM cisplatin. The result shows the corresponding densitometry analysis of the results. The values represent the mean ± standard deviation of 5 independent experiments.
** $P<0.01$ is the statistical significance of the difference in BAG-1 p29 isoform expression with Xrel3 induction relative to the non-induced state,
*$P<0.01$ is the statistical significance of the difference in BAG-1 p29 isoform expression with Xrel3 induction relative to the non-induced state.

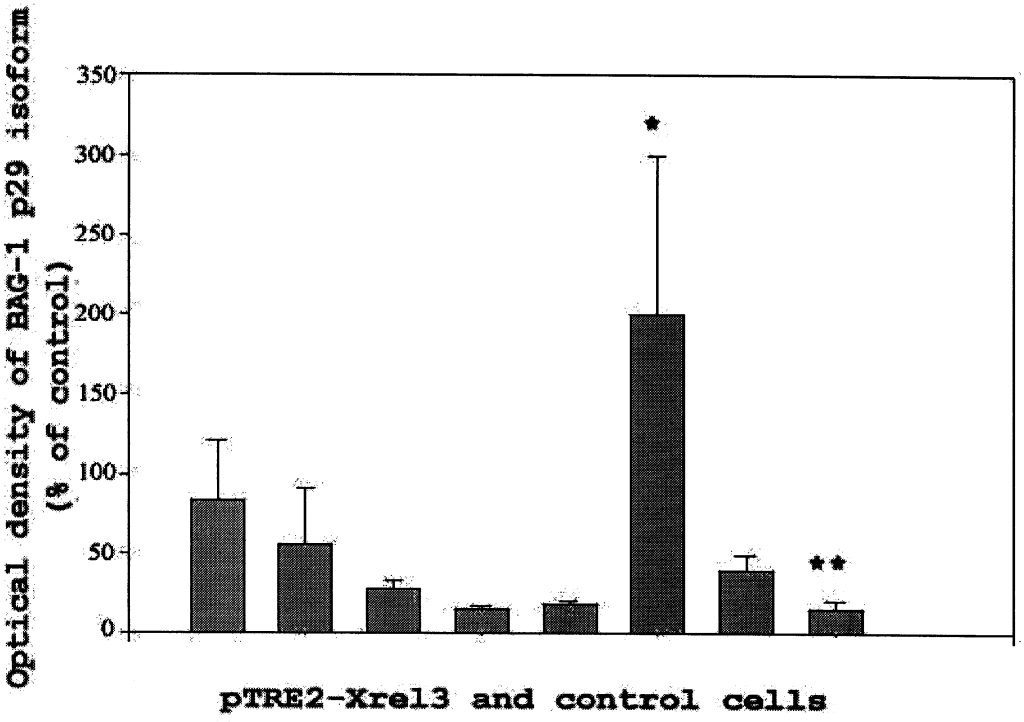
Optical density of BAG-1 p29 isoform
(% of control)
350
300
250
200
150
100
50
0
*
**
pTRE2-Xrel3 and control cells

Figure 3.26: Expression of HPV 16/18 E6 in pTRE2-Xrel3 intermediate level-expressing clone compared to the pTRE2 control +/- doxycycline and after 24 hours treatment with 1 and 5 μM cisplatin. The *upper panel* shows a Western blot analysis of the proteins extracted after 24 hours of treatment with 1 and 5 μM cisplatin from pTRE2-Xrel3 (Int.) cells in comparison with the pTRE2 control cells +/- doxycycline and +/- with 1 and 5 μM cisplatin. Protein expression was quantified by measuring the optical density of the bands at medium exposure of the X-ray film and then dividing the values by the corresponding β-actin values.
The *lower panel* shows the corresponding densitometry analysis of the results.

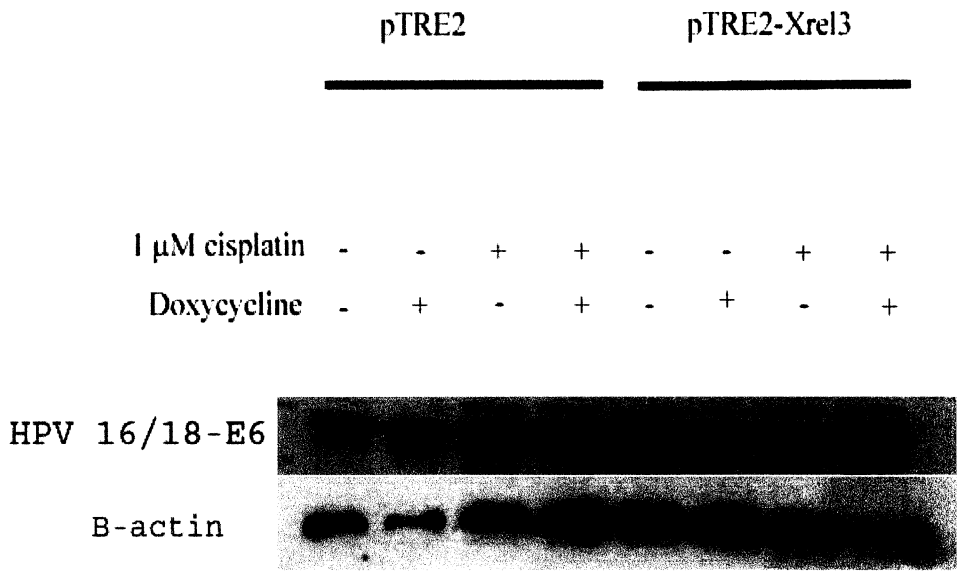

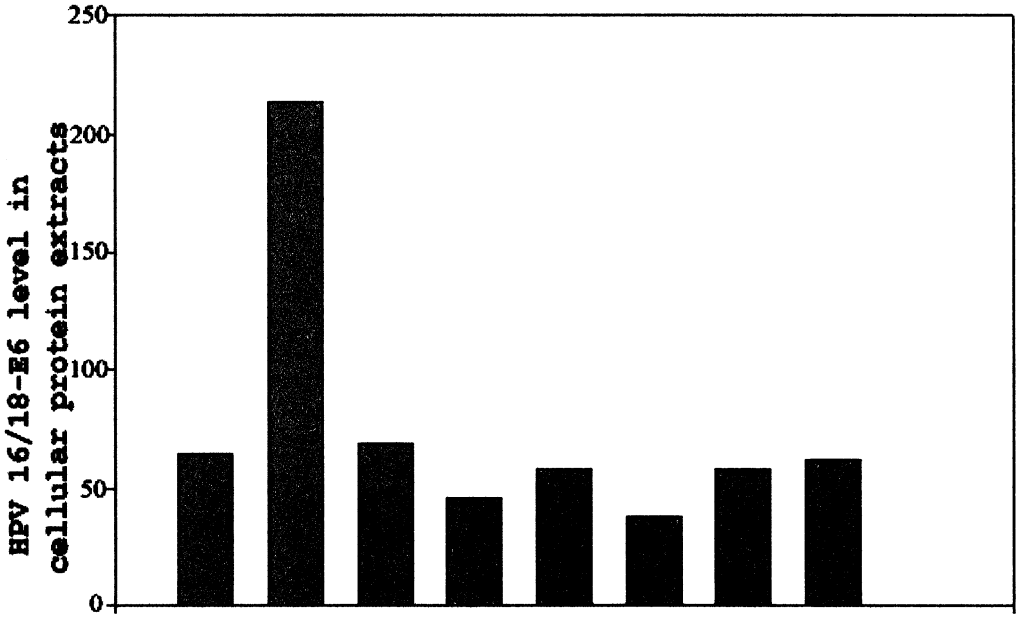

pTRE2 and pTRE2-Xrel3 +/- doxycycline and +/- 1 μM cisplatin

Summary: Effect of Xrel3 expression on HeLa cellular protein extracts

Apoptotic factors	No treatment	1 μM cisplatin	5 μM cisplatin
p53	Increase up to 4 fold compared to the non-induced state	Decrease up to 3 fold relative to the non-induced state.	Significant decrease $P<0.05$ relative to control.
Bax		Decrease $P<0.05$ relative to non-induced state.	Increase $P<0.05$ relative to control.
Bcl-2		Decrease $P<0.01$ relative to control and non-induced state.	Increase $P<0.01$ relative to control and non-induced state.
BCL-X_L		Decrease $P<0.01$ relative to control and $P<0.05$ relative to non-induced state.	Increase $P<0.01$ relative to control and $P<0.05$ relative to non-induced state.
Caspase-3		Decrease 0.3 fold relative to the non-induced state.	Increase $P<0.05$ relative to 1 μM cisplatin.
PARP	Increase $P<0.01$ relative to non-induced state and relative to the control	Increase up to 2 fold relative to the non-induced state.	Increase up to 3.1 fold relative to the non-induced state.
Caspase-8	Increase up to 6 fold relative to non-induced state	Decrease relative to control $P<0.05$	Increase $P<0.05$ relative to 1 μM cisplatin.
MDM-2		Decrease $P<0.01$ relative to both the non-induced state and to the control.	Increase $P<0.05$ relative to the non-induced state.

Cell cycle regulators			
p21	Increase relative to the non-induced and control cells.	Decrease up to 0.4 fold relative to the non-induced state.	Increase $P<0.01$ relative to control.
Cyclin D1		Increase 0.4 fold from control.	Increase 0.2 fold from non-induced state.
PCNA		Decrease $P<0.01$ relative to control and $P<0.05$ relative to non-induced state.	Increase $P<0.01$ relative to non-induced and the control.
Anti-apoptotic factors			
BAG-1		p29: Increase $P<0.05$ relative to both the non-induced and control cells. p33, 46, 50: Increase $P<0.01$ relative to both the non-induced and the control.	p29: Decrease $P<0.01$ relative to the non-induced state. p33, 46, 50: Increase $P<0.01$ relative to non-induced state.

Table 5: Modulation of the proteins by the effect of Xrel3

CHAPTER 4: DISCUSSION AND FUTURE DIRECTIONS

In this thesis, I wanted to determine the effect of *Xrel3* expression on HeLa cells in response to chemotherapeutic agents. Because of its homology to the mammalian *Rel/NF-κB* family and because of its effects in embryos, I speculated that *Xrel3* could have a role in promoting tumor formation. Its ability to support the survival of HeLa cells in the presence of 1 μM cisplatin indicated that it has a tumor-promoting activity by inhibiting apoptosis under mild-moderate stress conditions.

The objectives of this study were:

1. **Generation of *Xrel3* inducible system.** This was accomplished by creating an inducible Tet-On system that was capable of inducing the expression of *Xrel3* gene that is located downstream of the tet promoter. My results show a clear induction of Xrel3 from a baseline of no expression in at least 4 transfected pTRE2-Xrel3 clones (Figure 3.6). This inducible system is a convenient way of studying *Xrel3* expression as it allows *Xrel3* expression only upon the addition of doxycycline.

2. **To examine the effect of *Xrel3* expression on growth**. The growth of HeLa cervical cells expressing *Xrel3* was compared to similar cells not expressing *Xrel3*. The results of the growth assays were also compared to HeLa cells transfected with just the empty vector, which served as a control. In these experiments, I found that High and Low expressing clones did show a growth differential, but the Intermediate expressing clone showed the greatest growth inhibition in the presence of *Xrel3*. The reason behind these observations might be due to the slight differences in the genomic sequence encountered after the insertion of *Xrel3* into the HeLa cellular genome. Slight changes even by 1 or 2 nucleotides might have a great impact on gene expression and activity (Gerondakis *et al.,* 1999).
3. **To examine the effect of *Xrel3* on the growth of cisplatin treated HeLa cells**. I found that at 1 μM cisplatin, *Xrel3* provided an anti-apoptotic effect after 24 hours of treatment. This was based on the significantly lower levels of the apoptotic proteins, Bax ($P<0.05$), caspase-8 ($P<0.05$) and MDM-2 ($P<0.01$). Furthermore, the level of the tumor suppressor protein p53 was suppressed up to 3-fold, along with a reduction of caspase-3 and p21, as well. The anti-apoptotic

BAG-1 isoforms ($P<0.01$) were also upregulated. However, after 24 hours of 5 μM cisplatin treatment, a significant increase in the levels of the pro-apoptotic proteins was seen relative to controls. These included: Bax ($P<0.05$), MDM-2 ($P<0.05$), the cell cycle inhibitor p21 ($P<0.01$), cleaved PARP, caspase-8, and caspase-3. However, p53 was significantly decreased ($P<0.05$). BCL-2 ($P<0.01$) and BCL- X_L ($P<0.01$) were elevated significantly. The anti-apoptotic protein BAG-1 remained constant ($P<0.01$) in cisplatin-treated Xrel3-expressing cells. Despite the upregulation of BAG-1, the balance shifted towards apoptosis by the increased expression of the pro-apoptotic proteins.

4.1 Tet-On system and Xrel3 expression

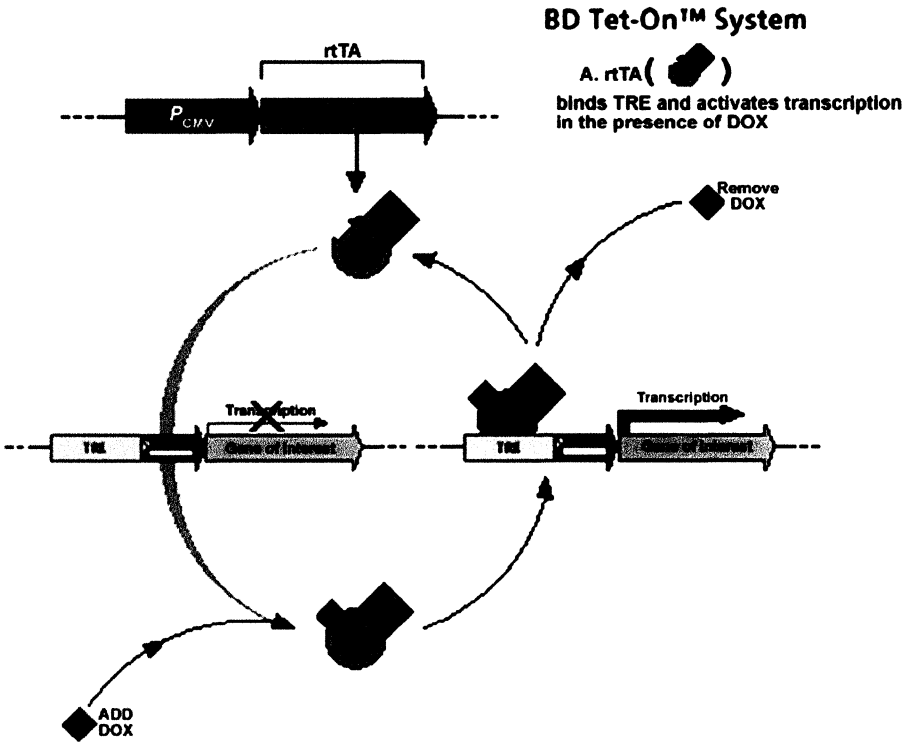

Figure 4.1: The mechanism of action of the Tet-On system (adapted from BD Biosciences Clontech catalog, 2003). The reverse tetracycline-controlled trans-activator (rtTA) induces transcription of the gene of interest only in the presence of doxycycline (1 μg/ml). The rtTA is in turn composed of the activation domain, VP16, and the reverse tet-repressor protein, rtetR sequences. The rtTA then binds the tetracycline-responsive element (TRE) and activates transcription in the presence of doxycycline.

The double-stable transfection of HeLa Tet-On cells with Xrel3 showed positive transcription of *Xrel3* as detected by Northern blotting. The rest of the clones were excluded because they expressed spurious sequences or exhibited leaky transcription, perhaps due to the integration of the transgene in a location on the heterochromatin that is of a high transcriptional activity (Alarcon *et al.,* 1999).

4.2 Effect of Xrel3 expression on growth

The expression of Xrel3 in the double-stable HeLa cell line transfected with pTRE2-Xrel3 was found to be associated with a significant decline in the rate of growth of cells as seen in 6 independent experiments. This decline was seen in all of the three selected clones with different levels of Xrel3 expression, that is, the highest-level, intermediate-level and lowest-level expressing clones. This decline was in comparison to the non-induced state when no doxycycline was added. As mentioned before, Xrel3 is a homolog of cRel, which is a member of the Rel/NF-κB family. However, NF-κB is not normally expressed in HeLa cells (Gerondakis *et al.,* 1999). It is interesting, therefore, that the stable integration and expression of Xrel3 in

HeLa cells caused their rate of growth to slow down in comparison to control cells transfected with pTRE2 vector. The decline in growth in the Xrel3-expressing clone was significant starting on day 3 in all of the tested clones, initiated with 4×10^4 cells seeded/well in 6-wells plates. This means that a lag period of 3 days was a consistant observation in all of the examined clones. This might be attributed to the anti-apoptotic effects of the Rel/NF-κB family and its ability to promote cell survival under mild-moderate stress conditions (See Introduction).

The intermediate-level expressing clone exhibited the highest differences in cell growth with and without induction as compared to the highest and lowest-Xrel3 expressing clones. The decline in the growth rate of HeLa cells after Xrel3 expression might be attributed to the ability of NF-κB to induce the expression of the cell cycle inhibitor p21 (Seitz *et al.,* 2000; Seitz *et al.,* 1998). My results showed a dramatic increase in p21 in the HeLa-transfected cells after induction of Xrel3 expression by doxycycline as compared to the decrease in p21 level in the untransfected cells induced by doxycycline. These observations were supported by previous findings. For example, the NF-κB subunits were found to arrest the growth of normal epithelial cells and this growth arrest was found to be coupled with high

$p21^{Cip1}$ expression (Seitz *et al.,* 2000; Seitz *et al.,* 1998). The p21 protein is one of the cell cycle regulators known to block the G1/S transition of the cell cycle and prevent aneuploidy by increasing the cell doubling time and G1-arrested cell cycle (for review, see Rich *et al.,* 2000; Chen *et al.,* 1996).

Interestingly, I also found that the cleaved PARP dramatically increased in Xrel3-expressing HeLa cells as compared to the non-induced and control cells. This suggests that the cells are undergoing extensive DNA repair (for review, see Rich *et al.,* 2000), thus cell exhaustion and decline in growth rate might be the possible consequences.

Another possible explanation is that the cells might be on the first steps of undergoing apoptosis. My results showed an increase in the caspase-8 catalytic subunit levels, which is used as an indicator of apoptosis, up to 6 fold relative to the non-induced pTRE2-Xrel3 transfected HeLa cells (for review, see Rich *et al.,* 2000). Caspase-8 is known to be a key molecule in the initiation of apoptosis (for review, see Krammer, 2000; Hengartner, 2000).

Furthermore, overexpression of c-Rel was found to be associated with apoptosis in bone marrow cells in vitro (Abbadie *et al.,* 1993) and in stably transfected HeLa cells depending on the stimulus (Kaltschmidt *et al.,* 2000).

Thus, the increased levels of p21 and consequent growth arrest followed by activation of caspase-8 might be the first steps in initiating apoptosis by Xrel3 overexpression. Further studies could be done to directly assay apoptosis using other cellular means such as TUNEL, TB exclusion and DNA fragmentation assays.

4.3 Effect of Xrel3 expression on cisplatin-treated HeLa cells.

Results of the cell viability assays showed lower numbers of cells surviving when Xrel3 was expressed in HeLa cells treated with 1 μM cisplatin over a period of six days as compared to the non-induced HeLa cells and control cells. The decline in the number of cells started to be significant on the third day of 1 μM cisplatin treatment. This might indicate that Xrel3 expression chemosensitizes the cells to cisplatin. However, this chemosensitization was not apparent on day 1 or day 2 of the experiment, but it started to appear on day 3 and continued till day 6 of the experiment. In previous studies, Rel/NF-κB was shown to provide a protective effect to the cells in response to stress (for review, see Chen *et al.,* 1998; Verma *et al.,* 1995). Rel/NF-κB is known to promote cell survival (Liou et Baltimore, 1993; May and Ghosh, 1998). These cell-survival effects of Rel/NF-κB

might be the reason behind the lag period of 2 days before a prominent chemosensitization was clear in HeLa cells.

With prolonged exposure to 1 μM cisplatin, chemosensitization was observed. It is possible that prolonged cisplatin exposure might initiate other apoptotic mechanisms that override the protective effect of Xrel3. I tried to examine the effect of 5 μM cisplatin on cell viability, but the cells showed such a fast rate of killing in the first 3 days that I could not examine whether Xrel3-induced chemosensitization will start from day 1 when the cells were exposed to a more potent dose stimulus.

NF-κB-induced chemosensitization is supported by previous research in the field. For example, NF-κB and AP-1 were found to stimulate the expression of the pro-apoptotic Fas ligand (Fas) protein and this was in direct response to chemotherapeutic drug treatment or T-cell activation signals (Baldwin, 2001; Barkett and Gilmore, 1999). Furthermore, NF-κB activation played a significant role in doxorubicin-induced apoptosis (Muller *et al.,* 2003) and in paclitaxel-induced apoptosis (Huang *et al.,* 2000). Still, in my experiments, the intermediate Xrel3-expressing clone showed the greatest variation on the growth curve +/- doxycycline after 1 μM cisplatin treatment, thus following a similar pattern to the growth curves without drug

treatment. These results and conclusions were based on 6 independent experiments, all of which showed the same pattern.

4.4 Modulation of protein expression by Xrel3 overexpression.

The overexpression of Xrel3 caused an anti-apoptotic effect on HeLa cells treated with 1 μM cisplatin for 24 hours. However, when HeLa cells were treated with 5 μM cisplatin for 24 hours, Xrel3 over expression caused an apoptotic effect synergistic to cisplatin when compared to the non-induced Xrel3-transfected HeLa cells and the control cells transfected with the empty vector.

Previous studies have shown that NF-κB might have an anti-apoptotic or a pro-apoptotic effect depending on the nature of the stimulus to which the cell is exposed (Kaltschmidt, 2000). The levels of the different proteins examined gave some insight on the possible mechanism of action of c-Rel overexpression in cisplatin-treated HeLa cells. When no drug was added, Xrel3 provided a cell survival and a protective effect to HeLa cells and this effect was demonstrated by slowing the growth of the cells as illustrated in the growth assays and the induction of p21, which promotes cell cycle arrest. Therefore, the cells may be protected from undergoing apoptosis by the

replicating cells that acquire more damage to their replicating DNA. Also Xrel3 provided an initial anti-apoptotic effect when the cells were treated with 1 μM cisplatin as measured by the expression of pro- and anti-apoptotic markers; however, with prolonged exposure to the 1 μM cisplatin or with 5 μM cisplatin, Xrel3 exhibited an apoptotic effect synergistic with the cisplatin and therefore caused chemosensitization of HeLa cells.

4.4.1 Xrel3 effect on protein expression at 1 μM cisplatin-treated HeLa cells.

The modulation of the different proteins expressed after 24 hours of 1 μM cisplatin-treated cells by the effect of Xrel3 suggests a mechanism of action of Xrel3. This was shown by the significant upregulation of anti-apoptotic factors and downregulation of apoptotic factors as follows:

1. A significant decrease in the apoptotic protein Bax ($P<0.05$) relative to the non-induced state.
2. A significant decrease in caspase-8 protein catalytic subunit (55-kDa) of the pro-apoptosis cascade ($P<0.05$) relative to the control cells was seen. The catalytic subunit is an indicator of active apoptosis.

3. Caspase-3 levels of the cleaved product at 17-kDa were decreased 0.3 fold relative to the non-induced state.
4. The tumor suppressor protein p53, showed a decrease of up to 3 fold indicating that NF-κB is potentiating the anti-apoptotic effect and promoting cell survival.
5. MDM-2, which is a p53-induced protein was significantly decreased ($P<0.01$) as is expected.
6. The BAG-1 anti-apoptotic isoforms p33, p46, p50 were found to be significantly increased presumably to promote survival and inhibit apoptosis.
7. Interestingly, p21 levels were decreased when HeLa cells were exposed to 1 μM cisplatin treatment, indicating that Xrel3 was working hard to prevent apoptosis and promote cell cycle progression and cell survival in response to the stimulus threatening the cells. But when no drug treatment was applied, NF-κB caused an induction of p21 levels in an attempt to arrest further cell growth and protect the cells from overproliferation. Thus, a decline in the growth rate was observed on day 3 of the experiment

8. The poly(ADP-ribose) polymerase , PARP, was increased up to 2 fold, perhaps cooperating with other factors in repairing the damage that is happening to the DNA by the effect of the 1 μM cisplatin treatment.
9. Cyclin D1, which is a cell cycle regulator showed a slight increase indicating that the cells are undergoing proliferation and mitosis. Cyclin D1 is known to be significantly upregulated in cancers (Yu *et al.,* 2001). However, recent studies have associated cell cycle arrest with high levels of cyclin D1 (Pratt and Niu, 2003).
10. The proliferating cell nuclear antigen (PCNA) levels were significantly decreased ($P<0.01$) relative to control and ($P<0.05$) relative to the non-induced state. This protein is responsible for proliferation and is usually upregulated in cancers. However, statistical studies have found that a high PCNA score has no significance in predicting chemosensitization or cell survival (Botti *et al.,* 1993).
11. The E6 oncoprotein expressed by HPV-16/18 showed no significant changes in both the Xrel3-expressing clone and the control.

Thus, at moderate stress levels, the molecular response of cells that express Xrel3 suggests a possible anti-apoptotic and cell survival effect. This was reinforced by the upregulation of the anti-apoptotic markers (BAG-1) and the downregulation of the pro-apoptotic markers (Caspase-3, Caspase-8, Bax, Bcl-2, p53, Mdm-2).

4.4.2 Xrel3 effect on protein expression at 5 μM cisplatin-treated HeLa cells.

The overexpression of Xrel3 demonstrated a synergistic apoptotic effect to the cisplatin when HeLa cells were treated with 5 μM cisplatin for 24 hours as assayed by marker expression analyses. The chemosensitization of HeLa cells to cisplatin after Xrel3 expression was clearly supported by the significant upregulation of the apoptotic proteins: caspase-3, caspase-8, Bax and MDM-2. Also p21, which is a cell cycle inhibitor, was upregulated significantly relative to the control cells transfected with the empty vector. The cleaved PARP level was increased up to 3.1 folds compared to the non-induced state. Interestingly, we found that p53 levels remained low and after 5 μM cisplatin treatment, the decrease in p53 levels became significant compared to the control cells transfected with just the empty vector. Recent

studies showed that tumor cells expressing high levels of p53 showed poor response to cisplatin treatment and consequent resistance (Nakayama *et al.,* 2003). Thus, the low levels of p53 caused by Xrel3 overexpression might be the reason behind the Xrel3-induced chemosensitivity. Another possible explanation of the chemosensitization is the ubiquitin-mediated degradation of p53 by the HPV18 E6 protein when HeLa cells were exposed to a more potent stimulus (5 μM cisplatin) (Cohen *et al.,* 2003). This idea is supported by the significantly high levels of MDM-2, which might have been induced by p53.

Another possible reason behind the low p53 levels is the high level of Bcl-2. Recent data showed that overexpression of Bcl-2 suppresses p53 expression (Jiang and Milner, 2003). My results showed that the anti-apoptosis BAG-1 p33, p46 and p50 protein isoforms levels remained significantly high after 5 μM cisplatin treatment. In contrast, there was a significant increase in the levels of Bcl-2 and Bcl-X_L relative to both the non-induced and control cells. Bcl-2 and Bcl-X_L are known anti-apoptotic factors, which promote cell survival and protect the cells from apoptosis (Shinoura *et al.,* 2000). However, recent research data provided evidence of the ability of Bcl-2 and Bcl-X_L to delay the cell cycle progression induced

by myc (Greider *et al.,* 2002). As previously mentioned, one of the mechanisms of action of NF-κB, as an anti-apoptotic protein, is the upregulation of myc (for review, see Foo and Nolan, 1999; Chen *et al.,* 1998). Strikingly, I found that Bcl-2 and Bcl-X_L levels increased significantly after 5 μM cisplatin treatment, when the cells are purportedly undergoing apoptosis. Therefore, overexpression of Bcl-2 and Bcl-X_L might contribute to the p53 suppression-mediated cell growth arrest and the synergistic apoptotic effect induced by Xrel3. Previous studies have shown that induction of Bcl-2 in glioblastoma cells promoted apoptosis (Shinoura *et al.,* 2000).

In conclusion, my results indicate that high concentrations of cisplatin cause significant upregulation of the apoptotic factors Bax, MDM-2, caspase-3 and caspase-8. Despite the upregulation of the anti-apoptotic factor BAG-1 isoforms by cisplatin and Xrel3 expression, the balance shifted towards apoptosis and a synergistic effect was achieved in promoting cell death by NF-κB when coupled with cisplatin. The study of the modulation of the different proteins expressed in response to Xrel3 expression provides new insights into the possible mechanism of action of

Rel/NF-κB in cell survival and apoptosis in response to chemotherapeutic drugs.

4.5 Future Directions

The HeLa-Tet On double transfected stable cell lines provide a powerful way of examining the effect of expression of any gene of interest inserted into the genome of HeLa cells. The expression of the gene of interest is simply turned on by the addition of doxycycline. However, no expression is detected in the absence of doxycycline. After examining the modulation of proteins caused by Xrel3 induction, more experiments are required to confirm and support the results obtained.

The following experiments can be done:

1. Detection of Fas, which is a marker of apoptosis mediated by the TNF receptor family. If Fas is detected when Xrel3 is expressed in the HeLa cells, it will support our results of the ability of Xrel3 to induce apoptosis.

2. Gene microarray technology is a highly sophisticated method in determining which genes, other than the ones I examined, might be turned on when Xrel3 is overexpressed. The knowledge of the concomittant expression of different genes might give a clear

representation of the pathways involved in cell survival and apoptosis induced by Xrel3. It will also allow understanding of the factors that shift the function of *Xrel3* from cell protection and promotion of survival to one of inducing cell death and apoptosis. This might be essential in targeting NF-κB for clinical therapeutic purposes.

3. The possible utilization of a different control than the empty vector. For example, a control that inhibits NF-κB translocation to the nucleus like IκB, might serve as a good control. Therefore, HeLa cells will be transfected with the same pTRE2-Xrel3 plasmid, but the control cells will be transfected with or without the pTRE2-Xrel3 plasmid with IκB in order to prevent the activation of NF-κB. In this case, the effects of induction and inhibition of NF-κB can be examined.

4. Examine the dose-response curve using various concentrations of cisplatin on different cell lines when NF-κB is activated and then determining the concentration associated with the shortest time required to achieve effective killing. Achieving tumor cell specificity is important for therapeutic purpose.

5. Examine other chemotherapeutic drugs belonging to different classes, for example: alkylating agents, nitrogen mustards, plant alkaloids and the miscellaneous group. These experiments will determine whether the other drugs affect the growth, apoptosis and expression of apoptosis regulating proteins of HeLa cells expressing or not expressing Xrel3 similarly to cisplatin or they show different responses depending on the group from which they are derived.

CHAPTER 5 REFERENCE LIST

Abbadie,C., Kabrun,N., Bouali,F., Smardova,J., Stehelin,D., Vandenbunder,B., & Enrietto,P.J. (1993). High levels of c-rel expression are associated with programmed cell death in the developing avian embryo and in bone marrow cells in vitro. Cell, 75(5), 899-912.

Adams,J.M., & Cory,S. (1998). The Bcl-2 Protein Family: Arbiters of Cell Survival. Science, 281, 1322-1326.

Alarcon,C.M., Pedram,M., Donelson,D.E. (1999). Leaky transcription of variant surface glycoprotein gene expression sites in bloodstream african trypanosomes. Journal of Biological Chemistry, 274(24),16884-16893.

Anonymous. (2002). Platinum compounds. British Medical Association,The Royal Pharmaceutical Society of Great Britain.

Ashkenazi,A., & Dixit,V.M. (1998). Death receptors: Signalling and Modulation. Science, 281, 1305-1308.

Baeuerle,P.A., & Baltimore,D. (1988). IκB: A Specific Inhibitor of the NF-κB Transcription Factor. Science, 242, 540-546.

Baldwin,A.S. (2001). Control of angiogenesis and cancer therapy resistance by the transcription factor NF- κB . The Journal of Clinical Investigation, 107, 241-246.

Barkett,M., & Gilmore,T.D. (1999). Control of apoptosis by Rel/NF- κB transcription factors. Oncogene, 18, 6910-6924.

Bash,J., Zong,W.X., Banga,S., Rivera,A., Ballard,D.W., Ron,Y., & Gelinas,C. (1999). Rel/NF- κB can trigger the Notch signaling pthway by inducing the expression of Jagged1, a ligand for Notch receptors. The EMBO Journal, 18, 2803-2811.

Bassuk,A.G., Anandappa,R.T., Leiden,J.M. (1997). Physical interactions between Ets and NF-kappaB/NFAT proteins play an important role in their cooperative activation of the human immunodeficiency virus enhancer in T cells. Journal of Virology, 71(5), 3563-3573.

Becton,D. (2003). The mechanism of action of the Tet-On system.

Beg,A.A., & Baldwin Jr.,A.S. (1993). The IκB proteins: multifunctional regulators of Rel/NF-κB trancription factors. Genes and Development, 7, 2064-2070.

Bennett,M.R., Macdonald,K., Chan,S.W., Boyle,J.J., Weissberg, P.L. (1998). Cooperative Interactions Between RB and p53 Regulate Cell Proliferation, Cell Senescence, and Apoptosis in Human Vascular Smooth Muscle Cells From Atherosclerotic Plaques. Circulation Research.;82:704-712.

Boise,L.H., Gottschalk,A.R., Quintans,J., & Thonpson,C.B. (1995). Bcl-2 and Bcl-2-related proteins in apoptosis regulation. Curr Top Microbiol Immunol., 200, 107-121.

Botti,G., Chiappetta,G., Aiuto,G., Angelis,E., Matteis,A., Montella,M., Picone,A., & Cascione,F. (1993). PCNA/cyclin and P-glycoprotein as prognostic factors in locally advanced breast cancer. An immunohistochemical, retrospective study. Tumori, 79, 214-218.

Boyd,J.M., Gallo,G.J., Elangovan,B., Houghton,A.B., Malstrom,S., Avery,B.J., Ebb,R.G., Subramanian,T., Chittenden,T., & Lutz,R.J. (1995). Bik, a novel death-inducing protein shares a distinct sequence motif with Bcl-2 family proteins and interacts with viral and cellular survival-promoting proteins. Oncogene, 11(9), 1921-1928.

Bukowski,R.M., Rayman,P., Uzzo,R., Bloom,T., Sandstrom,K., Peereboom,D., Olencki,T., Budd,T., McLain,D., Elson,P., Novick,A., & Finke,J.H. (1998). Signal Transduction Abnormalities in T Lymphocytes from Patients with Advanced Renal Carcinoma: Clinical Relevance and Effects of Cytokine Therapy. Clinical Cancer Research, 4, 2337-2347.

Bushdid,P.B., Brantley,D.M., Yull,F.E., Blaeuer,G.L., Hoffman,L.H., Niswander,L., & Kerr,L.D. (1998). Inhibition of NF-kappaB activity results in disruption of the apical ectodermal ridge and aberrant limb morphogenesis. Nature, 392, 615-618.

Castellsague,X., Bosch,F.X., & Munoz,N. (2002). Environmental co-factors in HPV carcinogenesis. Virus Research, 89, 191-199.

Castranova,V., Chen,F., Shi,X., & Demers,L.M. (1998,1999). New Insights into the Role of Nuclear Factor- κB, a Ubiquitous Transcription Factor in the Initiation of Diseases. Clinical Chemistry, 45, 7-17.

Chen,F., Castranova,V. & Shi,X. (2001). New Insights into the Role of Nuclear Factor- κB in Cell Growth Regulation. American Journal of Pathology, 159, 387-397.

Chen,J., Willingham,T., Shuford,M., Bruce,D., Rushing,E., Smith,Y., & Nisen,P.D. (1996). Effects of ectopic overexpression of p21(WAF1/CIP1) on aneuploidy and the malignant phenotype of human brain tumor cells. Oncogene, 13(7), 1395-1403.

Christensen,J.G., Romach,E.H., Healy,L.N., Gonzales,A.J., Anderson,S.P., Malarkey,D.E., Corton,J.C., Fox,T.R., Cattley,R.C., & Goldsworthy,T.L. (1999). Altered Bcl-2 family expression during non-genotoxic hepatocarcinogenesis in mice. Carcinogenesis, 20, 1583-1590.

Cogswell,P.C., Guttridge,D.C., Funkhouser,W.K., & Baldwin Jr.,A.S. (2000). Selective activation of NF- κB subunits in human breast cancer: potential roles for NF- κB2/p52 and for Bcl-3. Oncogene, 19, 1123-1131.

Cohen,C., Lohmann,C.M., Cotsonis,G., Lawson,D., & Santoianni,R. (2003). Survivin expression in ovarian carcinoma: correlation with apoptotic markers and prognosis. Mod Pathol, 16, 574-583.

Collins,T., Read,M.A., Neish,A.S., Whitley,M.Z., Thanos,D., & Maniatis,T. (1995). Transcriptional regulation of endothelial cell adhesion molecules: NF-kappa B and cytokine-inducible enhancers. FASEB J., 9(10), 899-909.

Cusack,J.C., Jr., Liu R. & Baldwin,A.S., Jr. (2000). Inducible Chemoresistance to 7-Ethyl-10-[4-(1-piperidino)-1-piperidino]carbonyloxycamptothecin (CPT-11) in Colorectal Cancer Cells and a Xenograft Model Is Overcome by Inhibition of Nuclear Factor-κB Activation. Cancer Research, 60, 2323-2330.

Deligdisch,L., Miranda,C.R.R., Wu,H.S., & Gil,J. (2003). Human papillomavirus-related cervical lesions in adolescents: a histologic and morphometric study. Gynecologic Oncology, 89, 52-59.

Evan,G., & Littlewood,T. (1998). A Matter of Life and Cell Death. Science, 281, 1317-1322.

Famuboni,A.K., Graveling, A.J., Markey,A.L., Minns,F.C., Patel,A. (2002). Apoptosis. http://www.portfolio.mvm.ed.ac.uk/studentwebs/session2/group28/index.html

Ferrer,I., & Planas,A.M. (2003). Signaling of cell death and cell survival following focal cerebral ischemia: life and death struggle in the penumbra. J Neuropathol Exp Neurol., 62(4), 329-339.

Fiers,W., Beyaert,R., Declercq,W., & Vandenabeele,P. (1999). More than one way to die: apoptosis, necrosis and reactive oxygen damage. Oncogene, 18, 7719-7730.

Finzer,P., Lemarroy,A.A., & Rosl,F. (2002). The role of human papillomavirus oncoproteins E6 and E7 in apoptosis. Cancer Letters, 188, 15-24.

Foo,S.Y., & Nolan,G.P. (1999). NF-κB to the rescue. Trends Genet, 15, 229-235.

Fuertes,M.A., Castilla,J., Alonso,C., & Perez,J.M. (2002). Novel concepts in the development of platinum antitumor drugs. Curr Med Chem Anti-Canc Agents, 2, 539-551.

Furman,R.R., Asgary,Z., Mascarenhas,J.O., Liou,H.C., & Schattner,E.J. (2000). Modulation of NF- κB Activity and Apoptosis in Chronic Lymphocytic Leukemia B Cells. Journal of Immunology, 164, 2200-2206.

Furomoto,H.IM., & Irahara. (2002). Human papilloma virus (HPV) and cervical cancer. J Med Invest, 49, 124-133.

Gadducci,A., Brunetti,I., Cisco,S., Giannessi,PG., Genazzani,AR., & Conte P. (1997). Platinum compounds and paclitaxel in advanced epithelial ovarian cancer. Anticancer Research, 17, 4703-4708.

Garcia,G.E., Xia,Y., Chen,S., Wang,Y., Ye,R.D., Harrison,J.K., Bacon,K.B., Zerwes,H.G., & Feng,L. (2000). NF- κB -dependent fractalkine induction in rat aortic endothelial cells stimulated by IL-1beta, TNF-alpha, and LPS. Journal of Leukocyte Biology, 67, 577-584.

Garland,S.M. (2002). Human papillomavirus update with a particular focus on cervical disease. Pathology, 34, 213-224.

Gerondakis,S., Grossmann,M., Nakamura,Y., Pohl,T., & Grumont,R. (1999). Genetic approaches in mice to understand Rel/NF- κB and I κB function: transgenics and knockouts. Oncogene, 18, 6888-6895.

Ghim,S.J., Basu,P.S., & Jenson,A. (2002). Cervical Cancer: Etiology, Pathogenesis, Treatment, and Future Vaccines. Asian Pac J Cancer, 3, 207-214.

Govind,S. (1999). Control of development and immunity by Rel transcription factors in Drosophila. Oncogene, 18, 6875-6887.

Green,A. (2003). Effect of Xrel3 on TGF-β Signalling Pathway in Human Cervical Cancer cells. Memorial University of Newfoundland.

Green,D.R., & Reed,J.C. (1998). Mitochondria and Apoptosis. Science, 281, 1309-1312.

Green,D.R. (2000). Apoptotic Pathways: Paper Wraps Stone Blunts Scissors. Cell, 102, 1-4.

Greider,C., Chattopadhyay,A., Parkhurst,C., & Yang,E. (2002). BCL-x_L and Bcl-2 delay Myc-induced cell cycle entry through elevation of p27 and inhibition of G1 cyclin-dependent kinases. Oncogene, 21(51), 7765-7775.

Grilli,M., Chen-Tran,A., & ,L.M.J. (1993). Tumor necrosis factor alpha mediates a T cell receptor-independent induction of the gene regulatory factor NF-kappa B in T lymphocytes. Mol Immunol.1993 Oct;30(14):1287-94., 30(14), 1287-1294.

Haddad,J. (2002). Science review: Redox and oxygen-sensitive transcription factors in the regulation of oxidant-mediated lung injury: role for nuclear factor-kappaB. Critical Care, 6, 481-490.

Heckman,C.A., Mehew,J.W., & Boxer,L.M. (2002). NF- κB activates Bcl-2 expression in t(14;18) lymphoma cells. Oncogene, 21, 3898-3908.

Heilmann,V., & Kreienberg,R. (2002). Molecular biology of cervical cancer and its precursors. Curr Womens Health Rep, 2, 27-33.

Hengartner,M.O. (2000). The biochemistry of apoptosis. Nature Insight, 407, 770-776.

Henkel,T., Machleidt,T., Alkalay,I., Kronke,M., Ben-Neriah,Y., & Baeuerle,P.A. (1993). Rapid proteolysis of I kappa B-alpha is necessary for activation of transcription factor NF-kappa B. Nature, 365, 182-185.

Hida,A., Kawakami,A., Nakashima,T., Yamasaki,S., Sakai,H., & Urayama,H.I.S. (2000). Nuclear factor-κB and caspases co-operatively regulate the activation and apoptosis of human macrophages. Immunology, 99, 553-560.

Higgins,K.A., Coleman,T.A., McComas,W.A., Perez,J.R., Dorshkind,K., Sarmiento,U.M., Rosen,C.A., & Narayanan,R. (1993). Antisense inhibition of the p65 subunit of NF-kappa B blocks tumorigenicity and causes tumor regression. Proc Natl Acad Sci U S A, 90(21), 9901-9905.

Hiscott,J., Kwon,H.& Genin,P. (2001). Hostile takeovers: viral appropriation of the NF-kB pathway. J. Clin. Invest., 107(2), 143 - 151.

Hogerlinden,M.V., Rozell,B.L., Richter,L.A., & Toftgard,R. (1999). Squamous Cell Carcinomas and Increased Apoptosis in Skin with Inhibited Rel/Nuclear Factor- κB Signaling. Cancer research, 59, 3299-3303.

Huang,Y., Johnson,K.R., Norris,J.S., & Fan,W. (2000). Nuclear Factor-κB /I κB Signaling Pathway May Contribute to the Mediation of Paclitaxel-induced Apoptosis in Solid Tumor Cells. Cancer research, 60, 4426-4432.

Jakupec,M.A., Galanski,M., & Keppler,B.K. (2003). Tumour-inhibiting platinum complexes--state of the art and future perspectives. Rev Physiol Biochem Pharmacol, 146-154.

Jiang,M., & Milner,J. (2003). Bcl-2 constitutively suppresses p53-dependent apoptosis in colorectal cancer cells. Genes Dev., 17, 832-837.

Jones,D.R., Broad,M., Madrid,L.V., Baldwin,A.S., Jr.& Mayo,M.W. (2000). Inhibition of NF-κB sensitizes non-small cell lung cancer cells to chemotherapy-induced apoptosis. Ann Thorac Surg, 70, 930-936

Josefson,D. (1999). Mild cervical dysplasia often reverts to normal. British Medical Journal, Feb 13, 1999.

Kaltschmidt,B., Kaltschmidt,C., Hofmann,T.G., Hehner,S.P., Droge,W., & Schmitz,M.L. (2000). The pro- or anti- apoptotic function of NF- κB is determined by the nature of the apoptotic stimulus. European Journal of Biochemistry, 267, 3828-3835.

Karin,M., Cao,Y., Greten, F.R.,Li, Z.W. (2002). NF-κB in cancer: From innocent bystander to major culprit. Nature Reviews ,Cancer **2**, 301 –310.

Kawakami,A., Nakashima,T., Sakai,H., Urayama,S., Yamasaki,S., Hida,A., Tsuboi,M., Nakamura,H., Ida,H., Migita,K., Kawabe,Y., & Eguchi,K. (1999). Inhibition of Caspase Cascade by HTLV-I Tax Through Induction of NF-κB Nuclear Translocation. Immunobiology, Blood, 94, 3847-3854.

Kim,C.J., Jeong,J.K., Park,M., Park,T.S., Park,T.C., Namkoong,S.E., & Park,J.S. (2003). HPV oligonucleotide microarray-based detection of HPV genotypes in cervical neoplastic lesions. Gynecologic Oncology, 89, 210-217.

Kim,D.W., Sovak,M.A., Zanieski,G., Nonet,G., Romieu-Mourez,R., Lau,A.W., Hafer,L.J., Yaswen,P., Stampfer,M., Rogers,A.E., Russo,J., & Sonenshein,G.E. (2000).
Activation of NF- κB /Rel occurs early during neoplastic transformation of mammary cells. Carcinogenesis, 21, 871-879.

Kim,J.-S., Kim,J.-S., Kim,S.Y., Kim,K.H., & Cho,M.J. (2003). Hyperfractionated Radiotherapy with Concurrent Chemotherapy for Para-aortic Lymph Node Recurrence in Carcinoma of the Cervix. Int.J.Radiation Oncology Biol.Phys., 55(1247), 1253

Koivusalo,R., Krausz,E., Ruotsalainen,P., Helenius,H., & Hietanen,S. (2002). Chemoradiation of Cervical Cancer Cells: Targeting Human Papillomavirus E6 and p53 Leads to Either Augmented or Attenuated Apoptosis Depending on the Platinum Carrier Ligand. Cancer research, 62, 7364-7371.

Krammer,P.H. (2000). CD95's deadly mission in the immune system. Nature Insight, 407, 789-795.

Lake,B.B., Ford,R., & Kao,K.R. (2001). Xrel3 is required for head development in Xenopus laevis. Development, 128(2), 263-273.

Liou,H.C., & Baltimore,D. (1993). Regulation of the NF- κB /rel transcription factor and I κB inhibitor system. Current Opinion in Cell biology, 5, 477-487.

Mackenzie,F.R., Connelly,M.A., Balzarano,D., Muller,J.R., Geleziunas,R., & Marcu,K.B. (2000). Functional Isoforms of I κB Kinase alpha (IKK alpha) Lacking Leucine and Helix-Loop-Helix Domains Reveal that IKK alpha and IKK beta Have Different Activation Requirements. Molecular and Cellular Biology, 20, 2635-2649.

Madrid,L.V., Wang,C.Y., Guttridge,D.C., Schottelius,A.J.G., Baldwin Jr.,A.S., & Mayo,M.W. (2000). Akt Suppresses Apoptosis by Stimulating the Transactivation Potential of the RelA/p65 Subunit of NF- κB. Molecular and Cellular Biology, 20, 1626-1638.

Maggirwar,S.B., Sarmiere,P.D., Dewhurst,S., & Freeman,R.S. (1999). Nerve Growth Factor-Dependent Activation of NF- κB Contributes to Survival of Sympathetic Neurons. The Journal of Neuroscience, 18, 10356-10365.

Manna,S.K., Mukhopadhyay,A., & Aggarwal,B.B. (2000). Resveratrol Suppresses TNF-Induced Activation of Nuclear Transcription Factors NF-

κB, Activator Protein-1, and Apoptosis: Potential Role of Reactive Oxygen Intermediates and Lipid Peroxidation. The Journal of Immunology, 164, 6509-6519.

Markman,M. (2003). Intraperitoneal antineoplastic drug delivery: rationale and results. The Lancet Oncology, 4, 277-283.

May,M.J., & Ghosh,S. (1998). Signal transduction through NF- κB. Immunology Today, 19, 80-88.

McFarland,E.D.C., Izumi,K.M., & Mosialos,G. (1999). Epstein-Barr virus transformation: involvement of latent membrane protein 1-mediated activation of NF- κB. Oncogene, 18, 6959-6964.

Meier,P., Finch,A., & Evan,G. (2000). Apoptosis in development. Nature Insight, 407, 796-801.

Mercurio,F., & Manning,A.M. (1999). Multiple signals concerging on NF-kappaB. Curr Opin Cell Biol, 11, 226-232.

Meyskens Jr.,F.L., Buckmeier,J.A., McNulty,S.E., & Tohidian,N.B. (1999). Activation of Nuclear Factor κB in Human Metastatic Melanoma

Cells and the Effect of Oxidative Stress. Clinical Cancer Research, 5, 1197-1202.

Mikeaelsdottir,E.K., Benediktsdottir,K.R., Olafsdottir,K., Arnadottir,T., Ragnarsson,G.B., Olafsson,K., Sigurdsson,K., Kristjansdottir,G.S., Imsland,A.K., Ogmundsdottir,H.M., & Rafnar,T. (2003). HPV subtypes and immunological parameters of cervical cancer in Iceland during two time periods, 1958-1960 and 1995-1996. Gynecologic Oncology, 89, 22-30.

Miller,L.J., & Marx,J. (1998). Apoptosis. Science, 281, 1301-1304.

Miyamoto,S., Maki,M., Schmitt,M.J., Hatanaka,M., & Verma,I.M. (1994). Tumor necrosis factor alpha-induced phosphorylation of I kappa B alpha is a signal for its degradation but not dissociation from NF-kappa B. Proc Natl Acad Sci U S A., 91(26), 12740-12744.

Mori,N., Fujii,M., Ikeda,S., Yamada,Y., Tomonaga,M., Ballard,D.W., & Yamamoto,N. (1999). Constitutive Activation of NF- κB in Primary Adult T-Cell Leukemia Cells. Blood, 2360-2368.

Mosialos,G. (1997). The role of Rel/NF-kappa B proteins in viral oncogenesis and the regulation of viral transcription. Semin Cancer Biol, 8, 121-129.

Muller,I., Pfister,S.M., Grohs,U., Zweigner,J., Handgretinger,R., Niethammer,D., & Bruchelt,G. (2003). Receptor Activator of Nuclear Factor κB Ligand Plays a Nonredundant Role in Doxorubicin-induced Apoptosis. Cancer research, 63, 1772-1775.

Munoz,N., Bosch,F.X., Sanjose,S., Herrero,R., Castellsague,X., Shah,K.V., Snijders,P.J., Meijer,C.J., & International Agency for Research on Cancer Multicenter Cervical Cancer Study Group. (2003). Epidemiologic classification of human papillomavirus types associated with cervical cancer. N Engl J Med, 348, 518-527.

Naishiro,Y., Adachi,M., Okuda,H., Yawata,A., Mitaka,T., Takayama,S., Reed,J.C., Hinoda,Y., & Imai,K. (1999). BAG-1 accelerates cell motility of human gastric cancer cells. Stockton Press, 3244-3251.

Nakayama,K., Takebayashi,Y., Nakayama,S., Hata,K., Fujiwaki,R., Fukumoto,M., & Miyazaki,K. (2003). Prognostic value of overexpression

of p53 in human ovarian carcinoma patients receiving cisplatin. Cancer Letters, 192, 227-235.

National Cancer Institute of Canada. 2003 Canadian Cancer Statistics. (2003). Anonymous.

Nicholson,D.W. (2000). From bench to clinic with apoptosis-based therapeutic agents. Nature Insight, 407, 810-816.

Nicoletti,V.G., & Stella,A.M. (2003). Role of PARP under stress conditions: cell death or protection? Neurochem Res., 28(2), 187-194.

Ondrey,F.G., Dong,G., Sunwoo,J., Chen,Z., Wolf,J.S., Crowl-Bancroft,C.V., Mukaida,N., & Waes,C.V. (1999). Constitutive Activation of Transcription Factors NF κB, AP-1, and NF-IL6 in Human Head and Neck Squamous Cell Carcinoma Cell Lines that Express Pro-inflammatory and Pro-angiogenic Cytokines. Molecular Carcinogenesis, 26, 119-129.

Packham,G., Brimmell,M., & Cleveland,J.L. (1997). Mammalian cells express two differently localized Bag-1 isoforms generated by alternative translation initiation. Journal of Biochemistry, 328, 807-813.

Park,J.S., Rhyu,J.W., Kim,C.J., Kim,H.S., Lee,S.Y., Kwon,Y.I., Namkoong,S.I., Sin,H.S., & Um,S.J. (2003). Neoplastic change of squamo-columnar junction in uterine cervix and vaginal epitheluim by exogenous estrogen in hpv-18 URR E6/E7 transgenic mice small star, filled. Gynecologic Oncology, 89, 360-368.

Ponnappan,U. (1998). Regulation of transcription factor NFkappa B in immune senescence. Frontiers in Bioscience, 3, D152-168.

Pratt,M.A.C., & Niu,M.Y. (2003). Bcl-2 Controls Caspase Activation Following a p53-dependent Cyclin D1-induced Death Signal. Journal of Biological Chemistry, 278, 14219-14229.

Ravi,R., Bedi,A., Fuchs,E.J., & Bedi,A. (1998). CD95 (Fas)-induced Caspase-mediated Proteolysis of NF- κB. Cancer research, 58, 882-886.

Reed,J.C. (1997). Double identity for proteins of the Bcl-2 family. Nature, 387, 776

Reedijk,J. (2003). New Clues for platinum antitumor chemistry: Kinetically controlled metal binding to DNA. National Academy of Sciences, 100, 3611-3616.

Reuning,U., Guerrini,L., Nishiguchi,T., Page,S., Seibold,H., Magdolen,V., Graeff,H., & Schmitt,M. (1999). Rel transcription factors contribute to elevated urokinase expression in human ovarian carcinoma cells. European Journal of Biochemistry, 259, 143-148.

Rich,T., & Allen,R.L.W.A.H. (2000). Defying death after DNA damage. Nature Insight, 407, 777-783.

Romano,M.F., Lamberti,A., Bisogni,R., Tassone,P., Pagnini,D., Storti,G., Vecchio,L.D., Turco,M.C., & Venuta,S. (2000). Enhancement of cytosine arabinoside-induced apoptosis in human myeloblastic leukemia cells by NF-κB /Rel- specific decoy oligodeoxynucleotides. Gene Therapy, 7, 1234-1237.

Rosenthal,A.N., Ryan,A., Al-Jejani,R.M., Storey,A., Harwood,C.A., & Jacobs I.J. (1998). p53 codon 72 polymorphism and risk of cervical cancer in UK. The Lancet, 352, 871-874.

Rudolph,D., Yeh,W.C., Wakeham,A., Rudolph,B., Nallainathan,D., Potter,J., Elia,A.J., & Mak,T.W. (2000). Severe liver degeneration and lack of NF- κB activation in NEMO/IKKγ-deficient mice. Genes and Development, 854-862.

Savill,J., & Fadok,V. (2000). Corpse clearance defines the meaning of cell death. Nature Insight, 407, 784-788.

Schottelius,A.J.G., Mayo,M.W., Sartor,R.B., & Baldwin Jr.,A.S. (1999). Interleukin-10 Signaling Blocks Inhibitor of κB Kinase Activity and Nuclear Factor-κB DNA Binding. The Journal of Biological Chemistry, 274, 31868-31874.

Seitz,C.S., Deng,H., Hinata,K., Lin,Q., & Khavari,P.A. (2000). Nuclear Factor- κB Subunits Induce Epithelial Cell Growth Arrest. Cancer research, 60, 4085-4092.

Shain,K.H., Jove,R., & Olashaw,N.E. (1999). Constitutive RelB Activation in v-Src-Transformed Fibroblasts: Requirement for I κB Degradation. Journal of Cellular Biochemistry, 73, 237-247.

Shinoura,N., Yoshida,Y., Nishimura,M., Muramatsu,Y., Asai,A., Kirino,T., & Hamada,H. (2000). Expression Level of Bcl-2 Determines Anti- or Proapoptotic Function. Cancer research, 59, 4119-4128.

Sisk,E.A., & Robertson,E.S. (2002). Clinical implications of human papillomavirus infection. Front Biosci, 1, e77-e84

Sonenshein,G.E. (1997). Rel/NF-kappaB transcription factors and the control of apoptosis. Semin Cancer Biol, 8, 113-119.

Stehlik,C., Rainer de Martin, Kumabashiri,I., Schmid,J.A., Binder,B.R., & Lipp,J. (1998). Nuclear Factor (NF)- κB -regulated X-chromosome-linked iap Gene Expression Protects Endothelial Cells from Tumor Necrosis Factor α-induced Apoptosis. J.Exp.Med, 188, 211-216.

Stuart,J.K., Myszka,D.G., Joss,L., Mitchell,R.S., McDonald,S.M., Xie,Z., Takayama,S., Reed,J.C., & Ely,K.R. (1998). Characterization of Interactions between the Anti-apoptotic Protein BAG-1 and Hsc70 Molecular Chaperones. The Journal of Biological Chemistry, 273, 22506-22514.

Sun,S.C., & Ballard,D.W. (1999). Persistant activation of NF- κB by the Tax transforming protein of HTLV-1: hijacking cellular I κB kinases. Oncogene, 18, 6948-6958.

Thornberry,N.A., & Lazebnik,Y. (1998). Caspases: Enemies Within. Science, 281, 1312-1316.

Tickle,C. (1998). Worlds in common through NF-kappaB. Nature, 392, 547-549.

United States Pharmacopeia, USP. (2003). Chemotherapeutic Drugs. In Anonymous,

Verma,I.M., Stevenson,J.K., Schwarz,E.M., & Antwerp,D.V. (1995). Rel/NF- κB /I κB family: intimate tales of association and dissociation. Genes and Development, 9, 2723-2735.

Villiers,E.M. (2003). Relationship between steroid hormone contraceptives and HPV, cervical intraepithelial neoplasia and cervical carcinoma. Int.J.Cancer, 103, 705-708.

Wang,W., Abbruzzese,J.L., Evans,D.B., & Chiao,P.J. (1999). Overexpression of urokinase-type plasminogen activator in pancreatic adenocarcinoma is regulated by constitutively activated RelA. Oncogene, 18, 4554-4563.

Wang,W., Abbruzzese,J.L., Evans,D.B., Larry,L., Cleary,K.R., & Chiao,P.J. (1999). The Nuclear Factor-κB RelA Transcription Factor is

Constitutively Activated in Human Pancreatic Adenocarcinoma Cells. Clinical Cancer Research, 5, 119-127.

Warbinek,R.H., Schmid,J.A., Stehlik,C., Binder,B.R., Lipp,J., & Martin,R. (2000). Activation of NF- κB by XIAP, the X Chromosome-linked Inhibitor of Apoptosis, in Endothelial Cells Involves TAK1. The Journal of Biological Chemistry, 275, 22064-22068.

Yang,X., Hao,Y., Ferenczy,A., Tang,S.C., & Pater,A. (1999). Overexpression of Anti-apoptotic Gene BAG-1 in Human Cervical Cancer. Experimental Cell Research, 247, 200-207.

Yang,X., Ferenczy,A., Tang,S.C., & Pater,A. (2000). Overexpression of anti-apoptotic gene BAG-1 in human cervical cancer. Experimental Cell Research, 2562-2583.

Yu,Q., Geng,Y., & Sicinski,P. (2001). Specific protection against breast cancers by cyclin D1 ablation. Nature, 411, 1001-1002.

Yuan,J., & Yanker,B.A. (2000). Apoptosis in the nervous system. Nature Insight, 407, 802-809.

Zhang,H.G., Huang,N., Liu,D., Bilbao,L., Zhang,X., Yang,P., Zhou,T., Curiel,D.T., & Mountz,J.D. (2000). Gene Therapy That Inhibits Nuclear Translocation of Nuclear Factor κB Results in Tumor Necrosis Factor alpha-induced Apoptosis of Human Synovial Fibroblasts. Arthritis and Rheumatism, 43, 1094-1105.

Zigarelli,B., Sheehan,M., & Wong,H.R. (2003). Nuclear factor- κB as a therapeutic target in critical care medicine. Critical Care Medicine, 31, S105-S111

zur Hausen,A., van Beek,J., Bloemena,E., ten Kate,F.J., Meijer,C.J., & van den Brule,A.J. (2003). No role for Epstein-Barr virus in Dutch hepatocellular carcinoma: a study at the DNA, RNA and protein levels. J Gen Virol, 84(7), 1863-1869.

APPENDIX 1

$$t = \frac{\bar{x} - \bar{y}}{\sqrt{s^2\left(\frac{1}{n} + \frac{1}{m}\right)}}$$ = (difference between means)/(weighted average of standard deviations)

$$S^2 = \frac{(n-1)s_x^2 + (m-1)s_y^2}{n+m-2}$$

$\bar{x}$ = the average for the first sample

$\bar{y}$ = the average for the second sample

n = number of data points in the first sample

m = number of data points in the second sample

S_x = standard deviation of first sample (in formula #2 above, square the standard deviation = s_x^2)

S_y = standard deviation of second sample (in formula #2 above, square the standard deviation = s_y^2)

Degrees of Freedom: d.f. = n + m – 2

Table 4: Computation of the Student's t-test.